TUM School of Life Sciences
Weihenstephan
Technische Universität München

Neuronal representation of amplitude modulated sounds in the juvenile and adult brain of the bat *Phyllostomus discolor* and its relation to vocal communication

Stephen Gareth Hörpel

Vollständiger Abdruck der von der TUM School of Life Sciences Weihenstephan der Technischen Universität München zur Erlangung des akademischen Grades eines

Doktor der Naturwissenschaften (Dr. rer. nat.)

genehmigten Dissertation.

Vorsitzender:

Prof. Dr. Martin Klingenspor

Prüfende der Dissertation:

1. Priv.-Doz. Dr. Uwe Firzlaff
2. Prof. Dr. Michael Schemann

Die Dissertation wurde am 29.05.2020 bei der Technischen Universität München eingereicht und durch die Fakultät TUM School of Life Sciences am 18.09.2020 angenommen.

Abstract

Bats use a set of communication calls for social interaction with conspecifics. Some of these communication calls are characterised by strong amplitude modulations (i.e. a periodic change of the sound pressure level), especially the calls used in an aggressive behavioural context. Due to the significance of this behavioural context and the possible consequences for the animal itself, the main objective of this thesis was to investigate how amplitude modulated sounds are represented in the auditory system and whether differences in encoding could be found depending on the location within the auditory system and the level of maturity of the animal under investigation.

In the first part of the project, I investigated how both artificial sounds and natural communication sounds are processed in the auditory cortex of the bat *Phyllostomus discolor* via extracellular recordings. A bias in neuronal response strength towards calls associated with aggressive behaviour was uncovered and furthermore, it was revealed that a subpopulation of neurons could follow artificial, sinusoidally amplitude modulated sounds (i.e. the amplitude of the sound increases and decreases periodically with a certain modulation frequency) with surprisingly high fidelity. These artificial calls used amplitude modulation frequencies comparable to those seen in the aggression calls, therefore, there seems to be a pre-adaptation of the neurons in the auditory cortex of *Phyllostomus discolor* to process amplitude modulated sounds.

The next part of the project followed up directly on the findings of the initial part as it focused on the encoding of amplitude modulated sounds in juvenile *Phyllostomus discolor* during their ontogeny. By measuring auditory brainstem responses, I analysed the development of the capability of the auditory brainstem to lock its neuronal response to the envelope (i.e. the outline of the waveform) of a periodic sound signal starting at postnatal day 7. It was shown, that this envelope locking capability is not matured at birth and further develops over a longer maturation period. However, lower modulation frequencies are more developed at birth, while higher modulation frequencies take more time to fully mature.

In the last part of this project, I focused more on the frontal auditory field, a small region located in the frontal cortex, which also receives acoustically driven input. Having performed single cells recordings, I was able to identify variations in the neuronal response properties. Unlike the auditory cortex with (mainly) low latency, short duration neuronal discharges, the frontal auditory field showed delayed neuronal responses with increased discharge duration. Additionally, the bias of the auditory cortex towards aggression calls could not be found in the frontal auditory field. Finally, I established the position of the frontal auditory field in *Phyllostomus discolor* and ran preliminary experiments outlining its connectivity to other brain regions.

Zusammenfassung

Fledermäuse verwenden eine Vielzahl an Kommunikationslauten um mit Artgenossen zu kommunizieren. Manche dieser Kommunikationslaute werden durch starke Amplitudenmodulationen (d.h. eine periodische Änderung des Schallpegels) charakterisiert, insbesondere jene, welche in einem aggressiven Verhaltenskontext verwendet werden. Aufgrund der Bedeutsamkeit dieses Verhaltenskontextes und den möglichen Folgen für das Tier lag das Hauptaugenmerk dieser Arbeit auf der Untersuchung der neuronalen Repräsentation von amplitudenmodulierten Tönen im auditorischen System. Insbesondere wurde untersucht, ob die Lage im auditorischen System und das Tieralter zu Unterschieden in der neuronalen Verarbeitung führen würden.

Im ersten Teil des Projekts analysierte ich mittels extrazellulärer Ableitungen, wie sowohl künstliche Laute als auch natürliche Kommunikationslaute im auditorischen Cortex der Fledermausart *Phyllostomus discolor* verarbeitet werden. Eine Präferenz der neuronalen Antwortstärke gegenüber Kommunikationslauten, welche mit aggressivem Verhalten assoziiert werden, konnte aufgedeckt werden. Des Weiteren wurde entdeckt, dass eine Untergruppe an Neuronen künstlichen, sinusförmig amplitudenmodulierten Lauten (d.h. die Amplitude des Tones steigt und fällt periodisch mit einer gewissen Frequenz) mit hoher Präzision folgen konnte. Diese künstlichen Töne verwendeten Amplitudenmodulationsfrequenzen vergleichbar mit jenen, welche in den natürlichen Aggressionslauten vorkommen. Somit scheint es eine Präadaptation der Neurone des auditorischen Cortex von *Phyllostomus discolor* hinsichtlich der Verarbeitung amplitudenmodulierter Laute zu geben.

Der nächste Abschnitt des Projekts baute direkt auf den Erkenntnissen des ersten Teils auf, da nun die neuronale Verarbeitung von amplitudenmodulierten Tönen in jungen *Phyllostomus discolor* während ihres Heranwachsens untersucht wurde. Durch Messung auditorischer Hirnstammantworten analysierte ich die Entwicklung der Fähigkeit des auditorischen Hirnstammes seine neuronalen Antworten an die Lautumhüllende (d.h. die Kontur des Lautes) eines periodischen Signals zu koppeln. Es konnte gezeigt werden, dass dieses Koppeln an die Lautumhüllende bei Geburt noch nicht vollständig ausgebildet ist und sich über eine bestimmte Reifeperiode hinweg fertig entwickelt. Tiefere Modulationsfrequenzen werden bei Geburt besser neuronal abgebildet, während die Abbildung höherer Modulationsfrequenzen mehr Zeit zur Entwicklung benötigt.

Im finalen Abschnitt dieses Promotionsvorhabens konzentrierte ich mich auf das frontale auditorische Feld, eine kleine Region im Bereich des frontalen Cortex, welche ebenfalls akustisch stimulierte Eingänge erhält. Nachdem ich Einzelzellableitungen durchgeführt hatte, konnte ich Unterschiede im neuronalen Antwortverhalten identifizieren. Im Gegensatz zu dem auditorischen Cortex mit seiner (überwiegend) geringen neuronalen Antwortlatenz und Antwortdauer offenbarte das frontale auditorische Feld eine verzögerte neu-

ronale Antwort, welche jedoch länger ausfiel als im Cortex. Des Weiteren konnte die Präferenz des auditorischen Cortex hinsichtlich Aggressionslauten im frontalen auditorischen Feld nicht nachgewiesen werden. Abschließend konnte ich die Position des frontalen auditorischen Feldes im Cortex von *Phyllostomus discolor* festlegen und führte vorbereitende Experimente durch, mit welchen die Verbindungen zu anderen Hirnregionen skizziert werden konnten.

Contents

Acronyms

ABR Auditory brainstem response.

AC Auditory cortex.

AVCN Anteroventral cochlear nuchleus.

BDA Biotinylated dextran.

BF Best frequency.

BM Basilar membrane.

CF Characteristic frequency.

DCN Dorsal cochlear nucleus.

DNLL Dorsal nucleus of the lateral lemniscus.

FAF Frontal auditory field.

HRTF Head related transfer function.

IC Inferior colliculus.

IHC Inner hair cells.

IQR Interquartile range.

ITD Inter-aural time differences.

LFP Local field potential.

LSO Lateral superior olivary complex.

MGB Mediageniculate body of the thalamus.

MNTB Medial nucleus of the trapezoid body.

MSO Medial superior olivary nucleus.

OHC Outer hair cells.

PFA Paraformaldehyde.

PFC prefrontal cortex.

PSTH Peri-stimulus time histogram.

PVCN Posteroventral cochlear nucleus.

SAM Sinusoidally amplitude modulated.

SC Superior colliculus.

SG Suprageniculate nucleus (of the thalamus).

SPL Sound pressure level.

TDT Tucker-Davis Technologies.

TM Tectorial membrane.

VNLL Ventral nucleus of the lateral lemniscus.

WPI World Precision Instruments.

List of Figures

1 Introduction

With over 1300 species, the Chiroptera or bats are the second largest group of mammals and they are the only mammals capable of sustained flight. Historically, they were divided into the suborders Microchiroptera and Megachiroptera, however, more recently, a re-classification of the Chiroptera based on genetic markers was proposed, which groups the former Megachiroptera and the Rhinolophoidea (i.e. horseshoe bats) to form the Yinpterochiroptera, while the remaining Microchiroptera form the Yangochiroptera (Springer et al. [2001]). Some Yinpterochiroptera (all Rhinolophoidea and some former Megachiroptera) and all Yangochiroptera rely on echolocation for navigation. This ability to successfully navigate and hunt in absolute darkness or when blinded was described in the late 18^{th} century by the Bishop of Padua (Neuweiler [1993]), however, the reason for their navigational skills was only discovered 150 years later by Donald Griffin, when a group of apparently silent bats revealed their noisy nature, when recorded with an ultrasonic microphone (Pierce and Griffin [1938]). However, not all bat vocalisations are short, ultrasonic echolocation calls. Being gregarious animals, which usually live in larger groups, they use a broad variety of social communication calls, which are not always limited to the ultrasonic frequency range, but can also be audible to humans. Unlike echolocation calls, communication calls are longer in duration, show complex spectro-temporal (i.e. amplitude and frequency) modulations and are in a lower frequency range when compared to the echolocation calls (Gillam and Fenton [2016], see Figure 1.1 for a spectrogram of both an echolocation call and an aggression call).

These communication calls serve many purposes, ranging from mother-pup recognition, over courtship songs to conveying outright aggression. In the bat *Phyllostomus discolor*, which was the subject used in my studies, social communication calls usually show frequency and/or amplitude modulations (Esser and Schmidt [1989], Lattenkamp et al. [2019], Lattenkamp et al. [2020]). Especially calls associated with aggressive behaviour can be identified and characterized by strong amplitude modulations and show a striking structural similarity across bat species (Russ et al. [2004], Gillam and Fenton [2016]).

As *Phyllostomus discolor* is a known vocal learner (Esser and Schubert [1998], Lattenkamp et al. [2018]) and a highly sociable species (Kwiecinski [2006]) and given the fact that the heavily amplitude modulated aggression calls convey vital information regarding social cohesion, it was of great interest to investigate the development of neuronal representations of amplitude modulated sounds during the ontogeny of juvenile bats and also to investigate adult bats, where fully matured neuronal representations of these amplitude modulations were to be expected. Furthermore, we analysed the neuronal responses to a variety of *Phyllostomus discolor* calls in light of "call detector" functionality (Pelleg-Toiba and Wollberg [1991], Schnupp et al. [2006]) in both the auditory cortex and the frontal auditory field to determine whether a neuronal preference for a certain type of communication call exists in the bat cortex.

This chapter will give the reader a general overview into neuronal sound processing, starting at the auditory periphery and moving along the ascending auditory pathway, highlighting bat specific features and laying the foundation for the following, more detailed chapters 3 and 4. While the auditory cortex and auditory brainstem have been the focus of numerous publications over the past decades, only very few publications

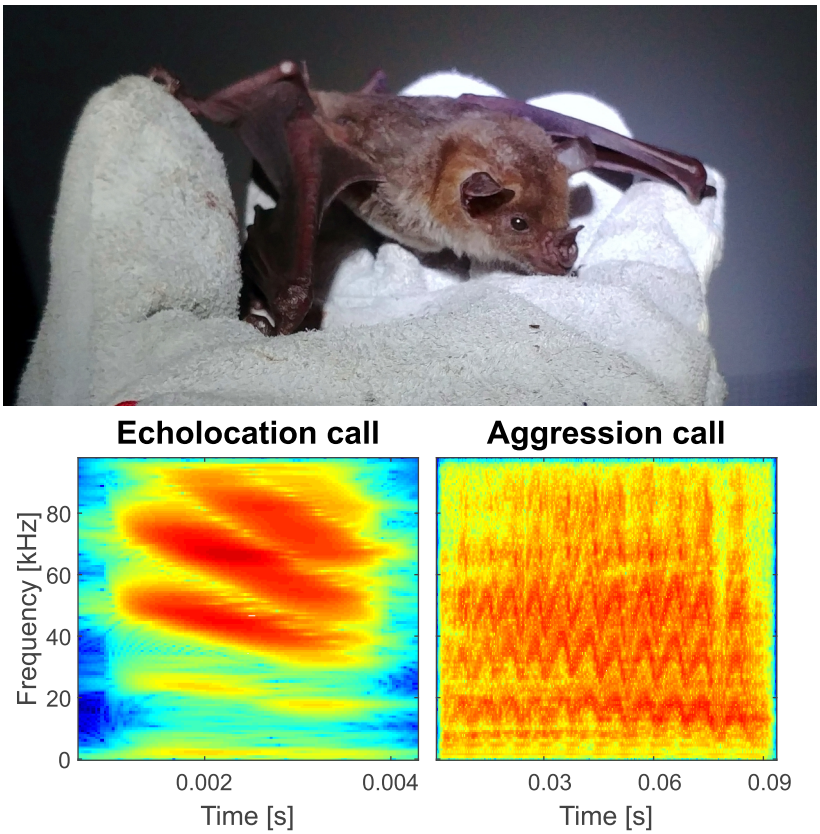

Figure 1.1: The bat *Phyllostomus discolor*, self-provided image (top) and spectrograms of a *Phyllostomus discolor* echolocation call and aggression call: Multiharmonic, short duration echolocation call on the bottom left and strongly amplitude and frequency modulated aggression call on the bottom right. Note the different timescales.

have covered the frontal auditory field, a small region of the frontal/prefrontal cortex which is acoustically driven and said to be involved in linking both auditory and motor-systems, as it is connected with several nuclei associated with either auditory processing or sensory-motor integration. It may therefore be involved in the control of vocalisation, in auditory feedback loops which coordinate vocalisation during vocal learning or in the coordination of both ear and head movement during sound localisation. Chapter 5 introduces the frontal auditory field of *Phyllostomus discolor*, highlighting its neuronal response properties to both artificial sounds and echolocation/social communication calls and uncovering the neurocircuitry innervating it.

1.1 The anatomical necessities for sound processing in bats

The outer ear of bats consists of the pinna and the external acoustic meatus, or ear canal. The pinna is both rotatable and tiltable and aids the bat in determining target angles (Mogdans et al. [1988]). Furthermore, it plays a vital role in the head related transfer function (HRTF), further aiding sound localisation in both azimuth and elevation (De Mey et al. [2008], Aytekin et al. [2004]). This is due to the fact that the pinna and ear canal function as a directional antenna, amplifying incoming sound waves within a certain frequency range, depending on the opening diameter of the pinna and, to some extent, of the opening diameter of the ear canal (Neuweiler [1993]).
Additional signal amplification and frequency filtering occurs in the middle ear. The size and rigidity of the auditory ossicles impact their frequency filtering capabilities. Mechanical amplification of sound is achieved in several ways. Firstly, the area of the tympanic membrane is very large compared to the area of the oval window on the cochlea (Nummela [1995]), therefore a small deflection of the tympanic membrane results in a large deflection of the oval window, resulting in an increased signal amplitude (Neuweiler [1993]). Secondly, the size of the auditory ossicles plays an important role in mechanical signal amplification. The leverage of the malleus (hammer) is larger than that of the incus (anvil), resulting in a slower but stronger movement of the stapes (stirrup) and therefore a large deflection of the oval window (Neuweiler [1993], Wilson and Bruns [1983]). The size and rigidity of the auditory ossicles impact their frequency filtering capabilities, with small, rigid bones leading to a higher resonance frequency (Henson [1960]) and therefore an increased frequency range.
In most cases, the basic structure of chiropteran cochlea is similar to the human cochlea and therefore typically mammalian, consisting of three liquid-filled cavities contained within a concentrically wound (2.25-3 turns, species-dependent) bone structure with two membrane covered openings (oval and round window) at the basal part of the structure (see Figure 1.2, Kössl and Vater [1995]).

These three cavities (scala vestibuli v, scala media m and scala tympani t, see Figure 1.2) are separated by flexible membranes from each other. Deflection of the membrane covering the oval window causes an increase in pressure of the perilymph within the scala vestibuli, which ultimately results in a travelling wave within the scala media, whose pressure differences are negated by movement of the round window (Neuweiler [1993]). The Reissners membrane (R) forms the roof of the scala media, while the floor is formed by the basilar membrane (BM, see Figure 1.2, Neuweiler [1993]), which is displaced by the travelling wave. The basilar membrane performs the first steps of frequency analysis in the cochlea, as its flexibility increases from base to apex (Von Békésy and Wever [1960]). This increase in flexibility leads to a tonotopy of the basilar membrane, as high-frequency sounds achieve maximum displacement of the basilar membrane at the basal end of the cochlea, whereas low frequency sounds cause maximum displacement towards the apical end (Bruns [1976]). Usually, each frequency range of one octave occupies the same distance along the basilar membrane (Neuweiler [1993]), however, in some bat species an acoustic fovea exists, where one frequency range is (heavily) overrepresented in the spatial distribution along the basilar membrane (Bruns [1976]).

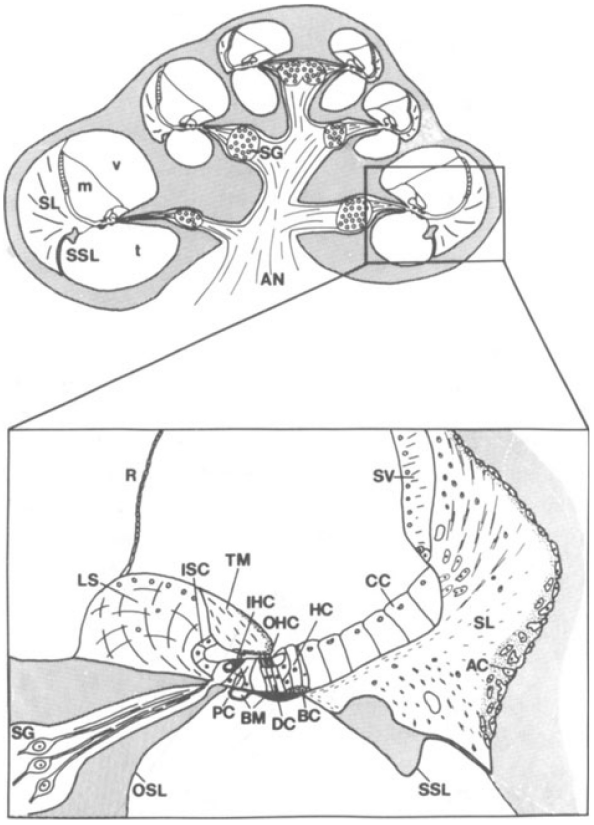

Figure 1.2: Cross-section of the cochlea of *Rhinolophus rouxii*: fluid-filled caveties (only marked in one basal half-turn): v, scala vestibuli; m, scala media; t, scala tympani. AC, anchoring cells; AN, auditory nerve; BM, basilar membrane; BC, Boettcher cells; CC, Claudius cells; DC, Deiters cells; HC, Hensens cells; IHC, inner hair cell; ISC, inner sulcus cells; LS, spiral limbus; OHC, outer hair cell; OSL, osseus spiral lamina; PC, pillar cells; R, Reissners membrane; SG, spiral ganglion; SL, spiral ligament; SSL, secondary spiral lamina; SV, stria vascularis; TM, tectorial membrane. ([Kössl and Vater, 1995, with permission from Springer Nature, see Figure B.1]).

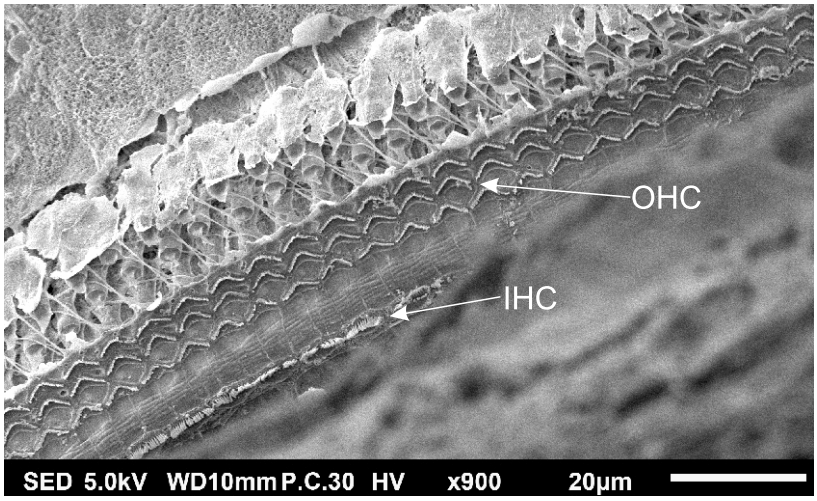

Figure 1.3: Scanning electron microscope image of the inner and outer hair cells of *Phyllostomus discolor:* The stereocilia of the 3 rows of OHC and 1 row of IHC are visible in this preparation, the TM was removed from the decalcified cochlea of an adult bat. Self-provided image with help from Gaby Schwabedissen using a JSM-F100 scanning electron microscope (Jeol GmbH, Freising, Germany).

First investigated by Corti [1851], the sensory epithelium of the cochlea, the organ of Corti, is supported by the basilar membrane. It consists of various supporting cells (Boettcher cells, *BC*; Claudis cells, *CC*; Deiters cells, *DC*; Hensens cells, *HC* and pillar cells, *PC*), the tectorial membrane (*TM*) and both one row of inner (*IHC*) and three rows of outer (*OHC*) hair cells (Kössl and Vater [1995], see Figure 1.3). These outer hair cells, each with a supporting Deiters cell at its base are attached to the basilar membrane, while their stereocilia are attached to the tectorial membrane (Vater and Lenoir [1992]). The inner hair cells are embedded in supporting inner border cells (Köles et al. [2019]) and their stereocilia are in close contact with the tectorial membrane (see Figure 1.2).

Vibration of the basilar membrane against the tectorial membrane causes the stereocilia of the IHC to bend, leading to a depolarisation of their membrane potential (Neuweiler [1993]). The IHC are innervated by the spiral ganglion (see Figure 1.2), whereas the OHC mainly act as a mechanical amplifier and frequency filter (Neuweiler [1993]). The axons of the neurons forming the spiral ganglion form the cochlear or auditory nerve (VIII, Figure 1.4), which projects to the cochlear nucleus (CN).

The cochlear nucleus is subdivided into three parts, the anteroventral cochlear nucleus (AVCN), the dorsal cochlear nucleus (DCN) and the posteroventral cochlear nucleus (PVCN).

The DCN and PVCN are involved in complex stimulus analysis and project directly onto the IC, whereas the AVNC amplifies the precision of temporal information encoded in neuronal firing Pickles [2015]. The information from the AVNC is passed on to the superior olivary complex (SOC, Figure 1.4), which consists of the medial superior olivary nucleus (MSO), the lateral superior olive (LSO) and the medial nucleus of the

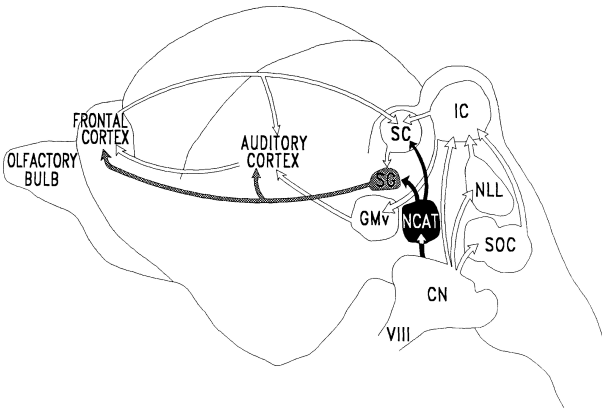

Figure 1.4: Summary diagram of auditory pathways to the auditory cortex and frontal auditory field in the bat *Pteronotus parnellii*: Summary diagram of auditory pathways to the auditory cortex and frontal auditory field. The components of the central acoustic tract are shown by the black arrows; those of the lemniscal system are shown by the white arrows. The grey arrows indicate further projections beyond the SG. CN, cochlear nucleus; GMv, ventral division of the medial geniculate body; IC, inferior colliculus; NCAT, nucleus of the central acoustic tract; NLL, nucleus of the lateral lemniscus; SC, superior colliculus; SG, suprageniculate nucleus; SOC, superior olivary complex; VIII, auditory nerve [Casseday et al., 1989, with permission from John Wiley and Sons, see Figure B.2].

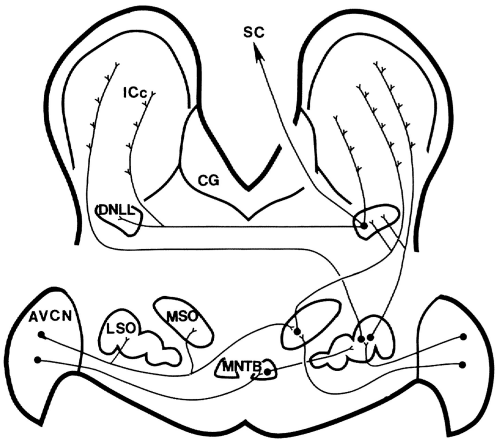

Figure 1.5: Summary diagram of ascending binaural pathways: For simplification only projections via right superior olivary complex are depicted. AVCN, anteroventral cochlear nucleus; CG, central grey; DNLL, dorsal nucleus of the lateral lemniscus; ICc, inferior colliculus; LSO, lateral superior olive; MNTB, medial nucleus of the trapezoid body; MSO, medial superior olivary nucleus; SC, superior colliculus [Pollak and Casseday, 1989, with permission from Elsevier, see Figure B.3].

trapeziod body (MNTB) as main nuclei (Figure 1.5). Sound localisation is one of the key features of the SOC. Inter-aural intensity differences (IID) are calculated in the LSO, which receives excitatory input from the ipsilateral AVCN and the inhibitory input from contralateral MNTB (Grothe and Park [2000]). In the MSO, sound localisation is achieved by calculation of inter-aural time differences (ITD), as it receives auditory input from both the ipsilateral and contralateral ear via the ipsilateral (excitatory input) and the contralateral AVCN (inhibitory input, see Figure 1.5, Pollak and Casseday [1989], Neuweiler [1993]), however, depending on the bat species, the ITD-calculation capabilities, are, if at all, limited (Neuweiler [1993]). The main output of the MSO is uncrossed and projects to both the ipsilateral IC and DNLL (dorsal nucleus of the lateral lemniscus), whereas the main output of the LSO crosses the centre line of the brainstem and projects to the contralateral IC, however, the LSO also projects to the ipsilateral DNLL and IC (Pollak and Casseday [1989], Neuweiler [1993]). The DNLL has several outputs, two cross and project to the contralateral DNLL and IC, while the other projections are to the ipsilateral IC and SC (superior colliculus, Pickles [2015]). Each IC projects to both the contralateral and ipsilateral MGB (mediageniculate body of the thalamus) and each MGB projects to the other MGB and its corresponding ipsilateral auditory cortex (Pickles [2015]). Furthermore, the SC projects to the suprageniculate nucleus (SG) of the thalamus, which itself projects to the auditory cortex (AC) and the frontal auditory field (FAF) (see Figure 1.4, Casseday et al. [1989]), which were the focus of our investigations in Chapter 3 and 5.

1.2 Neuronal representation of amplitude modulated sounds

Of all the known sensory systems, auditory perception outclasses the rest in terms of pure processing speed (Joris et al. [2004]). However, said processing speed varies depending on the location within the auditory system, as the response properties change drastically from the auditory nerve to the auditory cortex. This can be easily demonstrated with sinusoidally amplitude modulated stimuli (SAM), as these consist of a carrier signal, which is attenuated with a certain modulation rate (see Figure 1.6, top plot). A 400 ms long stimulus with a 5 Hz amplitude modulation has 2 modulation cycles, where the stimulus amplitude changes from a minimum to a maximum and then back again to minimum. An ideally synchronised neuron would fire every modulation cycle and the neuronal discharge would always occur at the same phase of the stimulus, hence the term phase-locked (Tollin and Yin [2009]). The described ideal neuron would produce a strong representation of the amplitude modulation frequency within both its firing pattern and rate (see Figure 1.6). However, a neuron can still present phase-locked responses, even if it does not discharge at every single modulation cycle, as long as the response occurs at the same stimulus phase.

Generally speaking, neuronal responses to amplitude modulated stimuli are typically limited in their ability to synchronise to very high modulation frequencies and the ability to synchronise to amplitude modulated stimuli diminishes when ascending the auditory pathway (Krishna and Semple [2000], Joris et al. [2004]). While neurons in the auditory

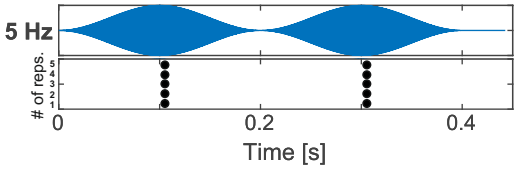

Figure 1.6: Amplitude modulated stimulus and synchronised neuronal discharge: Waveform of a high-frequency carrier with a 5 Hz amplitude modulation (top plot) and five repeated recordings of a highly synchronised neuronal discharge (bottom plot, indicated by black dots for each action potential)

nerve of cats were still capable of synchronising to a modulation frequency of 1400 Hz (Joris and Yin [1992]), only a single neuron in the CN of horseshoe bats was capable of synchronising to a modulation frequency greater than 800 Hz (Vater [1982]), therefore already limiting the phase-locking capabilities of the following auditory nuclei. This can be seen in the IC of horseshoe bats, where phase-locking only occurred for modulation frequencies up to 400 Hz (Reimer [1987]) and was limited to modulation frequencies lower than 100 Hz at the level of the auditory cortex (Ostwald [1988]). In the auditory cortex of *Carollia perspicillata*, a close relative of *Phyllostomus discolor*, synchronised neuronal firing could only be detected for modulation frequencies lower than 100 Hz (Martin et al. [2017], García-Rosales et al. [2018]), which is a typical limit for the mammalian auditory cortex, where the prevalent frequency range of the best synchronisation is below 50 Hz (Eggermont [1998], Gaese and Ostwald [1995], Schreiner and Urbas [1988]).
Loss of synchronisation or adaptation (i.e. decrease in neuronal discharge amplitude) are attributed to neuronal inhibition (Grothe [1994]). In the case of the MSO in the mustached bat *Pteronotus parnellii*, inhibitory projections from the MNTB inhibited synchronized neuronal discharge in the MSO when presented with an amplitude modulated stimulus of sufficient modulation frequency, as the inhibitory response to one modulation cycle effectively blocked the excitatory discharge of the following modulation cycle (Grothe [1994]), leading to a high modulation frequency cut-off. The low frequency cut-off follows a different mechanism, with the steepness of the stimulus' rise time being responsible for the neuronal discharge (Grothe [1994]), which was demonstrated in neurons of the Ventral nucleus of the lateral lemniscus (VNLL) in *Pteronotus parnellii* (O'Neill et al. [1992]). However, a loss of synchronisation does not mean a cessation of neuronal response, a neuron can still respond in an unsynchronised, tonal fashion, therefore shifting from a temporal code (i.e. information is contained in the level of synchronisation) to a rate code (i.e. information is contained in the firing rate). This shift can usually be seen along the ascending auditory pathway, where a high modulation frequency might still evoke synchronised neuronal firing in the lower parts of the pathway, but it will only evoke tonal neuronal responses at the level of the auditory cortex.

Chapter 3 of this thesis focusses entirely on the dorsal fields of the auditory cortex and their neuronal response properties, whereas the fourth chapter focusses more on the response properties of the lower auditory tract, i.e. from the cochlear nerve to the

inferior colliculus (see Figure 1.4 for further reference). In both chapters amplitude modulated stimuli were used to evoke and quantify neuronal responses in the aforementioned brain regions. While chapters 3 and 4 cover brain regions clearly associated with auditory processing, the 5th chapter concentrates on the frontal auditory field of *Phyllostomus discolor*, which is supposedly involved with linking both auditory processing and sensory-motor integration of several nuclei innervated by it. While no artificial amplitude modulated stimuli were presented, a call library consisting of echolocation calls and both amplitude modulated and/or frequency modulated social calls was used to measure the response properties of the frontal auditory field.

To summarise, the main objective of this thesis was to investigate how amplitude modulated sounds are represented in the auditory system and whether differences in encoding could be found depending on the location within the auditory system and the level of maturity of the animal under investigation.

2 Methods

2.1 The experimental animal Phyllostomus discolor

The pale spear-nosed bat *Phyllostomus discolor* is a medium sized bat belonging to the family of the Phyllostomidae (i.e. leaf-nosed bats). It is a neotropical bat and can be found from southern Mexico to Paraguay and southern Brazil (Costa-Pinto [2020], Kwiecinski [2006]). As mentioned, it is medium in size with a mean wingspan of 41.6 cm and a body weight between 30-45 g, depending on age and sex (Kwiecinski [2006]). Being omnivorous, *Phyllostomus discolor* feeds on different wilds fruits, nectar, pollen and insects (Heithaus et al. [1975]), which makes it easy to keep in captivity when compared to purely insectivorous bats.
Furthermore, this bat species is very sociable with colony sizes ranging up to 400 individuals (Bradbury [1977]), with a rich vocal repertoire (Lattenkamp et al. [2019]) and the ability to modify its vocalisations (i.e. vocal learning; Esser and Schubert [1998], Lattenkamp et al. [2018] and Lattenkamp et al. [2020]), making it the ideal experimental animal to study mammalian vocal learning.
All animals used for the experiments originated from a breeding colony situated in the Department Biology II of the Ludwig-Maximilians University of Munich. The animals were kept under semi-natural conditions (reversed 12 day/12 h night cycle, 65%-70% relative humidity, 28 °C) with free access to food and water. The animals used in the cortical recording experiments where kept isolated from other individuals, while the juvenile bats were kept with their mothers. All the experiments complied with the principles of laboratory animal care and were conducted following the regulations of the current version of the German Law on Animal Protection (cortical recordings: approval ROB-55.2-2532.Vet_02-13-147, Regierung von Oberbayern; ABR recordings: approval ROB-55.2-2532.Vet_02-17-218, Regierung von Oberbayern).

2.2 Anaesthesia and surgery

The initial surgery and all following electrophysiological experiments were performed under general anesthesia using a subcutaneously injected mixture of medetomidine (Dorbene®, Zoetis, Berlin, Germany), midazolam (Dormicum®, Hoffmann-La Roche, Mannheim, Germany) and fentanyl (Fentadon®, Albrecht, Aulendorf, Germany) at a dosage of 0.4, 4.0 and 0.04 μg/g body weight, respectively. Anaesthesia was maintained for up to 5 hours through additional injections containing 67% of the initial dose every 90 minutes. After completion of the surgery or the experiments on each day, anaesthesia was antagonized using a mixture of atipamezole (Alzane®, Novartis, Nürnberg, Germany), flumazenil (Flumazenil, Hexal, Holzkirchen, Germany) and naloxone (Naloxon- ratiopharm®, Ratiopharm, Ulm, Germany), which was injected subcutaneously (2.5, 0.5 and 1.2 μg/g body weight, respectively). To alleviate postoperative pain, an analgesic (0.2 μg/g body weight; Meloxicam, Metacam, Boehringer-Ingelheim) was administered after the surgery for four postoperative days. The bats were treated with antibiotics (0.5 μg/g body weight; enrofloxacin, Baytril®, Bayer AG) for four postoperative days.
To perform the surgery to mount a head bar to the skull of *Phyllostomus discolor*, the

animal was placed into a custom built holder to keep its skull in a fixed position (the operating room had been pre-heated to roughly 35°C). The hair covering the skull was removed with a depilatory cream bought locally. The cream was applied and after 5-10 minutes the cream and the hair was removed from the skull. The skin was then cleaned thoroughly with sterile water and sterilised for the surgery using an iodine solution. An initial incision was made along the dorsal midline of the skull, starting at the level of the eyes and ending shortly before the base of the skull. The skin and further subcutaneous tissue was loosened from the skull, pushed to either side and affixed there using surgical sponges inserted between the skull and the tissue. The periosteum covering the skull was further anaesthetised by administering lidocaine solution and after a short incubation period the periosteum was scraped from the skull, revealing the underlying bone. This removal was necessary, as the dental cement (iBond®Total Etch, Kulzer Gmbh, Hanau, Germany) used later in this procedure requires bone material to form a strong bond. In the next step, the position where the head bar would be glued to the skull was treated with an etching gel containing phosphoric acid. This gel was applied for 20-30 seconds and was then removed with water and surgical sponges, its goal was to increase the surface by slightly dissolving the bone structure, hereby increasing the bonding area and strength of the dental cement. Then, a bonder was applied to the etched bone area and it was activated by 20-30 seconds of intense UV light. This bonder later formed the foundation of the head bar. In a final step, dental cement was applied generously to the bonder and the head bar inserted via micromanipulator. The dental cement was also hardened using UV light and after an initial check of the correct positioning of the head bar, the animal was removed from the custom built holder and transferred into the pre-heated (± 35°C) anechoic chamber. It was inserted into a custom built stereotactic setup (Schuller et al. [1986]), where its skull profile line was scanned in both rostro-caudal and medio-lateral direction. These two profile lines were then compared with the standardised brain profile of *Phyllostomus discolor* (A. Nixdorf, T. Fenzl, B. Schwellnus, unpublished data). This method generally allows for precise reconstruction of recording site and also enables the user to locate and target small brain regions, which would otherwise be difficult to find. Due to the standardised profile line of *Phyllostomus discolor*, one can align the individual animal to achieve the same head position (e.g. "norm position") for every animal used in the experiments, therefore positioning the brain at the same spot in a standardised coordinate system. To perform either a recording or a tracer injection, one would identify the coordinates of the target region and use a dental burr to drill a 500 μm wide hole into the skull. A small piece of tungsten wire was used to penetrate the three meninges, as particularly the dura mater can bend electrodes or break off the tips of glass micropipettes used in the tracing experiments.

2.3 Extracellular recordings from the cortex of Phyllostomus discolor

In both the 3rd and the 5th chapter I performed extracellular recordings from the auditory cortex and the frontal cortex. I recorded from the brain three times a week for

five hours each, for up to a total of eight weeks (including the week with surgery). The responses recorded from neurons under general anaesthesia reflect the behavioural experiments of *Phyllostomus discolor* well (Firzlaff et al. [2006]). All extracellular recordings in the brain were performed using parylene-coated tungsten electrodes (5 MΩ impedance, Alpha Omega GmbH, Ubstadt-Weiher, Germany). Electrode penetrations were made either perpendicularly to the brain surface or at a certain rostro-caudal and medio-lateral angle, depending on the targeted region. A piezo-driven microstepper was used to drive the recording electrode into the brain. A thin silver wire was inserted between the skull and the tissue at the edges of the surgical wound to serve as a reference electrode. The recording electrode signal was digitalised using an analogue to digital converter (headstage: RA16, Tucker-Davis Technologies (TDT), Alachua, USA and either RX5-2 (TDT) or Fireface 400, RME, Haimhausen, Germany; sampling rate: 25 kHz, band-pass filter: 400-3000 Hz) and either the software Brainware (TDT) or Audiospike (HörTech gGmbH, Oldenburg, Germany) depending on the recording hardware utilised. Additionally, the electrode signal was passed on to a speaker and was also visualised on screen for monitoring purposes. The recorded action potentials were threshold discriminated (i.e. only signals exceeding this threshold are considered to be correct neuronal discharges) and stored for later offline analysis using Matlab (Mathworks, Natick, MA, USA).

All acoustic stimuli were computer-generated (Matlab), digital–analogue converted (either RX6 (TDT) or Fireface 400, RME; sampling rate 195.312 kHz with the RX6 or 192 kHz with the FireFace 400), amplified (AX-396, Yamaha Music Foundation, Tokyo, Japan) and presented via free-field loudspeaker (R2904/700000, Scan-Speak, Videbæk, Denmark). The loudspeaker had been calibrated for linear frequency response between 1 kHz to 96 kHz using a $\frac{1}{4}$ inch ultrasonic reference microphone (Type 4939 microphone attached to a Type 2610 measuring amplifier, Brüel & Kjær, Nærum, Denmark). To search for acoustically driven neuronal activity, the electrode was driven into the brain tissue along the Z-Axis using a piezo-driven microstepper, while presenting either short pure-tones with user defined frequency and sound pressure level or typical social vocalisations used by *Phyllostomus discolor*. Acoustically driven neuronal activity was identified both visually and acoustically and whenever possible, only single units were analysed. However, due to experimental limits is was not always possible to isolate the neuronal responses from single neurons, therefore, some recordings will contain responses from up to three neurons. More detailed descriptions of the overall experiments can be found in the respective chapters. On the last experimental day, a neuronal tracer (8 nl injection volume, BDA3000, biotinylated dextran, 3000 MW molecular weight, 1 mg BDA/ 20 μl phosphate-buffer, Sigma-Aldrich, St. Louis, USA) was pressure injected (Nanoliter2010 injector, World Precision Instruments (WPI), Sarasota, USA) into the brain at one position in order to reconstruct the position of the various recording sites in a standardised coordinate system (A. Nixdorf, T. Fenzl, B. Schwellnus, unpublished data). Thus, the coordinates of the pressure injection were noted down for later use.

Figure 2.1: Roughly 10 day old juvenile *Phyllostomus discolor*, self provided image: Note the lack of fur on the skull and shoulder area. Authors fingers for size reference.

2.4 Recording of auditory brainstem potentials in juvenile Phyllostomus discolor

In the 4th chapter I recorded summed auditory brainstem responses (ABR) from juvenile bats. The recording scheme varied from the one described in the previous chapter with eight recordings spread out over three months. The same anaesthesia protocol was used for the juvenile bats, however, the total duration of the experiment was roughly 80 minutes, so no further injections apart from the initial one were required. Also, no depilatory cream was necessary, as the juvenile bats initially only had little fur (see Figure 2.1) and even when their fur had grown, the subdermal electrodes could be placed without hair removal.

The electrodes were fabricated from hypodermic needles (0.3 x 12 mm, Henry Schein Inc., Melville, USA), as these have the advantage of being sterile and very sharp, facilitating easy subdermal placement. The electrodes were bent into a U-shape and inserted through the skin, with the rest of the Luer system acting as a retainer on the skin surface, hereby preventing the electrode from slipping out, while a small crocodile clamp was attached to the tip of the electrode, connecting it with the amplifier. A basic schematic of electrode placement can be seen in Figure 2.2.

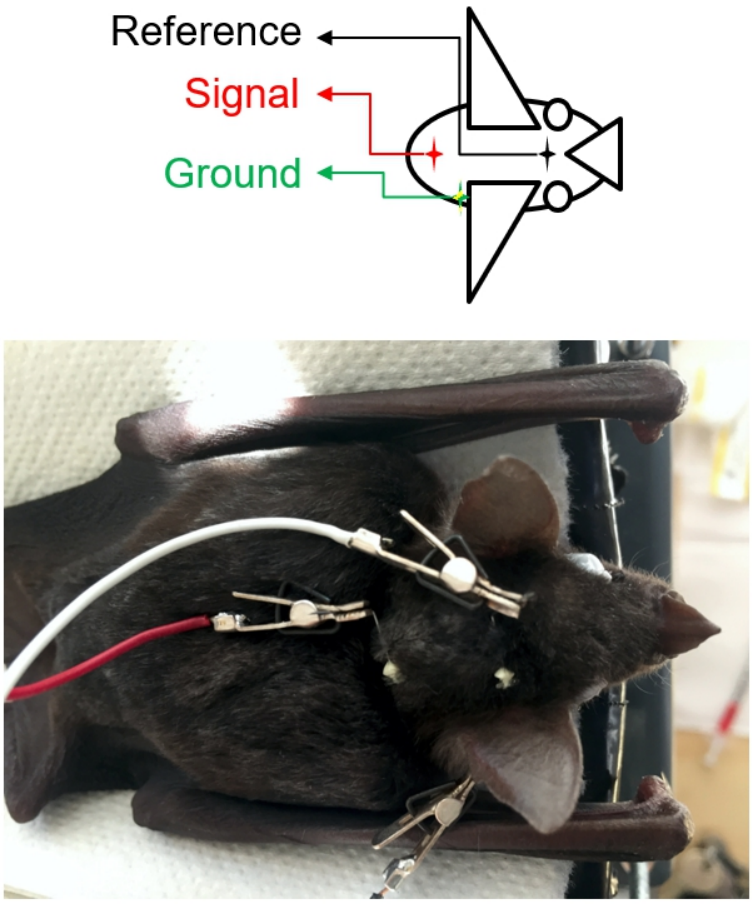

Figure 2.2: Basic schematic of the electrode placement on the head of the animal for ABR recordings (top) and actual placement on the animal (bottom): The bent electrodes have been pushed through the skin of the animal and are held in place by the rest of the Luer system acting as a retainer. Note differences in the cable colours between the schematic and the actual cable colours used in the setup. Schematic provided by the author and picture of the animal provided by Ella Z. Lattenkamp.

The bat was then placed on a styrofoam block within a custom-built, heavily sound-attenuated measuring setup, which was closely based on the setup used by Linnenschmidt and Wiegrebe [2019]. This setup was constructed from 4 cm thick veneer plywood and the insides of the setup were covered with 2 cm acoustic foam to attenuate any unwanted reflections of the stimuli. During the experiments, the setup was sealed with an acrylic glass lid and it was heated using two heating pads (110 x 77 mm, 12V, 12W, thermo Flächenheizungs GmbH, Rohrbach, Germany) connected to an external power supply (Voltcraft LPS 1153, Conrad Electronics SE, Hirschau, Germany). The temperature was controlled by an analogue thermometer tucked under the wings of the bat. Similar to the experiments described above, the sound stimuli used in this experiment (pure-tones and

amplitude modulated noise) were computer generated using Matlab, digital–analogue converted (Fireface 400, RME; sampling rate 192 kHz), amplified (AX-396, Yamaha Music Foundation) and presented via free-field loudspeaker (R2904/700000, Scan-Speak). The loudspeaker had been calibrated for linear frequency response between 1 kHz to 96 kHz using a $\frac{1}{4}$ inch ultrasonic reference microphone (Type 4939 microphone and Type 2610 measuring amplifier, Brüel & Kjær). The loudspeaker was roughly 8 cm from the bats ears with the animal placed on axis with it.

The amplifier for the electrode signals used in this set of experiments was a DAM80 (World Precision Instruments, Sarasota, USA), which was set to 20 dB amplification (0.1 Hz to 10 kHz bandpass filter). ABR measurements are susceptible to noise, as the signal picked up by the electrodes is in the range of μV, therefore the amplified signal was passed through a HumBug (Quest Scientific, North Vancouver, Canada) to remove any unwanted noise from the power mains without influencing the overall amplitude of the signal. The signals were then digitalised, further amplified (Fireface 400, RME; 192 kHz sampling rate, 10 dB amplification) and down-sampled for offline analysis (see Chapter 4).

2.5 Histology and coordinate reconstruction

After the injection of the neuronal tracer following the cortical recordings (see Chapter 3 & 5), the bats brain had to be harvested for further processing and for the reconstruction of the recording sites. Seeing as the bat was already anaesthetised for the injection, an intraperitoneal injection of pentobarbital (0.16 mg/g bodyweight, Narcoren®, Boehringer Ingelheim Vetmedica GmbH, Ingelheim am Rhein, Germany) was used to euthanise the animal. After breathing arrest, the visceral cavity was opened and the pericardium removed from around the heart. A hypodermic needle (0.45 x 25 mm, Sterican®G26, B. Braun Melsungen AG, Melsungen, Germany) was inserted into the left ventricle, which is easily identifiable due to its different colour when compared to the surrounding heart tissue. The right atrium was cut open using a pair of ophthalmic scissors and a peristaltic pump was activated, which pumped Heparin infused saline (1 ml per 100 ml of 0.9% saline, pH=7.4) into the heart and subsequently through the animal, rinsing out the blood. After 10 minutes, the perfusion solution was changed over to 4% paraformaldehyde (PFA, 4 g per 100 ml of phosphate buffer, pH=7.4) and the perfusion continued for another 30 minutes. Once the time had passed, the pump was shut off and the needle removed from the heart. A successful perfusion was easily identifiable due to the resulting stiffness of the fixed animal. The animal was then decapitated and the tissue attached to the skull was removed. A small tweezers was inserted into the base of the skull, paying great attention not to damage any tissue and the skull was cracked open, removing the bone bit by bit. Once the brain had been fully exposed, the meninges were cut and removed and a small pair of ophthalmic scissors was used to cut the nerves protruding from the base of the brain, thus releasing it from the skull. The removed brain was carefully cleaned and further fixed for one hour in 4% PFA solution. Subsequently, it was moved into 30% sucrose solution for cryoprotection

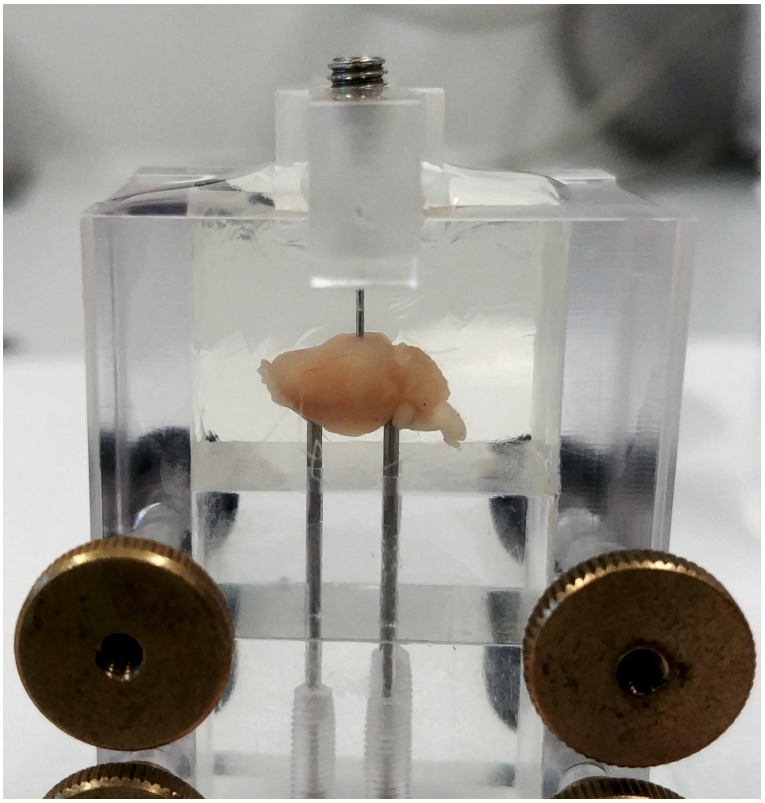

Figure 2.3: Self provided image on an embedded brain of *Phyllostomus discolor*: The brain was aligned with the embedding chamber using the three metal prongs visible and embedded in gelatine.

and kept refrigerated, until it was saturated (it no longer floats in the sucrose solution). Once this was achieved, the brain was transferred into the embedding chamber Schuller et al. [1986], aligned horizontally and vertically using three threaded metal prongs and then the chamber was filled with molten gelatine (see Figure 2.3). Once the gelatine had set, the chamber was dismantled and the embedded brain removed. It was further fixed in 4% PFA solution and soaked in 30% sucrose solution until it was saturated. In a final step, the brain was frozen using dry ice and sliced to 40 μm thickness using a sliding microtome (Microm HM440E, Thermo Fisher Scientific). The slices containing the tracer injection for reconstruction were stained using the ABC/DAB procedure (Avidin-Biotin Complex/ Diaminobenzidine). All slices were mounted, stained with neutral red and covered (DePeX mounting medium). The marking from the tracer injection was identified and the slice with the marking was compared to the corresponding slice according to the injections coordinates. Any deviation in the rostro-caudal position was noted, as this was the correction factor by which the rostro-caudal position of each recording had to be adjusted by to obtain the actual recording site in the brain.

2.6 Neuronal tracing utilising a dextran-linked fluorophore

The procedures for neuronal tracing were similar to the ones described above. Both the surgical procedure and the injection procedure were identical, however, a different neuronal tracer was used to trace the connectivity of the frontal auditory field of *Phyllostomus discolor*. Instead of BDA I injected (Nanoliter2010 injector, WPI) a dextran-linked fluorophore (18.2 nl of 10% Alexa Fluor 488, 10.000 MW, Thermo Fisher Scientific, Waltham, MA, USA) into the FAF. A fluorophore is a fluorescent chemical compound that can re-emit light upon light excitation, in the case of Alexa Fluor 488 blue light is used for excitation, with green light being re-emitted by the molecule. After the injection, the incubation period begins, while the neuronal tracer is absorbed by the neurons surrounding the injection site. Depending on the type of neuronal tracer, it is either transported to the cell body of the neuron (retrograde tracer) or it is transported away from the cell body and towards the axon terminal of the neuron (anterograde tracer). The tracer used to trace the connectivity of the frontal auditory field in *Phyllostomus discolor* shows both anterograde and retrograde tracing capabilities. The duration of the incubation period is dictated by the size of the molecule (larger molecules are transported slower) and by the chosen tracing distance, as connected areas close to the injection site will be labelled faster than further distant areas. After the incubation period had passed, the animals were euthanised and perfused (see above). Then, the animals were dissected and the brains cryoprotected in 30% sucrose solution. They were then embedded (Schuller et al. [1986]), sliced to 40 μm thickness using a sliding microtome (Microm HM440E, Thermo Fisher Scientific)and mounted (VECTASHIELD® HardSet^{TM} Antifade Mounting Medium H-1400). During all these procedures, the tissue should be protected from both artificial light and sunlight, as these will cause the fluorescence of the tracer to dimmish. The slides were then be digitised using a fluorescence microscope set to the excitation wavelength of the tracer utilised (10 times magnification, 20 layer Z-stack, Axio Scan.Z1, Carl Zeiss Microscopy GmbH, Jena, Germany). Successfully labelled fibres and neurons were identified manually by observation of the images and their position was determined by comparing the results to a brain atlas of *Phyllostomus discolor* (Radtke-Schuller et al., in prep.).

3 Processing of temporal sound features

The third chapter of this thesis covers how social communication calls, in particular, their temporal sound features, and artificial amplitude modulated sounds are encoded in the auditory cortex of *Phyllostomus discolor*. Bats are usually social animals which live together in large groups and they rely on a large repertoire of social vocalisations for interactions with conspecifics. These social vocalisations are often characterised by sinusoidally amplitude and frequency modulations, with an emphasis on the 100 to 130 Hz modulation frequency range. However, the mammalian brain is typically limited to modulation frequencies below 100 Hz, so my supervisor and I devised a set of experiments designed to investigate how neurons in the auditory cortex of *Phyllostomus discolor* process sinusoidally amplitude modulations. We chose to use a set of natural echolocation and social communication calls as well as artificial amplitude modulated pure-tones as stimuli. In total, I recorded 142 cortical units from a region in the auditory cortex in four bats and analysed the data offline. Firstly, I identified six different response classes to sinusoidally amplitude modulated pure-tones ranging from phase-locked bandpass type responses over high- and lowpass responses to no variation in response at all. Furthermore, I could show that neurons in the AC of *Phyllostomus discolor* are capable of synchronising their discharges to unusually high modulation frequencies with a best rate and temporal modulation transfer function of 130 Hz, which is exceedingly higher than the typical mammalian value of 50 Hz. Additionally, I could show that this high preferential modulation frequency matches the fast amplitude and frequency modulations of social vocalisations, especially the calls of *Phyllostomus discolor* typically associated with aggressive behaviour. I calculated a selectivity index d_{i}, showing that a subpopulation of neurons (with bandpass type temporal modulation transfer functions and phasic discharge patterns) had a strong preference for sinusoidally amplitude modulated aggression calls, therefore corroborating the likely predisposition, that parts of auditory cortex of *Phyllostomus discolor* are tuned to reliably encode fast amplitude modulations like the ones seen in the social communication calls. The individual contributions can be broken down as follow: Both my supervisor and I conceived and designed the research. I performed the experiments and we both analysed the data and interpreted the results. I prepared the figures and drafted the manuscript, which was edited and revised by both of us. My supervisor approved the final version of the manuscript, which was then published in the *Journal of Neurophysiology* (Hörpel and Firzlaff [2019]). The license for reproduction in this thesis has been attached (see Appendix C, Figure B.4 for further confirmation).

J Neurophysiol 121: 1501–1512, 2019.
First published February 20, 2019; doi:10.1152/jn.00748.2018.

RESEARCH ARTICLE | *Sensory Processing*

Processing of fast amplitude modulations in bat auditory cortex matches communication call-specific sound features

Stephen Gareth Hörpel and Uwe Firzlaff
Chair of Zoology, Department of Animal Sciences, Technical University of Munich, Freising, Germany

Submitted 2 November 2018; accepted in final form 15 February 2019

Hörpel SG, Firzlaff U. Processing of fast amplitude modulations in bat auditory cortex matches communication call-specific sound features. *J Neurophysiol* 121: 1501–1512, 2019. First published February 20, 2019; doi:10.1152/jn.00748.2018.—Bats use a large repertoire of calls for social communication. In the bat *Phyllostomus discolor*, social communication calls are often characterized by sinusoidal amplitude and frequency modulations with modulation frequencies in the range of 100–130 Hz. However, peaks in mammalian auditory cortical modulation transfer functions are typically limited to modulation frequencies below 100 Hz. We investigated the coding of sinusoidally amplitude modulated sounds in auditory cortical neurons in *P. discolor* by constructing rate and temporal modulation transfer functions. Neuronal responses to playbacks of various communication calls were additionally recorded and compared with the neurons' responses to sinusoidally amplitude-modulated sounds. Cortical neurons in the posterior dorsal field of the auditory cortex were tuned to unusually high modulation frequencies: rate modulation transfer functions often peaked around 130 Hz (median: 87 Hz), and the median of the highest modulation frequency that evoked significant phase-locking was also 130 Hz. Both values are much higher than reported from the auditory cortex of other mammals, with more than 51% of the units preferring modulation frequencies exceeding 100 Hz. Conspicuously, the fast modulations preferred by the neurons match the fast amplitude and frequency modulations of prosocial, and mostly of aggressive, communication calls in *P. discolor*. We suggest that the preference for fast amplitude modulations in the *P. discolor* dorsal auditory cortex serves to reliably encode the fast modulations seen in their communication calls.

NEW & NOTEWORTHY Neural processing of temporal sound features is crucial for the analysis of communication calls. In bats, these calls are often characterized by fast temporal envelope modulations. Because auditory cortex neurons typically encode only low modulation frequencies, it is unclear how species-specific vocalizations are cortically processed. We show that auditory cortex neurons in the bat *Phyllostomus discolor* encode fast temporal envelope modulations. This property improves response specificity to communication calls and thus might support species-specific communication.

amplitude modulation; auditory cortex; social communication; temporal processing

INTRODUCTION

The analysis of temporal sound features is one of the hallmarks of the auditory system of mammals and other vertebrates. Precise timing information about sound onset and envelope is essential for processing of interaural time differences for sound localization, but the analysis of temporal structure of sounds is also crucial for species-specific communication (Bohn et al. 2008). Temporal amplitude and frequency modulations are, among other sound features, important characteristics of human speech and animal communication sounds (Bohn et al. 2008; Gaucher et al. 2013; Nourski and Brugge 2011; Schwartz et al. 2007). Temporal processing in the auditory system has been intensively studied over the last decades for different stages of the ascending auditory pathway in different animal models (Joris et al. 2004; Langner 1992). Responses to sinusoidally amplitude-modulated (SAM) sounds can be quantified either in terms of a rate code or in terms of the synchronization of spikes to the modulator ("phase-locking"). It has been shown that the ability to encode temporal modulation in a phase-locked manner decreases from the auditory brain stem to the auditory cortex (AC). Neurons in the auditory nerve can follow the carrier up to around 10 kHz in owls (Köppl 1997) and up to 2 kHz in cats (Joris and Yin 1992). Yet, neurons in the inferior colliculus (IC) show phase-locking only up to 320 Hz in the rat (Rees and Møller 1987) and up to 500 Hz in Parnell's mustached bat (Burger and Pollak 1998). On the level of the AC, typically only modulation frequencies below 30 Hz in cats (Whitfield and Evans 1965) and guinea pigs (Creutzfeldt et al. 1980) and 35 Hz in macaques (Cohen et al. 2007) and marmosets (DiMattina and Wang 2006) are encoded with a phase-locked response. However, Hoglen et al. (2018) recently showed significant phase-locking in the AC of squirrel monkeys to modulation frequencies of up to 128 Hz. In comparison to the temporal modulation transfer functions (tMTF) responses in the AC, the rate modulation transfer functions (rMTF) responses usually extend to higher modulation frequencies. Yet, the majority of rate best modulation frequencies (rBMFs) in the AC of anesthetized animals are typically below 50 Hz (Eggermont 1998; Gaese and Ostwald 1995; Schreiner and Urbas 1988), although studies in awake animals have reported rBMFs exceeding this value (gerbils, Schulze and Langner 1997; squirrel monkeys, Bendor and Wang 2008; Bieser and Müller-Preuss 1996).

In bats, precise temporal processing is required to detect prey and avoid obstacles by echolocation. Numerous studies have revealed precise processing of echo delay and stimulus duration as the hallmark of the bat auditory system (Ehrlich et al. 1997; Greiter and Firzlaff 2017; Hagemann et al. 2010;

Address for reprint requests and other correspondence: S. G. Hörpel, Dept. of Animal Sciences, Technical University of Munich, Liesel-Beckmann-Str. 4, 85354 Freising, Germany (e-mail: stephen.hoerpel@tum.de).

Mittmann and Wenstrup 1995; Olsen and Suga 1991; O'Neill and Suga 1979; Sayegh et al. 2014). The neural structures in bats required for hearing are similar to those of other mammals and have simply been adapted to a more specialized role, i.e., echolocation (Covey 2005). Furthermore, neuronal responses to SAM and sinusoidally frequency-modulated stimuli in the bat auditory brain stem are not very different from those in other mammals (Covey et al. 1995; Grothe et al. 2001). This is astonishing, considering the rich vocal repertoire of these animals, which is often characterized by strong and fast temporal modulation or repetitive patterns of short sounds, especially in so-called distress and aggression calls (August 1979; Fenton et al. 1976; Gadziola et al. 2012; Hechavarría et al. 2016; Kanwal et al. 1994; Russ et al. 2004). In our animal model, the bat *Phyllostomus discolor*, the temporal amplitude modulation patterns of these calls are in the range of 100–130 Hz (Fig. 1*D*, *left* and *right*).

The representation of communication calls in the bat auditory system has been investigated in the AC (e.g., Esser et al. 1997; Washington and Kanwal 2008, 2012) and IC (Andoni et al. 2007; Andoni and Pollak 2011), as well as in the amygdala (Gadziola et al. 2012, 2016; Naumann and Kanwal 2011; Peterson and Wenstrup 2012). Neuronal responses were often influenced by the temporal modulation patterns and/or tempo-

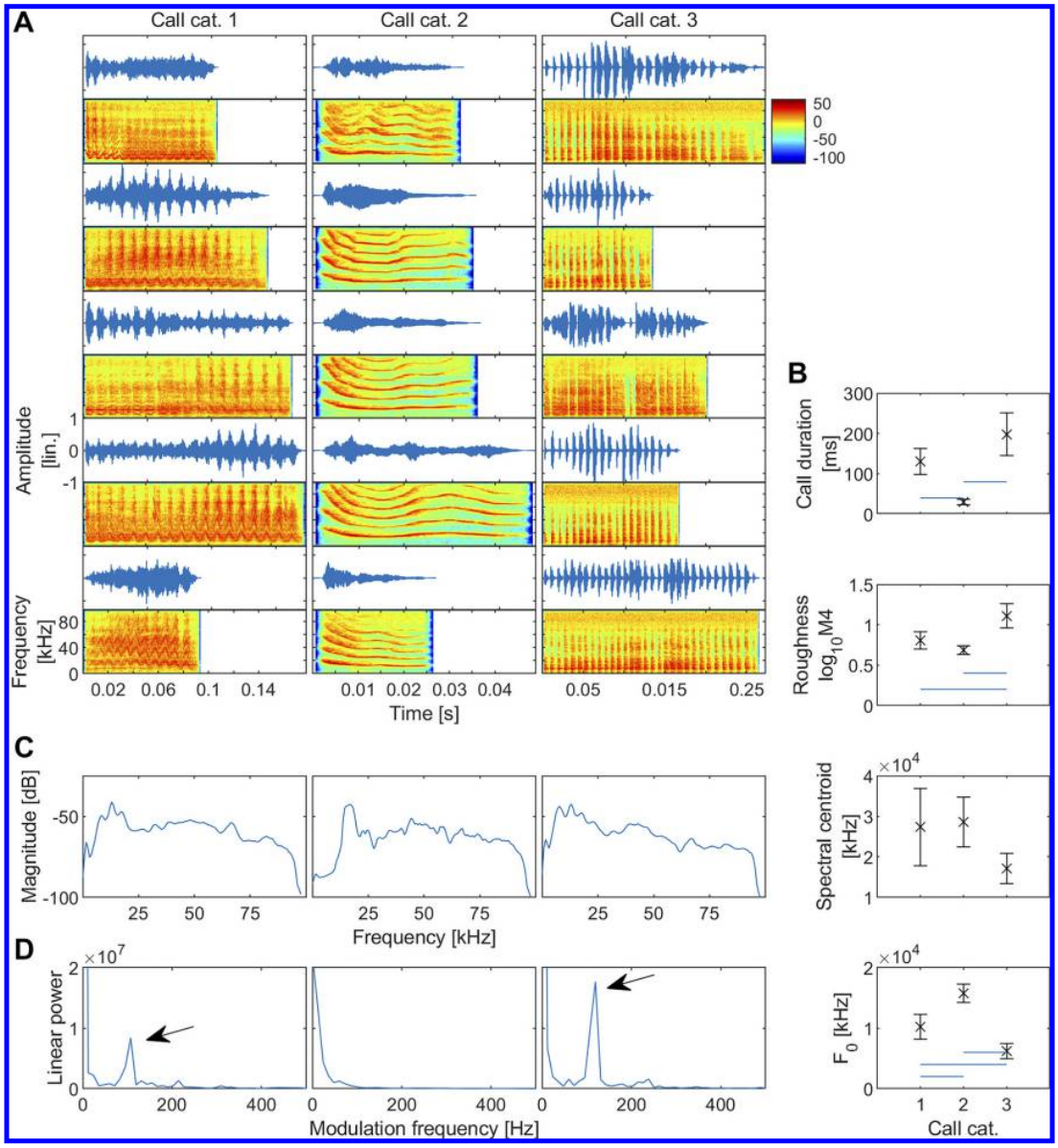

Fig. 1. Natural communication call categories of *Phyllostomus discolor* and their acoustic properties. *A*: waveforms and spectrograms of aggression calls (call *category 1* and call *category 3*) and appeasement/contact calls (call *category 2*) used as natural stimuli (cat., category). *B*: comparison of call duration, roughness ($\log_{10}$M4, where M4 = 4th moment of the envelope waveform), spectral centroid, and fundamental frequency (F_0) of the 3 call classes. Values are means (±SD). Blue lines indicate significant ($P < 0.05$, ANOVA) differences between call categories. *C*: frequency spectra of *category 1* (*left*), *category 2* (*middle*), and *category 3* (*right*) communication calls. *D*: amplitude modulation spectra of *category 1* (*left*), *category 2* (*middle*), and *category 3* (*right*) communication calls. Prominent peaks appear around 100–130 Hz in *category 1* and *category 3* (arrows) spectra. Note the lack of peak in call *category 2* spectrum.

ral order of syllable combinations. In the bat AC, communication calls were often encoded in areas that were also sensitive to a combination of echolocation calls and echoes separated by a certain delay and thus serving for target detection during echolocation (Esser et al. 1997; Kanwal and Ehret 2011; Kanwal and Rauschecker 2007). However, cortical neurons in bats could precisely encode the temporal envelope of SAM stimuli or naturalistic sequences of vocalizations up to frequencies around 20 Hz only (Jen et al. 1993; Martin et al. 2017). Recently, it was reported (García-Rosales et al. 2018a) that a subpopulation of units in the AC of *Carollia perspicillata* showed best synchronization to modulation frequencies of communication calls at roughly 60 Hz. Because temporal modulation patterns of behaviorally relevant communication calls were reflected in the response patterns of neurons in the primary AC of other mammals (Nagarajan et al. 2002; Wang et al. 1995), this raises the question how the fast temporal modulation found in bat communication sounds are represented in the AC.

We investigated the coding of temporal envelope modulation in neurons of the non-tonotopic dorsal fields of the AC of the bat *P. discolor*. By measuring rMTFs and tMTFs in response to SAM stimuli, we could show that a population of cortical neurons had an rBMF of around 130 Hz, whereas the temporal best modulation frequency (tBMF) peaked at 87 Hz, and had 50% cutoff frequencies up to 230 Hz. This ability to encode surprisingly fast temporal modulations might be an adaptation to the fast modulations found in certain types of species-specific communication calls and, so far, has not been reported for other bat species.

METHODS

Surgery

All the experiments complied with the principles of laboratory animal care and were conducted following the regulations of the current version of the German Law on Animal Protection (approval ROB-55.2-2532.Vet_02-13-147, Regierung von Oberbayern). The bats (*P. discolor*; 3 adult females, 1 adult male) originated from a breeding colony situated in the Department of Biology II of the Ludwig-Maximilian University of Munich. For experiments, animals were kept separated from other bats under seminatural conditions (12:12-h day-night cycle, 65–70% relative humidity, 28°C) with free access to food and water.

The surgical procedures are described in detail in a previous publication (Hoffmann et al. 2008) and will be mentioned only briefly. The bats were anesthetized using a combination of medetomidine (Dorbene; Zoetis), midazolam (Dormicum; Hoffmann-La Roche), and fentanyl (Fentadon; Albrecht) at dosages of 0.4, 4.0, and 0.04 μg/g body wt, respectively. Anesthesia was maintained through additional injections containing two-thirds of the initial dose every 1.5 h. The skin overlying the skull was opened along the midline, and the skull surface was freed from tissue. A small metal tube was then fixed to the skull using a microglass composite to fix the animal to a stereotaxic device. Details of the stereotaxic device and the procedure used to reconstruct the recording sites are described elsewhere (Schuller et al. 1986). In brief, the alignment of the animal's skull and the underlying brain within the stereotaxic coordinate system was measured by scanning the characteristic profile lines of the skull in the parasagittal and frontal planes. These profiles were then digitally fitted to a standardized skull profile in a standardized coordinate system.

To alleviate postoperative pain, an analgesic (0.2 μg/g body wt meloxicam; Metacam; Boehringer-Ingelheim) was administered after the surgery for 4 postoperative days. The anesthesia was antagonized with a mixture of atipamezole (Alzane; Novartis), flumazenil (Flumazenil; Hexal), and naloxone (Naloxon-ratiopharm; Ratiopharm), which was injected subcutaneously (2.5, 0.5, and 1.2 μg/g body wt, respectively). The bats were treated with antibiotics (0.5 μg/g body wt enrofloxacin; Baytril; Bayer) for 4 postoperative days.

Acoustic Stimulation

To measure the neuronal response properties to SAM sounds, the following procedure was used: a frequency-response curve of the neuron under test was established by presenting pure tone stimuli with a frequency range from 5 to 80 kHz (logarithmically spaced in ⅛ octave steps) and with sound pressure level (SPL) from 80 to 15 dB referenced to 20 μPa. The duration of each pure tone was 20 ms, and the stimuli were preceded by 50 ms of silence. The repetition rate was 2 Hz. The neuronal response was measured in a response window starting at stimulus onset and lasting 250 ms. The stimuli were each presented in random order and repeated 10 times. The data were plotted using the BrainWare analysis tools [Tucker-Davis Technologies (TDT), Gainesville, FL], and the characteristic frequency (CF; frequency at which a given neuron responds to the lowest sound intensity) and corresponding threshold SPL were identified. To create the SAM stimuli, a 400-ms (t) pure tone carrier (f_c) at the CF of the unit was modulated with 15 different modulation sinusoids (f_m) logarithmically spaced from 5 to 1,500 Hz, as shown in Fig. 2. The modulation depth (m) was 100% (*Eq. 1*; Joris et al. 2004).

$$\left[1 + m\sin\left(2\pi f_m t\right)\right]\sin\left(2\pi f_c t\right) \qquad (1)$$

The modulation frequencies were each randomly presented 20 times at 10–15 dB above the CF SPL. Each stimulus was preceded by a 50-ms silent period. Repetition rate was ~1.1 Hz.

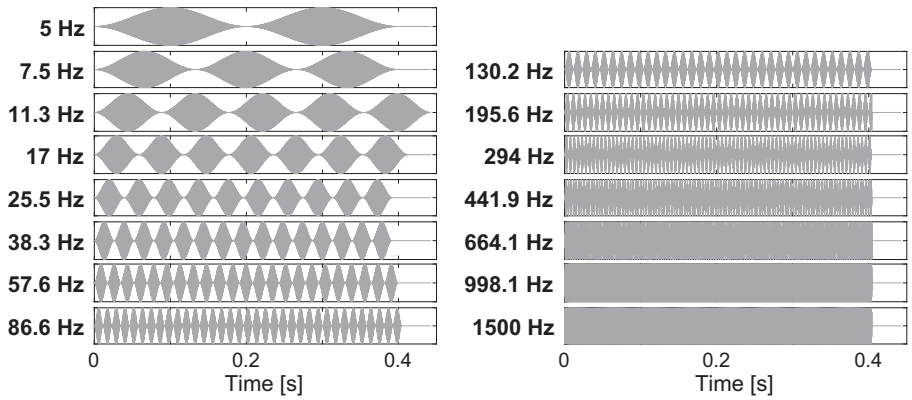

Fig. 2. Sinusoidally amplitude-modulated (SAM) stimuli. Waveforms of the SAM stimuli are shown (carrier frequency, 20 kHz) at modulation frequencies of 5–1,500 Hz in 15 logarithmically spaced steps (modulation depth 100%). Note small variations in stimulus length to permit full modulation cycle.

Communication Calls

To test whether neuronal responses to SAM sounds could be related to responses of communication sounds, we presented 15 *P. discolor* communication sounds (Fig. 1*A*). The sounds were selected from a library of 269 calls recorded in the *P. discolor* colony in the Department of Biology II of the Ludwig-Maximilian University of Munich.

The 15 selected communication sounds were grouped into three categories on the basis of differences in several acoustic parameters such as duration, fundamental frequency F_0, roughness (Fig. 1*B*), and occurrence of amplitude and frequency modulations in the call envelope and spectrogram, respectively (Fig. 1*D*). *Category 1* calls consisted of long amplitude and frequency-modulated calls with relatively low fundamental frequency of ~13 kHz (see Fig. 1*C*, *left*), whereas the amplitude modulation spectrum showed a peak around 100–130 Hz (Fig. 1*D*, *left*). *Category 2* calls showed no amplitude modulations, were shorter in duration, had a higher fundamental frequency of ~17 kHz and a strongly harmonic spectrum, and displayed shallow frequency modulations (Fig. 1*D*, *middle*). *Category 3* calls consisted of a varying number of short broadband sound elements separated by ~8 ms and thus giving rise to strong amplitude modulations. In contrast to *category 1* calls, *category 3* calls showed no frequency modulations and had a significantly lower fundamental frequency of ~7.5 kHz. Similarly to *category 1* calls, *category 3* calls also displayed a peak amplitude modulation frequency of 100–130 Hz (Fig. 1*D*, *right*). Unlike the fundamental frequencies of the respective call categories, the spectral centroid did not differ significantly between the categories. The roughness values ($\log_{10}$M4; Fig. 1*B*) are given as the base 10 logarithm of the envelope roughness, which was quantified in terms of the fourth moment (M4; the envelope waveform raised to the power of 4 divided by the squared waveform raised to the power of 2; Firzlaff et al. 2006; Hartmann and Pumplin 1988). The envelope roughness of *category 3* calls is significantly higher than that of the other two call categories. The calls were randomly presented with 20 repetitions (repetition rate ~0.7 Hz) at a level of ~15–20 dB above CF threshold.

Because a comprehensive call repertoire of social calls has not been published for *P. discolor*, clear assertions about the behavioral context of the calls recorded in the present study are not possible. However, calls of *category 1* and *category 3* resembled typical aggression and distress calls as described for other bat species (Gadziola et al. 2012; Hechavarría et al. 2016). *Category 2* calls resembled maternal contact calls or appeasement calls of *P. discolor* (Esser and Schubert 1998) and other bat species (Gadziola et al. 2012).

Electrophysiological Recordings

After initial surgery, experiments were conducted in a sound-attenuated and heated (~35°C) chamber. Extracellular recordings were made with parylene-coated tungsten microelectrodes (5-MΩ impedance; Alpha Omega) in anesthetized bats (see *Surgery*). Note that the responses recorded from cortical units under this anesthesia regime reflect the behavioral performance of *P. discolor* well (Firzlaff et al. 2006). Recording sessions took place 3 days per week for up to 8 weeks (with at least 1 day off between consecutive experiments) and could last up to 5 h per day. Dorsoventral (DV) electrode penetrations in the AC were run obliquely to the brain surface with different mediolateral (ML) and rostrocaudal (RC) angles. The electrode signal was recorded using an analog-to-digital converter (TDT RA16 and RX5; sampling rate 25 kHz, bandpass filter 400-3,000 Hz) and BrainWare (TDT). The action potentials were threshold discriminated and saved for later offline analysis. We tried to isolate single neurons whenever possible; however, it was not always possible to clearly discriminate the activity of a single neuron. Therefore, the term "unit" is used in this article to describe the collective activity of one to three neurons recorded at a recoding site. A comparison of neuronal responses from single units and multiple units revealed no differences.

To search for acoustically driven neural activity, either a natural echolocation call (downward modulated, multiharmonic, main energy between 40 and 90 kHz, duration ~1.2 ms) or an aggression call (frequency and amplitude modulated, main energy between 0 and 20 kHz, duration ~170 ms) was presented periodically. During the search, the SPLs were varied while neural activity was monitored visually and acoustically. All acoustic stimuli were computer generated (MATLAB; The MathWorks, Natick, MA), digital-to-analog converted (TDT RX6; sampling rate 195,312 Hz), attenuated (TDT PA5), amplified (Yamaha AX-396), and presented via a free-field loudspeaker (Scan-Speak R2904-7000-00), which had been calibrated for linear frequency response between 1 and 95 kHz. The loudspeaker was positioned contralaterally ~30° off the head midline at a distance of ~20 cm, and the search stimuli were presented with a repetition rate of 2 Hz. After the experiments were completed, a neuronal marker (BDA 3000; Sigma-Aldrich; 1 mg/20 μl phosphate buffer) was pressure-injected (Nanoliter 2010 injector; World Precision Instruments) into the brains to reconstruct the position of the recording sites in standardized stereotaxic coordinates (Schuller et al. 1986) of a brain atlas of *P. discolor* (Nixdorf A, Fenzl T, Schwellnus B, unpublished observations). The animals were then euthanized by an intraperitoneally applied lethal dose of pentobarbital sodium (0.16 mg/g body wt) and subsequently perfused transcardially with 4% paraformaldehyde.

Data Analysis

Spike responses from the 15 SAM and 15 natural stimuli were displayed as peristimulus time histograms (PSTHs; bin width 1 ms) and raster plots. Few units showed spontaneous activity and, when present, the spontaneous spike rate was very low (<10 spikes/s). For the natural stimuli, the mean spike rates of the neuronal responses to aggression (call *categories 1* and *3*, R_{agg}) and appeasement/contact calls (call *category 2*, R_{cont}) were calculated over a 400-ms response window, starting at the stimulus presentation. By using *Eq. 2* (Schnupp et al. 2006; Wang et al. 1995; Wang and Kadia 2001), the "selectivity index" d_i of each unit was calculated.

$$d_i = \frac{R_{agg} - R_{cont}}{R_{agg} + R_{cont}} \quad (2)$$

The d_i ranges from +1 to −1, indicating a neuron responding only to the aggression call (+1) or only to the contact call (−1), with a 50% difference between R_{agg} and R_{cont}, resulting in a d_i value of ±0.3.

In the case of SAM stimuli, rMTFs were constructed by plotting the median response rate (for 20 repetitions) calculated in a fixed PSTH window (from 50 to 450 ms, 1-ms binning) over modulation frequency. Because many units responded to the onset of a SAM stimulus with a strong phasic response, onset responses were eliminated for the construction of temporal modulation transfer functions (tMTFs) as suggested by Heil et al. (1995). To do so, the response window was adjusted to remove the response to the first modulation cycle for each modulation frequency. The ability of the units to synchronize spikes to the modulation frequency of SAM stimuli was measured using the vector-strength (VS) analysis in *Eq. 3* (Goldberg and Brown 1969; Martin et al. 2017).

$$VS = \frac{\sqrt{(\sum x_i)^2 + (\sum y_i)^2}}{n} \quad (3)$$

The VS values ranged from 0 (homogenous spike distribution across stimulus period) to 1 (perfect synchronization, all spikes occurring at same stimulus phase). Rayleigh's test (Buunen and Rhode 1978) with $P \leq 0.01$ was used to test the significance of the vector strength. Nonsignificant responses were set to 0. To finally yield the tMTF, the VS was plotted over modulation frequency. In rare cases ($n = 3$; ~2%), phase-locking occurred to every second modulation cycle for higher modulation frequencies. These units were omitted from tMTF

calculations. rMTFs were classified as bandpass, high pass, low pass, or unspecific. Bandpass rMTFs were characterized by a decrease of the spike rate of at least 50% on both sides of the maximum. High-pass and low-pass rMTFs had a decrease of spike rate of at least 50% on only one side (the low or the high modulation frequency side, respectively), but not on the other side. Unspecific rMTFs lacked a 50% decrease on either side of the maximum. To quantify the 50% cutoff values of rMTFs, polynomials were fitted to the flanks of the functions and the 50% point between the highest and lowest rate was determined on each polynomial. tMTFs were classified accordingly.

To see if the envelope modulation of *P. discolor* communication calls is reflected in the temporal spike pattern of cortical units, the temporal response properties to aggression and appeasement/contact calls of *P. discolor* were analyzed by computing the PSTH autocorrelation (PSTH 1-ms binning) and subsequently extracting spectral information (Wang et al. 1995). The call envelopes were extracted via Hilbert transformation and were smoothed with a second-degree Butterworth filter. Following this step, we compared frequency components of both the call envelope spectrum and the PSTH autocorrelation spectrum around 100–130 Hz using a multitaper method [MATLAB *pmtm* function; confidence level 0.95, time-halfbandwidth product (*nw*) 4, sample rate 192 kHz, fast Fourier transform size determined by length of the signal]. If repetitive firing of the units occurred following the temporal envelope of the aggression calls, a significant peak could be detected in this frequency range.

RESULTS

In total, we recorded from 142 units from both hemispheres of the AC of *P. discolor* [4 adult animals: 3 females (102 units) and 1 male (40 units)]. Recordings were derived mainly from cortical layers III and IV. As shown in Fig. 3, the majority of the units recorded were located in the anterior dorsal (ADF) and posterior dorsal fields (PDF; Hoffmann et al. 2008). The CFs of the recorded units overlapped with the fundamental frequencies of the vocalizations with a median CF of 20 kHz (mean 32.9 kHz) and with the maximum of the CF distribution at 18 kHz. As expected from previous studies (Hoffmann et al. 2008), there was no correlation between the RC position and the CF of the units in the dorsal AC.

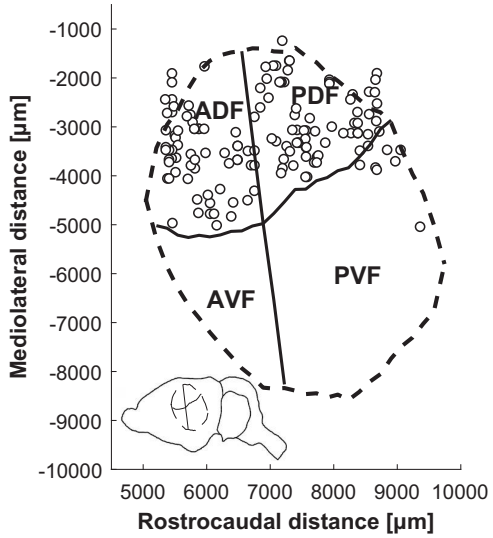

Fig. 3. Recording sites and subfields in the auditory cortex (AC) of *Phyllostomus discolor*. Shown are projections of recording sites (circles) on an unrolled and flattened cortical surface with schematic AC subfields: anterior dorsal field (ADF), posterior dorsal field (PDF), anterior ventral field (AVF), and posterior ventral field (PVF). *Inset* shows overall position of the AC in the brain of *P. discolor*.

Neuronal Response Classes to SAM Stimuli in the Dorsal AC

Neuronal responses to SAM stimuli were assigned to six different classes, based on the type of the rMTF (bandpass, high pass, low pass, all pass) and the temporal response pattern (on response, tonic response, phase-locked response).

Class I units ($n = 38$; Fig. 4) had a bandpass rMTF. The temporal response pattern was characterized by a phasic on response followed by a prolonged response component that showed significant phase-locking to a limited range of modulation frequencies.

Class II units ($n = 33$; Fig. 4) also had a bandpass rMTF, but the temporal response pattern lacked the onset response and phase-locking behavior. Instead, responses consisted of a tonic component.

Class III units ($n = 22$; Fig. 4) were not selective for certain modulation frequencies but responded equally to all SAM stimuli (all pass). Temporal response patterns were tonic without onset response and phase-locking.

Class IV units displayed high-pass rMTFs ($n = 25$; Fig. 4). These units showed either pure onset responses, an additional tonic response component or displayed a tonic response pattern only.

A tonic response pattern and a low-pass rMTF were found in *class V* units ($n = 4$; Fig. 4). Units in *classes IV* and *V* did not show phase-locking to SAM stimuli.

Finally, a number of units ($n = 20$; not shown) displayed rMTFs and/or temporal response patterns that were not unequivocally classifiable by our criteria. These units were labeled *class VI* and excluded from any further calculations.

The population of bandpass units (*class I* and *class II*) recorded had a median best rate response at 86.6 Hz [interquartile range (IQR) = 91.8 Hz] with a peak at 130-Hz modulation frequency (Fig. 5*A*). The median 50% lower cutoff frequency was 23 Hz, and the median 50% upper cutoff frequency was 241 Hz for the rate response. In detail, *class I* bandpass units had a median best rate response of 86.6 Hz (IQR = 91.8 Hz), whereas *class II* bandpass units reached a median best rate response of 130.2 Hz (IQR = 93.7 Hz).

The calculation of a median rate response in units with an onset response and/or high-pass rMTFs is futile, because it would highly depend on the range of modulation frequency tested. Therefore, we only show the lower 50% cutoff value for *class IV*: 24 Hz (IQR = 33.3 Hz). The low-pass *Class V* units had a median best rate response of 7.5 Hz (IQR = 40.8 Hz).

Furthermore, of the 122 units included in the calculations, 35 units (i.e., *class I*, 28.7%) showed significant phase-locking according to the VS analysis. The median highest frequency that evoked phase-locking was 130.2 Hz (Fig. 5*B*; IQR = 65.5 Hz), with the median best phase-locking frequency being 25.5 Hz (IQR = 44.9 Hz). The median 50% upper cutoff frequency for phase-locking was 162.9 Hz (IQR = 81.9 Hz).

Neuronal Responses to Communication Calls

Call selectivity. The selectivity index d_i quantifies the selectivity of a unit for either aggressive calls (*category 1* and

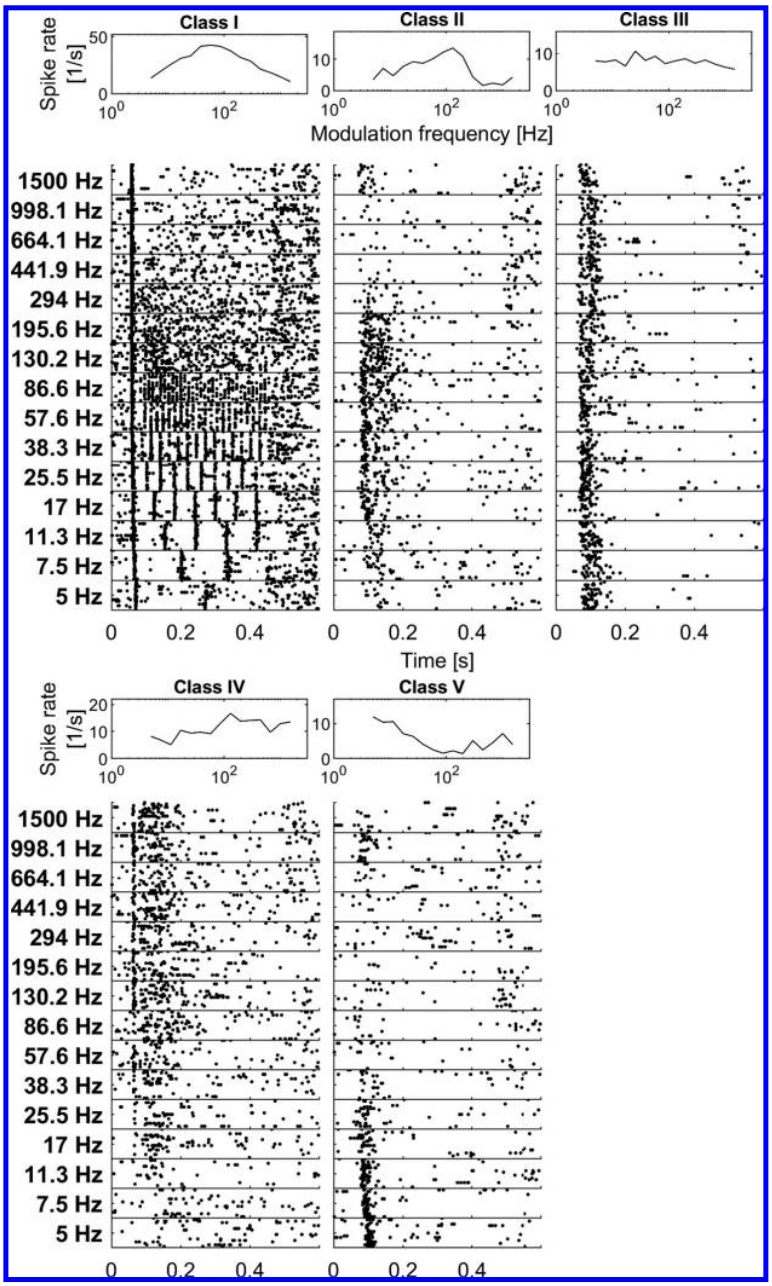

Fig. 4. Response classes of cortical units. Representative examples are rate modulation transfer functions (rMTFs) and raster plots of the 5 different response classes. *Class I* and *class II* units have bandpass rMTFs with phasic onset responses and significant phase-locking to a limited range of modulation frequencies (*class I*) or tonic responses lacking the onset response and phase-locking behavior (*class II*). *Class III* units have tonic, nonselective, all-responsive units lacking onsets and phase-locking. *Class IV* units have high-pass rMTFs. *Class V* units have low-pass rMTFs.

category 3) or contact calls (*category 2*). A total of 61 units (50%) had a strong preference for the aggression calls ($d_i \geq 0.3$). Only 4 units (3.3%) had a negative d_i value and thus showed preference toward the contact/appeasement calls, whereas 57 units (46.7%) showed no selectivity or only a small preference toward the aggression calls ($0 \leq d_i < 0.3$). The mean d_i value of all recorded units was 0.3153 ± 0.2055 (median $d_i = 0.3011$).

Call selectivity of different SAM response classes. To see if the units' call-type preferences are related to the response classes for SAM stimuli, we plotted their selectivity indexes against their corresponding response classes, which is depicted in a heat map (Fig. 6). For simplification, the negative d_i values were grouped with all the other values <0.1 and their respective d_i values were set to 0. Of the 61 units with a selectivity index exceeding the median d_i value of 0.3011, 35 units ($>57\%$) responded in a bandpass manner, and the phase-locked bandpass units in particular exhibited higher than average selectivity. In other words, if units showed a high degree of call selectivity, they most probably had bandpass rMTFs.

Furthermore, we checked for an existing correlation between the best rMTF frequency and the selectivity index d_i. In Fig. 7*A*, the best rMTF frequencies of *class I* (*left*) and *class II* (*right*) band pass units were plotted against their respective d_i values. It can be seen that *class I* units with higher best rMTF frequencies also show increased selectivity toward aggression calls (Pearson correlation coefficient $r = 0.69$, $P < 0.00001$). *Class II* units also show an increased selectivity toward these

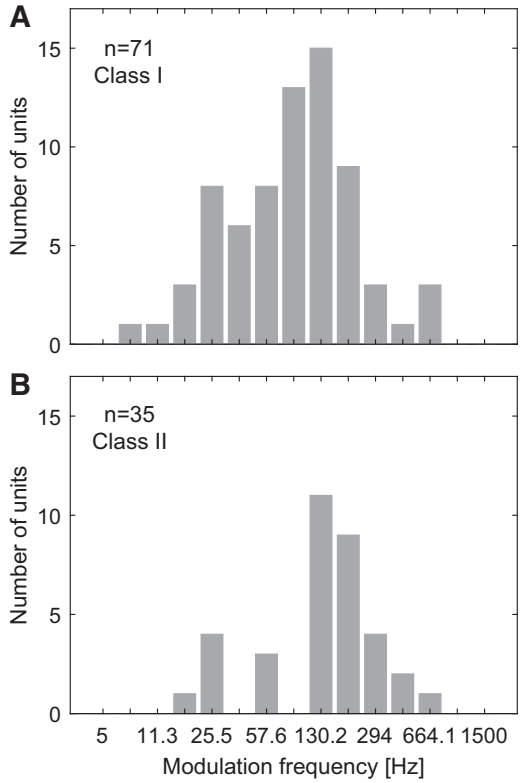

Fig. 5. Distribution of best rate modulation transfer function (rMTF) and highest temporal modulation transfer function (tMTF) bandpass units. *A*: histogram of the best modulation frequencies (BMF) of the rMTF of the 71 *class I* and *class II* bandpass units. The median best rate response is at 86.6 Hz with a maximum of the distribution at 130-Hz modulation frequency. *B*: histogram of the highest phase-locking frequency of the 35 *class I* bandpass units (3 units were omitted because they phase-locked to every 2nd modulation cycle for higher modulation frequencies). The median highest phase-locked response and the maximum of the distribution are at 130-Hz modulation frequency.

calls; however, in this case, the correlation between the best rMTF frequencies of the units and their selectivity is weaker ($r = 0.41$, $P = 0.0166$).

Cortical distribution of bandpass rMTFs. Additionally, we also investigated the relationship between the different neuronal classes and their corresponding position in the AC of *P. discolor*. In Fig. 7*B*, the RC and DV distances of *class I* (*left*), *class II* (*right*), and *class III–V* units (*left and right*) can be seen. In both plots of Fig. 7*B*, there is a conspicuous accumulation of bandpass-type units in the more caudal and dorsal parts of the AC, which is highly significant (2-sample *t*-test, $P < 0.001$; Fig. 7*C*). This dorsocaudal region corresponds roughly to the PDF of the AC of *P. discolor* (Hoffmann et al. 2008; see also Fig. 3 for outlines of cortical fields).

Call selectivity and temporal spike pattern. Finally, we analyzed if envelope modulation of *P. discolor* communication calls is reflected in the temporal spike pattern of cortical units. In Fig. 8*A*, one can see the waveform of a typical aggression call (call *category 3*) and its corresponding envelope (Fig. 8*B*). The response of a cortical unit to this specific call is depicted in Fig. 8*C*, and one can see that the neural responses phase-lock to the envelope of the communication call. By comparing the spectrum of the autocorrelation of the units' response PSTH (Fig. 8*D*) with the envelope modulation spectra (Fig. 8*E*), this becomes even clearer, because both spectra show distinct peaks between 100 and 130 Hz. In other words, several units locked to the envelope precisely and thereby encoded its modulation frequency. A total of 18 units (14.8%) showed peaks in the PSTH autocorrelation spectra as a response either to *category 1* or *3* calls or to calls from both categories. In detail, four units (3.3%) showed peaks in the PSTH autocorrelation spectra as a response to *category 1* calls and one unit (0.8%) as a response to *category 2* calls, whereas all units (18 units, 14.8%) showed peaks in the PSTH autocorrelation spectra as a response to *category 3* calls. Only a single unit showed responses to all three call categories. The median selectivity index d_i values of units preferring *category 1* or *category 3* calls are noticeably higher than the median d_i value of all units [0.3794 (*category 1*) or 0.3763 (*category 2*) vs. 0.3011]. Furthermore, 16 of the 18 units belonged to the group of *class I* bandpass units. In summary, units that phase-locked to the call envelope could better differentiate between aggressive and nonaggressive communication calls.

DISCUSSION

The present study investigated coding of temporal sound features in cortical units of the bat *P. discolor*. Responses to SAM sounds revealed the ability of a population of units to encode high modulation frequencies (100–130 Hz) in their firing rate but also as temporal code in phase-locked spike patterns. These units often preferably responded to communications calls used in an aggressive context, which are characterized by temporal envelope modulations around 130 Hz. In the following we compare our findings in *P. discolor* with results on temporal processing in other bats and other mammals, discuss possible neuronal mechanisms in *P. discolor* that might lead to the observed ability to encode fast temporal modulations of sound envelope, and depict possible functional

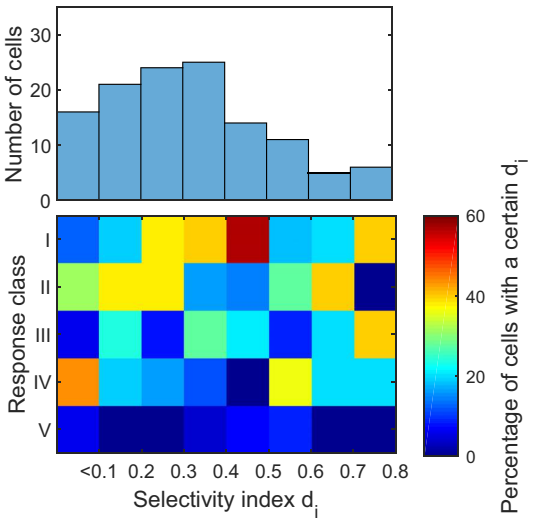

Fig. 6. Call class selectivity of sinusoidally amplitude-modulated (SAM) stimuli response classes. Heat map (*bottom*) shows the units' selectivity index d_i plotted against the 5 response classes with histogram (*top*) shown to visualize the distribution of the units (mean d_i of the units = 0.3153). The color bar indicates the percentage of units within a certain d_i range; the majority of the units are *class I*, *II*, and *III* types.

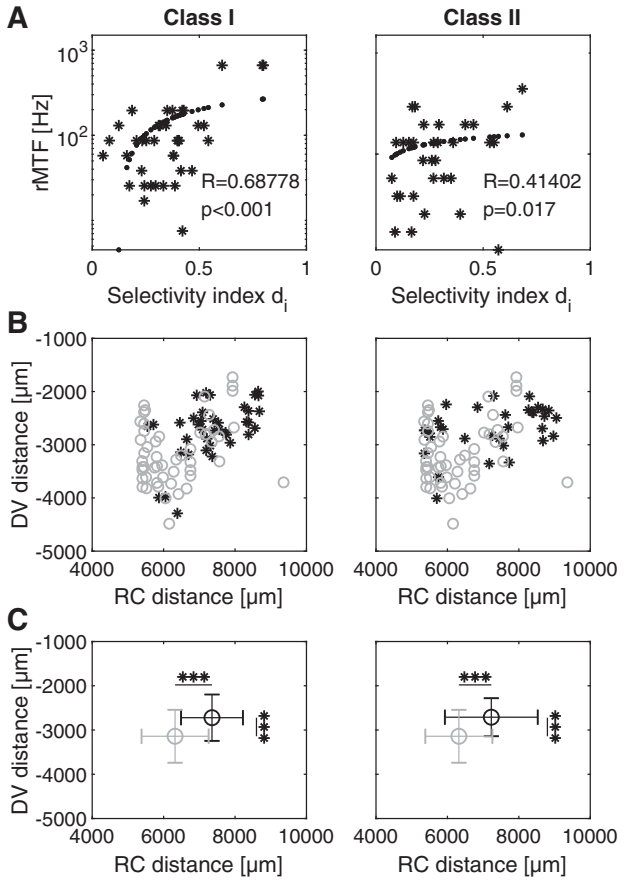

Fig. 7. Correlation of selectivity index and best rate modulation transfer function (rMTF) of *class I* and *class II* bandpass units and their spatial position in the auditory cortex (AC). *A*: correlation of selectivity index d_i plotted against the best rMTF of *class I* (*left*) and *class II* (*right*) bandpass units with regression curve indicated as a dotted line. *B*: rostrocaudal (RC) distance plotted against dorsoventral (DV) distance for *class I* (*left*; asterisks) and *class II* (*right*; black asterisks) compared with *class III–V* units (*left* and *right*; gray circles). *C*: mean RC distance plotted against mean DV distance with added standard deviations for *class I* (*left*, black error bars) and *class II* (*right*; black error bars) compared with *class III–V* units (*left* and *right*; gray error bars). The accumulation of the *class I* and *class II* units in the more caudal parts of the AC (mainly the posterior dorsal field) is highly significant (***$P < 0.001$, 2-way *t*-test).

implications of our findings for neural processing of vocal communication.

Temporal Processing in the AC of Bats and 0

In most studies, the range of rBMFs in the AC of mammals is limited to modulation frequencies below 50 Hz (Joris et al. 2004; Martin et al. 2017; Schreiner and Urbas 1988), although exceptions are possible (Schulze and Langner 1997). Phase-locked responses are typically also observed up to this range (Creutzfeldt et al. 1980; Whitfield and Evans 1965). So far, results from the AC of bats did not differ from findings from other mammals: in most (~89%) cortical units of *C. perspicillata*, a species closely related to *P. discolor*, significant phase-locking to the sound envelope was observed only below 23 Hz (García-Rosales et al. 2018b), although it was recently reported for the same species that 25% of units in the AC showed best synchronization to modulation frequencies of communication calls at roughly 60 Hz (García-Rosales et al. 2018a). In *Myotis lucifugus*, most units could not exceed phase-locking frequencies of 30 Hz (Condon et al. 1997). In the big brown bat *Eptesicus fuscus*, units in the AC could only follow pulse trains up to 10-Hz repetition frequency (Jen et al. 1993). These findings are somewhat surprising because for the bat bio-sonar systems, high temporal resolution is crucial to the precise detection of obstacles and prey. Indeed, units in the so-called chronotopic map of bats are sharply tuned to best delays between emitted echolocation calls and reflected echoes as short as 1 ms (Bartenstein et al. 2014; Hechavarría et al. 2013; O'Neill and Suga 1979).

Martin et al. (2017) investigated SAM coding in the primary AC of *C. perspicillata*. In contrast, our present study in *P. discolor* investigated units in the nonprimary dorsal fields (Hoffmann et al. 2008) of the AC. The chronotopic delay map in *P. discolor* is located in the PDF (Greiter and Firzlaff 2017), and most units with bandpass rMTFs with peaks around 130 Hz and high phase-locking abilities were located in this field, too (see Fig. 3 and Fig. 7, *B* and *C*). The vocal communication repertoires of *C. perspicillata* and *P. discolor* are quite similar (Hechavarría et al. 2016; compare Fig. 1), and both bats are

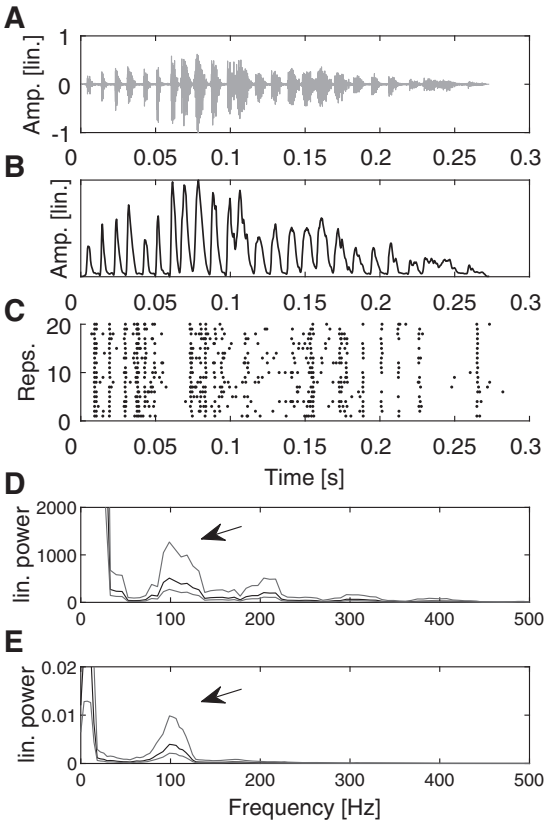

Fig. 8. Encoding of natural call envelope modulation frequency. *A*: temporal waveform of a *P Phyllostomus discolor* aggression call (spectrum from Fig. 1*A*, call *category 3*, 1st call). *B*: temporal envelope of the aggression call shown in *A*. *C*: raster plot of the corresponding neuronal response to the call shown in *A*. *D*: modulation spectrum of the peristimulus time histogram autocorrelation of the neuronal response shown in *C*. Gray lines are 0.95 confidence level borders. *E*: modulation spectrum of the call envelope shown in *B*. Gray lines are 0.95 confidence level borders. Both spectra (*D* and *E*) show distinct peaks between 100 and 130 Hz (arrows).

phylogenetically closely related and share many of their ecological preferences. Therefore, the profound differences in the responses to SAM sounds might be attributed to differences in the neural circuitry of the primary and nonprimary dorsal fields. However, one must be aware that coding of SAM sounds and coding of call-echo delay are thought to be based on different neuronal mechanisms.

Neuronal Mechanisms of Temporal Envelope Coding

As shown in RESULTS, we found two types of units with a bandpass response pattern caused by different mechanisms. Generally, a neuron with a phase-locked response will not respond to modulation frequencies exceeding its upper cutoff limit, thereby creating a typical bandpass modulation transfer function (see Fig. 4, *class I*). Additionally, units with pure rate responses can also show this characteristic, decreasing their spike rate/count after leaving their preferred frequency range (see Fig. 4, *class II*).

Rate responses of units in the cochlear nucleus are typically not tuned to certain modulation frequencies, but modulation frequency is encoded as a temporal code (Rhode and Greenberg 1994). On later stages of the ascending auditory pathway, rMTFs become generally more diverse and are created by multiple neuronal interactions (e.g., Heil et al. 1995; Krishna and Semple 2000). Synchronized excitatory inputs have been discussed as a mechanism for this at the level of the IC (Hewitt and Meddis 1994; Krishna and Semple 2000), although inhibition might contribute to the shape of rMTFs by suppressing responses to certain modulation frequencies. A model for low-pass responses proposed for the medial superior olive in mustached bats by Grothe (1994) is based on inhibitory inputs delayed with respect to excitation by a constant amount. Depending on modulation period, inhibitory and excitatory inputs might temporally overlap and thus restrict the range of modulation frequencies to which the neuron is responsive.

For the stages of the auditory pathway above the IC, Eggermont (1996) suggested that the tBMF is mainly determined by processes intrinsic to the cortical-thalamic network, whereas intrinsic pyramidal cell mechanisms influence the cutoff frequency. Furthermore, Eggermont (2002) described two main components of the envelope synchronization, i.e., the degree of input/presynaptic synchrony and shape of the temporal filter, which in turn is determined by properties of synaptic dynamics.

In contrast to SAM stimuli coding, delay tuning in bats is first observed on the level of the IC (Mittmann and Wenstrup 1995) and is created by spectrotemporal integration of inputs from the lateral lemniscus. Neural mechanisms for creating delay sensitivity employ coincidence of glycinergic postinhibitory rebound facilitation (Sanchez et al. 2008), but paradoxical latency shifts are also discussed as mechanisms for delay tuning in other bats (Feng 2011; Hechavarría and Kössl 2014; Sullivan 1982). Interestingly, Hechavarría and Kössl (2014) suggested that cortical units in the bat *C. perspicillata* might inherit delay-tuning properties from auditory stations below the AC. Following this line of argumentation, a possible (although hypothetical) explanation for the unusually high best modulations frequencies in rMTFs and tMTFs observed in our study can be supposed: temporal modulation properties of IC units might mainly be passed without further modification to the dorsal AC in *P. discolor*. This might therefore represent a fundamental scheme for this area. This hypothesis is supported by the fact that the dorsal field of AC in other bats often receive input from different subregions of the auditory thalamus (i.e., the medial geniculate body) than the primary cortex (Radtke-Schuller et al. 2004). Special functional properties in terms of temporal processing might come with those special thalamocortical connections. This was also recently suggested for the fast synchronization of local field potentials of cortical units in the AC of *C. perspicillata* (García-Rosales et al. 2018a). Furthermore, it might also be possible that coding of fast amplitude modulation in the PDF of *P. discolor* is facilitated by the temporal delay-tuning properties often found in neurons of this cortical region. Delay tuning of neurons in the chronotopic map of *P. discolor* is well observed in the range around 10 ms (Greiter and Firzlaff 2017). These neurons might therefore be preadapted to the processing of temporal envelope modulations in the frequency range around 100 Hz. Fast envelope modulation coding observed in our study might thus be considered to be an epiphenomenon, explaining the different results of our study and the study of Martin et al. (2017) in the primary AC of *C. perspicillata*.

Possible Influence of Anesthesia

In this study, we used a combination of medetomidine, midazolam, and fentanyl. Medetomidine did not produce an observable effect on neural activity in the IC and the primary AC of the Mongolian gerbil (Ter-Mikaelian et al. 2007). Immunoreactivity for endogenous opioids such as enkephalin is generally low or absent in the primary AC and the medial geniculate body but is abundant in other nuclei of the auditory pathway (Aguilar et al. 2004; Robertson and Mulders 2000). The main effect of enkephalin seems to be inhibition of the cochlear neural output via the descending olivocochlear bundle (Bürki et al. 1993). Thus the opioid fentanyl used in our study might have had a nonspecific overall inhibitory effect on neural activity to acoustic stimulation.

Midazolam, like other benzodiazepines, enhances $GABA_A$-mediated inhibition and might be the main source of possible anesthesia effects in this study. Temporal processing was influenced by GABAergic disinhibition in that the phase-locking ability of bat IC neurons was increased (Lu et al. 1998). In addition, anesthesia with pentobarbital sodium (which also enhances $GABA_A$-mediated inhibition) reduced stimulus-induced activity in neurons in the rat AC (Gaese and Ostwald 2001). The use of midazolam in our study might therefore have led to a decrease in overall neural activity and in temporal coding precision. However, previous studies have shown that neural responses measured in bats anesthetized with medetomidine, midazolam, and fentanyl reflected the behavioral performance of the bats well (Firzlaff et al. 2006, 2007). The influence of the anesthesia should therefore only be moderate.

Coding of Communication Calls in Relation to SAM Stimuli

The dorsal AC is also an important area in terms of the processing of species-specific communication sounds in bats. The delay-tuning properties of units in the AC of the mustached bat seem also to facilitate the responses to combination of syllables of communication calls (Esser et al. 1997; Ohle-

miller et al. 1996), therefore serving processing of syntax in bat vocal communication. Interestingly, nonlinear temporal and spectral integration appear to underlie processing of communication sounds in other mammals, thus representing a general principle in vocal communication (Kanwal and Rauschecker 2007).

Selectivity indexes of the recorded units in our study (mean d_i value 0.3153) were similar to values reported for the marmoset A1 (mean d_i values between 0.335 and 0.479; Wang and Kadia 2001) but substantially higher than the cat A1 (mean d_i values between 0.047 and 0.086; Wang and Kadia 2001). Wang and colleagues (Wang et al. 1995; Wang 2000) described aforementioned call selectivity in marmoset A1 units, and they hypothesized a specialization in fast and precise detection of frequently heard vocalizations, which also seems applicable to the units in the AC of *P. discolor*. Additionally, we found that the temporal envelope-coding properties of units often correlated with a preference for aggression calls (showing strong amplitude modulations around 130 Hz) expressed by neuronal firing rate as well as in spike timing patterns reflecting the temporal call envelope. Quite similar findings were reported for the primary AC of anesthetized marmosets, where responses to twitter calls correlated with responses to SAM sounds with comparable modulation rates (Nagarajan et al. 2002) and responses of units were phase-locked to parts of the envelope of communications calls (Wang et al. 1995). Whether this response correlation to sound envelope is enough to create a call-specific representation in single units or is used to synchronize a larger neuronal population, i.e., to create a population code for vocalizations (Wang et al. 1995), is still not clear for the dorsal AC in *P. discolor* and has to be investigated in future experiments.

The fact that response PSTH spectra often showed peaks in the 100- to 130-Hz range, reflecting peaks in the call envelope spectra, does not mean, per se, that the complete call envelope is thoroughly encoded in the response pattern. For SAM stimuli, phase-locking to higher modulation frequencies of did not occur over the full range of modulation cycles, i.e., not over the complete stimulus duration (e.g., Fig. 4). In addition, strong overall fluctuations of call intensity superimposed on faster envelope modulation might impair the neural response when becoming subthreshold. We therefore can only demonstrate the principle ability of *P. discolor* neurons to respond to high-frequency modulations in the call envelope of communication calls in this study, but we cannot demonstrate high-fidelity coding of the complete call envelope that might be necessary for response specificity to individual calls.

In conclusion, our results show that units in the dorsal AC of the bat *P. discolor* can encode fast temporal envelope modulations as both rate and temporal code. This ability is partly reflected in the neuronal response preference to certain types of species-specific communication calls characterized by temporal envelope modulations in the same frequency range. Therefore, neural processing in the dorsal AC of bats seems to be specifically adapted to the high envelope modulation rates occurring in the vocal repertoire and might therefore play an important role in vocal communication.

ACKNOWLEDGMENTS

We thank Lutz Wiegrebe for providing the experimental animals and Wolfgang Greiter for comments and input into the analysis.

GRANTS

This work was supported by Human Frontier Science Program Grant RGP0058 (to U. Firzlaff).

DISCLOSURES

No conflicts of interest, financial or otherwise, are declared by the authors.

AUTHOR CONTRIBUTIONS

S.G.H. and U.F. conceived and designed research; S.G.H. performed experiments; S.G.H. and U.F. analyzed data; S.G.H. and U.F. interpreted results of experiments; S.G.H. prepared figures; S.G.H. drafted manuscript; S.G.H. and U.F. edited and revised manuscript; U.F. approved final version of manuscript.

REFERENCES

Aguilar LA, Malmierca MS, Coveñas R, López-Poveda EA, Tramu G, Merchán M. Immunocytochemical distribution of Met-enkephalin-Arg6-Gly7-Leu8 (Met-8) in the auditory system of the rat. *Hear Res* 187: 111–121, 2004. doi:10.1016/S0378-5955(03)00333-2.

Andoni S, Li N, Pollak GD. Spectrotemporal receptive fields in the inferior colliculus revealing selectivity for spectral motion in conspecific vocalizations. *J Neurosci* 27: 4882–4893, 2007. doi:10.1523/JNEUROSCI.4342-06.2007.

Andoni S, Pollak GD. Selectivity for spectral motion as a neural computation for encoding natural communication signals in bat inferior colliculus. *J Neurosci* 31: 16529–16540, 2011. doi:10.1523/JNEUROSCI.1306-11.2011.

August PV. *Distress Calls in Artibeus jamaicensis: Ecology and Evolutionary Implications*, edited by Eisenberg JF. Washington, DC: Smithsonian Institution Press, 1979.

Bartenstein SK, Gerstenberg N, Vanderelst D, Peremans H, Firzlaff U. Echo-acoustic flow dynamically modifies the cortical map of target range in bats. *Nat Commun* 5: 4668, 2014. doi:10.1038/ncomms5668.

Bendor D, Wang X. Neural response properties of primary, rostral, and rostrotemporal core fields in the auditory cortex of marmoset monkeys. *J Neurophysiol* 100: 888–906, 2008. doi:10.1152/jn.00884.2007.

Bieser A, Müller-Preuss P. Auditory responsive cortex in the squirrel monkey: neural responses to amplitude-modulated sounds. *Exp Brain Res* 108: 273–284, 1996. doi:10.1007/BF00228100.

Bohn KM, Schmidt-French B, Ma ST, Pollak GD. Syllable acoustics, temporal patterns, and call composition vary with behavioral context in Mexican free-tailed bats. *J Acoust Soc Am* 124: 1838–1848, 2008. doi:10.1121/1.2953314.

Burger RM, Pollak GD. Analysis of the role of inhibition in shaping responses to sinusoidally amplitude-modulated signals in the inferior colliculus. *J Neurophysiol* 80: 1686–1701, 1998. doi:10.1152/jn.1998.80.4.1686.

Bürki C, Felix D, Ehrenberger K. Enkephalin suppresses afferent cochlear neurotransmission. *ORL J Otorhinolaryngol Relat Spec* 55: 3–6, 1993. doi:10.1159/000276344.

Buunen TJ, Rhode WS. Responses of fibers in the cat's auditory nerve to the cubic difference tone. *J Acoust Soc Am* 64: 772–781, 1978. doi:10.1121/1.382042.

Cohen YE, Theunissen F, Russ BE, Gill P. Acoustic features of rhesus vocalizations and their representation in the ventrolateral prefrontal cortex. *J Neurophysiol* 97: 1470–1484, 2007. doi:10.1152/jn.00769.2006.

Condon CJ, Galazyuk A, White KR, Feng AS. Neurons in the auditory cortex of the little brown bat exhibit selectivity for complex amplitude-modulated signals that mimic echoes from fluttering insects. *Aud Neurosci* 3: 269–287, 1997.

Covey E. Neurobiological specializations in echolocating bats. *Anat Rec A Discov Mol Cell Evol Biol* 287: 1103–1116, 2005. doi:10.1002/ar.a.20254.

Covey E, Carolina DN, Hawkins HL, Port RF (Editors). *Neural Representation of Temporal Patterns*. New York: Springer, 1995. doi:10.1007/978-1-4615-1919-5.

Creutzfeldt O, Hellweg FC, Schreiner C. Thalamocortical transformation of responses to complex auditory stimuli. *Exp Brain Res* 39: 87–104, 1980. doi:10.1007/BF00237072.

DiMattina C, Wang X. Virtual vocalization stimuli for investigating neural representations of species-specific vocalizations. *J Neurophysiol* 95: 1244–1262, 2006. doi:10.1152/jn.00818.2005.

Eggermont JJ. How homogeneous is cat primary auditory cortex? Evidence from simultaneous single-unit recordings. *Aud Neurosci* 2: 79–96, 1996.

Eggermont JJ. Representation of spectral and temporal sound features in three cortical fields of the cat. Similarities outweigh differences. *J Neurophysiol* 80: 2743–2764, 1998. doi:10.1152/jn.1998.80.5.2743.

Eggermont JJ. Temporal modulation transfer functions in cat primary auditory cortex: separating stimulus effects from neural mechanisms. *J Neurophysiol* 87: 305–321, 2002. doi:10.1152/jn.00490.2001.

Ehrlich D, Casseday JH, Covey E. Neural tuning to sound duration in the inferior colliculus of the big brown bat, *Eptesicus fuscus*. *J Neurophysiol* 77: 2360–2372, 1997. doi:10.1152/jn.1997.77.5.2360.

Esser K-H, Condon CJ, Suga N, Kanwal JS. Syntax processing by auditory cortical neurons in the FM-FM area of the mustached bat *Pteronotus parnellii*. *Proc Natl Acad Sci USA* 94: 14019–14024, 1997. doi:10.1073/pnas.94.25.14019.

Esser KH, Schubert J. Vocal dialects in the lesser spear-nosed bat *Phyllostomus discolor*. *Naturwissenschaften* 85: 347–349, 1998. doi:10.1007/s001140050513.

Feng AS. Neural mechanisms of target ranging in FM bats: physiological evidence from bats and frogs. *J Comp Physiol A Neuroethol Sens Neural Behav Physiol* 197: 595–603, 2011. doi:10.1007/s00359-010-0533-5.

Fenton MB, Belwood JJ, Fullard JH, Kunz TH. Responses of *Myotis lucifugus* (Chiroptera: Vespertilionidae) to calls of conspecifics and to other sounds. *Can J Zool* 54: 1443–1448, 1976. doi:10.1139/z76-167.

Firzlaff U, Schörnich S, Hoffmann S, Schuller G, Wiegrebe L. A neural correlate of stochastic echo imaging. *J Neurosci* 26: 785–791, 2006. doi:10.1523/JNEUROSCI.3478-05.2006.

Firzlaff U, Schuchmann M, Grunwald JE, Schuller G, Wiegrebe L. Object-oriented echo perception and cortical representation in echolocating bats. *PLoS Biol* 5: e100, 2007. doi:10.1371/journal.pbio.0050100.

Gadziola MA, Grimsley JMS, Shanbhag SJ, Wenstrup JJ. A novel coding mechanism for social vocalizations in the lateral amygdala. *J Neurophysiol* 107: 1047–1057, 2012. doi:10.1152/jn.00422.2011.

Gadziola MA, Shanbhag SJ, Wenstrup JJ. Two distinct representations of social vocalizations in the basolateral amygdala. *J Neurophysiol* 115: 868–886, 2016. doi:10.1152/jn.00953.2015.

Gaese BH, Ostwald J. Temporal coding of amplitude and frequency modulation in the rat auditory cortex. *Eur J Neurosci* 7: 438–450, 1995. doi:10.1111/j.1460-9568.1995.tb00340.x.

Gaese BH, Ostwald J. Anesthesia changes frequency tuning of neurons in the rat primary auditory cortex. *J Neurophysiol* 86: 1062–1066, 2001. doi:10.1152/jn.2001.86.2.1062.

García-Rosales F, Beetz MJ, Cabral-Calderin Y, Kössl M, Hechavarria JC. Neuronal coding of multiscale temporal features in communication sequences within the bat auditory cortex. *Commun Biol* 1: 200, 2018a. doi:10.1038/s42003-018-0205-5.

García-Rosales F, Martin LM, Beetz MJ, Cabral-Calderin Y, Kössl M, Hechavarria JC. Low-frequency spike-field coherence is a fingerprint of periodicity coding in the auditory cortex. *iScience* 9: 47–62, 2018b. doi:10.1016/j.isci.2018.10.009.

Gaucher Q, Huetz C, Gourévitch B, Laudanski J, Occelli F, Edeline JM. How do auditory cortex neurons represent communication sounds? *Hear Res* 305: 102–112, 2013. doi:10.1016/j.heares.2013.03.011.

Goldberg JM, Brown PB. Response of binaural neurons of dog superior olivary complex to dichotic tonal stimuli: some physiological mechanisms of sound localization. *J Neurophysiol* 32: 613–636, 1969. doi:10.1152/jn.1969.32.4.613.

Greiter W, Firzlaff U. Echo-acoustic flow shapes object representation in spatially complex acoustic scenes. *J Neurophysiol* 117: 2113–2124, 2017. doi:10.1152/jn.00860.2016.

Grothe B. Interaction of excitation and inhibition in processing of pure tone and amplitude-modulated stimuli in the medial superior olive of the mustached bat. *J Neurophysiol* 71: 706–721, 1994. doi:10.1152/jn.1994.71.2.706.

Grothe B, Covey E, Casseday JH. Medial superior olive of the big brown bat: neuronal responses to pure tones, amplitude modulations, and pulse trains. *J Neurophysiol* 86: 2219–2230, 2001. doi:10.1152/jn.2001.86.5.2219.

Hagemann C, Esser K-H, Kössl M. Chronotopically organized target-distance map in the auditory cortex of the short-tailed fruit bat. *J Neurophysiol* 103: 322–333, 2010. doi:10.1152/jn.00595.2009.

Hartmann WM, Pumplin J. Noise power fluctuations and the masking of sine signals. *J Acoust Soc Am* 83: 2277–2289, 1988. doi:10.1121/1.396358.

Hechavarría JC, Beetz MJ, Macias S, Kössl M. Distress vocalization sequences broadcasted by bats carry redundant information. *J Comp Physiol A Neuroethol Sens Neural Behav Physiol* 202: 503–515, 2016. doi:10.1007/s00359-016-1099-7.

Hechavarría JC, Kössl M. Footprints of inhibition in the response of cortical delay-tuned neurons of bats. *J Neurophysiol* 111: 1703–1716, 2014. doi:10.1152/jn.00777.2013.

Hechavarría JC, Macías S, Vater M, Voss C, Mora EC, Kössl M. Blurry topography for precise target-distance computations in the auditory cortex of echolocating bats. *Nat Commun* 4: 2587, 2013. doi:10.1038/ncomms3587.

Heil P, Schulze H, Langner G. Ontogenetic development of periodicity coding in the inferior colliculus of the Mongolian gerbil. *Aud Neurosci* 1: 363–383, 1995.

Hewitt MJ, Meddis R. A computer model of amplitude-modulation sensitivity of single units in the inferior colliculus. *J Acoust Soc Am* 95: 2145–2159, 1994. doi:10.1121/1.408676.

Hoffmann S, Firzlaff U, Radtke-Schuller S, Schwellnus B, Schuller G. The auditory cortex of the bat *Phyllostomus discolor*: localization and organization of basic response properties. *BMC Neurosci* 9: 65, 2008. doi:10.1186/1471-2202-9-65.

Hoglen NEG, Larimer P, Phillips EA, Malone BJ, Hasenstaub AR. Amplitude modulation coding in awake mice and squirrel monkeys. *J Neurophysiol* 119: 1753–1766, 2018. doi:10.1152/jn.00101.2017.

Jen PHS, Hou T, Wu M. Neurons in the inferior colliculus, auditory cortex and pontine nuclei of the FM bat, *Eptesicus fucus* respond to pulse repetition rate differently. *Brain Res* 613: 152–155, 1993. doi:10.1016/0006-8993(93)90466-Z.

Joris PX, Schreiner CE, Rees A. Neural processing of amplitude-modulated sounds. *Physiol Rev* 84: 541–577, 2004. doi:10.1152/physrev.00029.2003.

Joris PX, Yin TC. Responses to amplitude-modulated tones in the auditory nerve of the cat. *J Acoust Soc Am* 91: 215–232, 1992. doi:10.1121/1.402757.

Kanwal JS, Ehret G. Communication sounds and their cortical representation. In: *The Auditory Cortex*, edited by Winer JA, Schreiner CE. Boston, MA: Springer, 2011, p. 343–367.

Kanwal JS, Matsumura S, Ohlemiller K, Suga N. Analysis of acoustic elements and syntax in communication sounds emitted by mustached bats. *J Acoust Soc Am* 96: 1229–1254, 1994. doi:10.1121/1.410273.

Kanwal JS, Rauschecker JP. Auditory cortex of bats and primates: managing species-specific calls for social communication. *Front Biosci* 12: 4621–4640, 2007. doi:10.2741/2413.

Köppl C. Phase locking to high frequencies in the auditory nerve and cochlear nucleus magnocellularis of the barn owl, *Tyto alba*. *J Neurosci* 17: 3312–3321, 1997. doi:10.1523/JNEUROSCI.17-09-03312.1997.

Krishna BS, Semple MN. Auditory temporal processing: responses to sinusoidally amplitude-modulated tones in the inferior colliculus. *J Neurophysiol* 84: 255–273, 2000. doi:10.1152/jn.2000.84.1.255.

Langner G. Periodicity coding in the auditory system. *Hear Res* 60: 115–142, 1992. doi:10.1016/0378-5955(92)90015-F.

Lu Y, Jen PH, Wu M. GABAergic disinhibition affects responses of bat inferior collicular neurons to temporally patterned sound pulses. *J Neurophysiol* 79: 2303–2315, 1998. doi:10.1152/jn.1998.79.5.2303.

Martin LM, García-Rosales F, Beetz MJ, Hechavarría JC. Processing of temporally patterned sounds in the auditory cortex of Seba's short-tailed bat, *Carollia perspicillata*. *Eur J Neurosci* 46: 2365–2379, 2017. doi:10.1111/ejn.13702.

Mittmann DH, Wenstrup JJ. Combination-sensitive neurons in the inferior colliculus. *Hear Res* 90: 185–191, 1995. doi:10.1016/0378-5955(95)00164-X.

Nagarajan SS, Cheung SW, Bedenbaugh P, Beitel RE, Schreiner CE, Merzenich MM. Representation of spectral and temporal envelope of twitter vocalizations in common marmoset primary auditory cortex. *J Neurophysiol* 87: 1723–1737, 2002. doi:10.1152/jn.00632.2001.

Naumann RT, Kanwal JS. Basolateral amygdala responds robustly to social calls: spiking characteristics of single unit activity. *J Neurophysiol* 105: 2389–2404, 2011. doi:10.1152/jn.00580.2010.

Nourski KV, Brugge JF. Representation of temporal sound features in the human auditory cortex. *Rev Neurosci* 22: 187–203, 2011. doi:10.1515/rns.2011.016.

O'Neill WE, Suga N. Target range-sensitive neurons in the auditory cortex of the mustache bat. *Science* 203: 69–73, 1979. doi:10.1126/science.758681.

Ohlemiller KK, Kanwal JS, Suga N. Facilitative responses to species-specific calls in cortical FM-FM neurons of the mustached bat. *Neuroreport* 7: 1749–1755, 1996. doi:10.1097/00001756-199607290-00011.

Olsen JF, Suga N. Combination-sensitive neurons in the medial geniculate body of the mustached bat: encoding of target range information. *J Neurophysiol* 65: 1275–1296, 1991. doi:10.1152/jn.1991.65.6.1275.

Peterson DC, Wenstrup JJ. Selectivity and persistent firing responses to social vocalizations in the basolateral amygdala. *Neuroscience* 217: 154–171, 2012. doi:10.1016/j.neuroscience.2012.04.069.

Radtke-Schuller S, Schuller G, O'Neill WE. Thalamic projections to the auditory cortex in the rufous horseshoe bat (*Rhinolophus rouxi*). II. Dorsal fields. *Anat Embryol (Berl)* 209: 77–91, 2004. doi:10.1007/s00429-004-0425-y.

Rees A, Møller AR. Stimulus properties influencing the responses of inferior colliculus neurons to amplitude-modulated sounds. *Hear Res* 27: 129–143, 1987. doi:10.1016/0378-5955(87)90014-1.

Rhode WS, Greenberg S. Encoding of amplitude modulation in the cochlear nucleus of the cat. *J Neurophysiol* 71: 1797–1825, 1994. doi:10.1152/jn.1994.71.5.1797.

Robertson D, Mulders WHAM. Distribution and possible functional roles of some neuroactive peptides in the mammalian superior olivary complex. *Microsc Res Tech* 51: 307–317, 2000. doi:10.1002/1097-0029(20001115)51:4<307:AID-JEMT2>3.0.CO;2-4.

Russ JM, Jones G, Mackie IJ, Racey PA. Interspecific responses to distress calls in bats (Chiroptera: Vespertilionidae): A function for convergence in call design? *Anim Behav* 67: 1005–1014, 2004. doi:10.1016/j.anbehav.2003.09.003.

Sanchez JT, Gans D, Wenstrup JJ. Glycinergic "inhibition" mediates selective excitatory responses to combinations of sounds. *J Neurosci* 28: 80–90, 2008. doi:10.1523/JNEUROSCI.3572-07.2008.

Sayegh R, Casseday JH, Covey E, Faure PA. Monaural and binaural inhibition underlying duration-tuned neurons in the inferior colliculus. *J Neurosci* 34: 481–492, 2014. doi:10.1523/JNEUROSCI.3732-13.2014.

Schnupp JW, Hall TM, Kokelaar RF, Ahmed B. Plasticity of temporal pattern codes for vocalization stimuli in primary auditory cortex. *J Neurosci* 26: 4785–4795, 2006. doi:10.1523/JNEUROSCI.4330-05.2006.

Schreiner CE, Urbas JV. Representation of amplitude modulation in the auditory cortex of the cat. II. Comparison between cortical fields. *Hear Res* 32: 49–63, 1988. doi:10.1016/0378-5955(88)90146-3.

Schuller G, Radtke-Schuller S, Betz M. A stereotaxic method for small animals using experimentally determined reference profiles. *J Neurosci Methods* 18: 339–350, 1986. doi:10.1016/0165-0270(86)90022-1.

Schulze H, Langner G. Periodicity coding in the primary auditory cortex of the Mongolian gerbil (*Meriones unguiculatus*): two different coding strategies for pitch and rhythm? *J Comp Physiol A Neuroethol Sens Neural Behav Physiol* 181: 651–663, 1997. doi:10.1007/s003590050147.

Schwartz C, Tressler J, Keller H, Vanzant M, Ezell S, Smotherman M. The tiny difference between foraging and communication buzzes uttered by the Mexican free-tailed bat, *Tadarida brasiliensis*. *J Comp Physiol A Neuroethol Sens Neural Behav Physiol* 193: 853–863, 2007. doi:10.1007/s00359-007-0237-7.

Sullivan WE 3rd. Neural representation of target distance in auditory cortex of the echolocating bat *Myotis lucifugus*. *J Neurophysiol* 48: 1011–1032, 1982. doi:10.1152/jn.1982.48.4.1011.

Ter-Mikaelian M, Sanes DH, Semple MN. Transformation of temporal properties between auditory midbrain and cortex in the awake Mongolian gerbil. *J Neurosci* 27: 6091–6102, 2007. doi:10.1523/JNEUROSCI.4848-06.2007.

Wang X. On cortical coding of vocal communication sounds in primates. *Proc Natl Acad Sci USA* 97: 11843–11849, 2000. doi:10.1073/pnas.97.22.11843.

Wang X, Kadia SC. Differential representation of species-specific primate vocalizations in the auditory cortices of marmoset and cat. *J Neurophysiol* 86: 2616–2620, 2001. doi:10.1152/jn.2001.86.5.2616.

Wang X, Merzenich MM, Beitel R, Schreiner CE. Representation of a species-specific vocalization in the primary auditory cortex of the common marmoset: temporal and spectral characteristics. *J Neurophysiol* 74: 2685–2706, 1995. doi:10.1152/jn.1995.74.6.2685.

Washington SD, Kanwal JS. DSCF neurons within the primary auditory cortex of the mustached bat process frequency modulations present within social calls. *J Neurophysiol* 100: 3285–3304, 2008. doi:10.1152/jn.90442.2008.

Washington SD, Kanwal JS. Sex-dependent hemispheric asymmetries for processing frequency-modulated sounds in the primary auditory cortex of the mustached bat. *J Neurophysiol* 108: 1548–1566, 2012. doi:10.1152/jn.00952.2011.

Whitfield IC, Evans EF. Responses of auditory cortical neurons to stimuli of changing frequency. *J Neurophysiol* 28: 655–672, 1965. doi:10.1152/jn.1965.28.4.655.

4 Post-natal development of processing of temporal sound features

The fourth chapter of this thesis covers the development of envelope following responses in juvenile *Phyllostomus discolor*. Based on the findings of Hörpel and Firzlaff [2019], I chose to analyse the maturation of envelope following responses during the maturation period of juvenile *Phyllostomus discolor* and recorded from three individuals. Seeing as the auditory cortex showed a preference for strongly amplitude modulated calls associated with aggressive behaviour I assumed that the auditory brainstem would most likely be fully capable of synchronising its discharges to sinusoidally amplitude modulated stimuli. However, given the significance of correct processing of said aggression calls for the animal itself, we chose to investigate whether the ability of the auditory brainstem to synchronise to amplitude modulations is innate (and would therefore show no changes during the ontogeny of the animal) or if this ability is subject to changes during the maturation of the animal. This synchronised neural discharge is typically called the envelope following response, as it synchronises its firing pattern to the envelope or outline of the sound stimulus used. On each experimental day, the sound pressure threshold for the auditory brainstem responses was determined by presenting broadband click stimuli (4 to 96 kHz) at various sound pressure levels (40 to 120 dB SPL). Once the threshold had been determined I presented a stimulus library consisting of seven different frozen noise sounds (200 ms duration, frequency range between 2 and 95 kHz), which had been sinusoidally amplitude modulated (modulation frequencies logarithmically spaced between 11 and 130 Hz) at a sound pressure level of 80 dB RMS. I could show, that the sound pressure threshold for all three animals fluctuated only slightly over the full maturation period and deviated between 50 and 60 dB SPL. Furthermore, I was able to prove (in two out of three animals) that the envelope following response is basically developed by postnatal day 8 and that it further matures until postnatal day 33. However, this maturation period is dependant on the modulation frequency of the stimulus used, as low modulation frequencies (11 to 58 Hz) matured faster than high modulation frequencies (87 to 130 Hz).

Both my supervisor and I were involved in the conceptualisation of the experiments, the methodology and software required, also the writing of the original draft and the visualisation of the results. Additionally, I performed all the experiments, while my supervisor contributed both the project supervision and project funding. This chapter published in *Hearing Research* (Hörpel and Firzlaff [2020]). Being the author, no special permission for reproduction in this thesis was necessary as was communicated by the copyright owner (see Appendix B, Figure B.5 for further confirmation).

Hearing Research 388 (2020) 107904

Contents lists available at ScienceDirect

Hearing Research

journal homepage: www.elsevier.com/locate/heares

Research Paper

Post-natal development of the envelope following response to amplitude modulated sounds in the bat *Phyllostomus discolor*

Stephen Gareth Hörpel *, Uwe Firzlaff

Department of Animal Sciences, Technical University of Munich, Liesel-Beckmann-Str. 4, 85354, Freising, Germany

ARTICLE INFO

Article history:
Received 4 November 2019
Received in revised form
20 December 2019
Accepted 24 January 2020
Available online 30 January 2020

Keywords:
Temporal processing
Auditory brainstem responses
Amplitude modulation
Hearing development

ABSTRACT

Bats use a large repertoire of calls for social communication, which are often characterized by temporal amplitude and frequency modulations. As bats are considered to be among the few mammalian species capable of vocal learning, the perception of temporal sound modulations should be crucial for juvenile bats to develop social communication abilities. However, the post-natal development of auditory processing of temporal modulations has not been investigated in bats, so far. Here we use the minimally invasive technique of recording auditory brainstem responses to measure the envelope following response (EFR) to sinusoidally amplitude modulated noise (range of modulation frequencies: 11–130 Hz) in three juveniles (p8-p72) of the bat, *Phyllostomus discolor*. In two out of three animals, we show that although amplitude modulation processing is basically developed at p8, EFRs maturated further over a period of about two weeks until p33. Maturation of the EFR generally took longer for higher modulation frequencies (87–130 Hz) than for lower modulation frequencies (11–58 Hz).

1. Introduction

Human speech and animal communication sounds are characterized by, among other sound features, temporal amplitude and frequency modulations (Gaucher et al., 2013; Nourski and Brugge, 2011). This holds also true for species-specific communication in bats, which exhibit a rich vocal repertoire (Bohn et al., 2008; Knörnschild, 2014; Knörnschild et al., 2014; Lattenkamp et al., 2019). Furthermore, bats are among the few mammals species considered to be capable of vocal learning (Boughman, 1998; Knörnschild, 2014; Prat et al., 2015). For the bat *Phyllostomus discolor*, it has been reported that contact calls important for mother infant communication show a less prominent amount of temporal modulations in hand-reared pups compared to pups reared together with their mothers (Esser and Schmidt, 1989). Therefore, the ontogeny of the auditory system in these bats should reflect the need for processing of temporal sound modulations.

Generally, hearing onset is defined as the point during the maturation of an animal, where behavioral (Moore, 1982) or neuronal (Sonntag et al., 2009) responses can by elicited by sound pressure levels within physiological ranges. Common model animals are typically born deaf, e.g. gerbils (hearing onset at p11-p12, Heil et al., 1995; Magnusson et al., 2005), rats (hearing onset at p11, Smith et al., 2000) and mice (hearing onset at p12, Mikaelian and Ruben, 1965; Kraus and Aulbach-Kraus, 1981). In bats, hearing onset seems to vary between different species. However, for most species hearing onset is reported to occur within the first week if not as early as on postnatal day p1-p2 (p7-p8, *Antrozous pallidus*, Brown et al., 1978; Razak and Fuzessery, 2007; p1-p2, *Pteronotus parnellii*, Vater et al., 2010 and *Carollia perspicillata*, Sterbing, 2002; first and second postnatal week, *Hipposideros speoris* & *Rhinolophus rouxi*, Rübsamen et al., 1989). *P. discolor* was shown to react to maternal directive calls within the first day after birth (Esser and Schmidt, 1990), which is supported by data from Linnenschmidt and Wiegrebe (2019), who showed that hearing onset in this bat has already occurred at p5. It should certainly be clear, that an early hearing onset is of advantage in mother-pup communication.

The post-natal development of processing of temporal modulations has been already investigated in several mammalian species, e.g. gerbils (Heil et al., 1995; Khurana et al., 2012), mice (Müller et al., 2019), harbour porpoises (Linnenschmidt et al., 2013) and in humans (Draganova et al., 2018; Rance et al., 2006; Walker et al., 2019). However, data for bats are lacking so far. In order to analyze the development of temporal modulation processing ability in bats, we recorded envelope following responses (EFRs) from pups of *P. discolor*.

* Corresponding author.
E-mail address: stephen.hoerpel@tum.de (S.G. Hörpel).

https://doi.org/10.1016/j.heares.2020.107904
0378-5955/

The EFR is a subclass of auditory brainstem response (ABR) evoked by periodic auditory stimuli. As the EFR is typically phase-locked to the waveform and/or the envelope of a periodic stimulus (Moushegian et al., 1973), it has been used in animals as well as in humans to quantify the temporal processing abilities of the auditory system (Dimitrijevic et al., 2016; Prado-Gutierrez et al., 2012; Venkataraman and Bartlett, 2013).

More generally, the ABR signal reflects the summed electrical response potentials of both the auditory nerve fibers and nuclei of the ascending auditory pathway (Burkard et al., 2007). ABR recordings are ideal for measuring ontogenetic changes of the auditory pathway for mainly two reasons: first, the ABR waveform generally changes substantially during the ontogeny of the animal, reflecting the changes during the maturation of the auditory pathway. Second, being a minimally invasive recording method, it allows for long-term observations from the same animal and is especially suited for new porn pups, which might not be suitable for more invasive techniques.

ABR recordings have been utilized in bat auditory research several times (e.g. *Myotis lucifugus & Plecotus townsendii*, Grinnell, 1963; *Noctilio leporinus*, Wenstrup, 1984; *Lasiurus borealis*, Obrist and Wenstrup, 1998; *Pipistrellus abramus*, Simmons et al., 2015; *Eptesicus fuscus*, Simmons et al., 2016 and *Phyllostomus discolor*, Linnenschmidt and Wiegrebe, 2019), but the EFR has not been recorded in bats, so far.

Here we describe the EFR of juvenile *Phyllostomus discolor* at ages between p8 and p72. EFRs of individual animals showed a considerable amount of variability. In two out of three animals, the EFR developed with age, showing an increase in peak amplitude within the ABRs modulation spectra. Age related changes were stronger for high modulation frequencies (87–130 Hz) compared to lower modulation frequencies (11–58 Hz).

2. Methods

2.1. Animals

All the experiments complied with the principles of laboratory animal care and were conducted following the regulations of the current version of the German Law on Animal Protection (approval ROB-55.2-2532.Vet_02-17-218, Regierung von Oberbayern). The bats (*Phyllostomus discolor*; two juvenile females, one juvenile male, aged p8 on the first day of experiments) originated from a breeding colony situated in the Department Biology II of the Ludwig-Maximilian University of Munich. For experiments, animals were kept together with their mothers under semi-natural conditions (12 h day/12 h night cycle, 65%–70% relative humidity, 28 °C) with free access to food and water.

2.2. Anaesthesia

The bats were anaesthetized using a combination of medetomidine (Dorbene®, Zoetis), midazolam (Dormicum®, Hoffmann-La Roche) and fentanyl (Fentadon®, Albrecht) at a dosage of 0.4, 4.0 and 0.04 μg/g body weight, respectively.

The anaesthesia was antagonized with a mixture of atipamezole (Alzane®, Novartis), flumazenil (Flumazenil, Hexal) and naloxone (Naloxon-ratiopharm®, Ratiopharm), which was injected subcutaneously (2.5, 0.5 and 1.2 μg/g body weight, respectively). During the experiments, the eyes of the animals were covered with a vitamin A cream (VitA POS®, Ursapharm) to prevent them from drying, whereas the puncture wounds of the ABR electrodes were treated with panthenol (Bepanten®, Bayer).

2.3. Acoustic box setup

The setup used during the experiments is a close copy of the setup used by Linnenschmidt and Wiegrebe (2019). All recordings were made in a small, heavily sound-attenuated box (outside dimensions 34x34 × 34 cm) constructed from veneer plywood (4 cm thick) and covered with a removable acrylic glass lid (2.5 cm thick). The walls and floor were covered in 2 cm acoustic foam to dampen unwanted reflections of the stimuli. During the experiments, the bats were placed on a styrene foam block on axis with the loudspeaker. Two heating pads (11.0 × 7.7 cm, 12V, 12 W, thermo Flächenheizungs GmbH, Rohrbach, Germany) were located on either side of the animal. These were supplied by an external power supply (Voltcraft LPS 1153, Conrad Electronics SE, Hirschau, Germany). The temperature was monitored by an analogue thermometer tucked under the wing right next to the body of the bat and maintained at 37 °C air-temperature.

2.4. Acoustic stimulation

In order to measure the ABR properties to sinusoidally amplitude modulated (SAM) sounds, we followed the procedure used by Linnenschmidt and Wiegrebe (2019). First, the response threshold was established by presenting short, broadband (4–96 kHz, flat power spectrum, 256 repetitions) click stimuli to the animals. The stimuli were presented at nine different sound pressure levels (SPL) ranging from 40 to 120 dB (peak-equivalent, re 20 μPa) in 10 dB steps with every second stimulus played phase-inverted.

To evaluate the envelope following properties of the auditory brainstem a 200 ms frozen noise carrier (2–95 kHz, flat power spectrum) was modulated with seven different modulation sinusoids logarithmically spaced from 11 to 130 Hz. This range of modulation frequencies (MF) is most prominent in the temporal envelope of communication sound of *P. discolor* (Hörpel and Firzlaff, 2019).The modulation depth was 100%. The modulation frequencies were each randomly presented 256 times (every second stimulus was phase-inverted) at a level of 80 dB RMS (99 dB peSPL). The repetition rate was approximately 1.2 Hz.

All acoustic stimuli were computer-generated (Matlab®, 2018b; Mathworks, Natick, MA, USA), digital–analogue converted (Fireface 400, RME, Haimhausen, Germany; sampling rate 192 kHz), amplified (AX-396, Yamaha Music Foundation, Tokyo, Japan) and presented *via* free-field loudspeaker (R2904/700000, Scan-Speak, Videbæk, Denmark). The loudspeaker had been calibrated for linear frequency response between 1 kHz and 96 kHz and was positioned on the midline roughly 8 cm from the bats ears.

2.5. Electrophysiological recordings

To record the auditory brainstem responses, the setup was connected via small alligator clips to three subdermal electrodes (clipped 0.3 × 12 mm hypodermic needles, Henry Schein Inc., Melville, USA), which were pushed through the skin of the animal. The recording electrode was placed centrally at the base of the skull above the brainstem (Nape) while the reference electrode was placed centrally on top of the skull at the height of the foremost edge of the ears (Vertex). A ground electrode was inserted into the tissue caudally of the base of the right ear. The signals were initially amplified by 20 dB (DAM80, World Precision Instruments, Sarasota, USA) with the amplifier set to its widest filter settings (0.1 Hz–10 kHz band-pass filter). A HumBug (Quest Scientific, North Vancouver, Canada) was used to remove noise from the power mains, but did not affect the ABR signal. The signals were then analog-to-digitally converted (Fireface 400; 192 kHz sampling rate), additionally amplified by 10 dB and down-sampled 10 times

to reduce the amount of required storage. Then, each of the 256 repetitions per stimulus and sound level was saved into one combined file for offline analysis.

2.6. Data analysis

In order to establish click evoked ABRs waveforms recorded from the 256 stimuli, the repetitions were averaged and filtered (100 Hz–3000 Hz band-pass). To determine click evoked ABR SPL thresholds, we utilized a bootstrap analysis as described in Lv et al. (2007) and used by Linnenschmidt and Wiegrebe (2019). An analysis window of 6.8 ms (0.2 ms–7 ms after stimulus onset) was chosen. The bootstrap method is based on repeatedly drawing random samples of that window size (with replacement) from the original data (500 repetitions). It is then assessed in which percentage of cases the RMS of the resampled waveform exceeds the RMS of the original waveform. An ABR is considered significant when more than 99% of resampled waveforms have a lower RMS than the original waveform (Linnenschmidt and Wiegrebe, 2019; Lv et al., 2007).

ABRs evoked by SAM-noise were also established by averaging the recorded waveforms to 256 stimulus repetitions (but no filtering occurred). We then analyzed the modulation spectra of the averaged waveforms. In detail, we calculated the FFT (Fast Fourier transform, Matlab®) of the waveforms Hilbert envelope. EFRs were quantified by the height of the peak in the modulation spectra within the MF frequency range. However, the ABR amplitude (and thus the height of the envelope modulation spectra peaks) may not only be influenced by undesired factors like small differences in the positions of the recording electrode, but also by growth of the animal during post-natal development (Linnenschmidt and Wiegrebe, 2019; Walsh et al., 1986). Therefore, as a check, we also analyzed the EFR based on root mean square (RMS)-normalized average waveforms.

3. Results

In total, we recorded ABRs on 24 different occasions (3 animals, 8 recordings spread over 3 months from day p8-p72).

3.1. Development of click evoked ABRs

Click evoked ABRs with stable waveforms with multiple positive peaks were obtained for all animals. Examples of click evoked ABRs from two different bats are shown in Fig. 1a,b,d,e for different presentation levels ranging from 40 dB peSPL up to 120 dB peSPL. For the highest presentation level, the waveform typically consisted of 7 distinguishable waves and one pre-potential. The pre-potential occurred ca. 0.8 ms after stimulus onset, while the dominant waves I–V followed between 1.7 and 5 ms. Waves I and II were partly merged, i.e. they were protruding from each others rising or falling flanks. The same was observed for waves III-V. This waveform pattern was most prominent in early stages of the juvenile development (Fig. 1 a,d), and became more ambiguous in older bats (Fig. 1b,e). During development of the juveniles, the overall RMS amplitude of the click evoked ABRs generally decreased (Fig. 1c,f) for higher presentation levels, although this trend was not strictly linear in all three bats. For example, in Bat 1 (Fig. 1c) the ABR RMS amplitude resulting from the loudest presentation level increased slightly until p15 before a strong decrease was observed over the following period of juvenile development up to p69.

In Bat 3 click evoked ABR waveforms showed less distinguishable waves (Supplement S1). Contrarily to Bat 1 and 2, waves I and II were barely indistinguishable from each other and wave VII was missing.

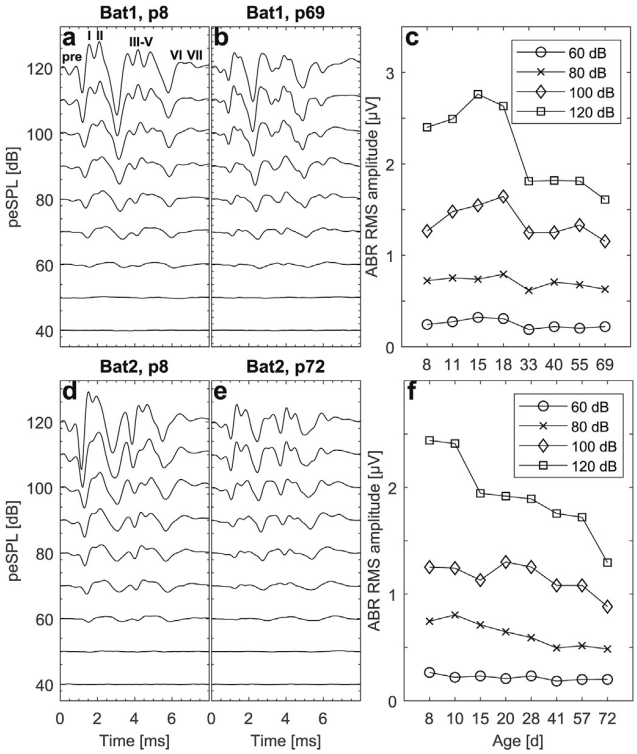

Fig. 1. Influence of stimulus level and age on click evoked ABR waveforms in P. *discolor* in Bat 1 (a, b) and Bat 2 (d, e). c, f. Summary data for ABR RMS amplitudes for all recording dates for Bat 1 and Bat 2, respectively. Analysis window for RMS calculation was from 0.2 to 7 ms.

Using click stimuli, significant ABRs could be evoked for presentation levels as low as 50 dB SPL in all three animals. This threshold did not change during development (Fig. 1a,b,d,e; S1), but fluctuated between 50 dB SPL and 60 dB SPL in all three animals.

3.2. Envelope following response

When comparing Fig. 1 with Fig. 2, the differences in fine structure between the ABR waveforms resulting from click stimulation or amplitude modulated noise stimulation become apparent: While the ABR waveform evoked by clicks is of limited duration (~7 ms, see Fig. 1a,b,d,e), the SAM evoked waveform is longer and more complex. Moreover, single waveform components within the click ABR waveform get less distinguishable and the overall RMS amplitude decreases during development (see Fig. 1a,b,d,e). Contrarily, age dependent changes in the waveform structure visible for the SAM-noise ABR waveform show the opposite trend.

Fig. 2 (left column) shows a 90 ms excerpt (i.e. one modulation cycle), of a SAM-noise evoked ABR waveform for a modulation frequency of 11 Hz, with the envelope of one modulation cycle of the stimulus (frozen noise) shown in the top panel. As the stimulus was frozen noise, the envelopes are not smooth, but show different numbers of prominent peaks within one modulation period. This is somewhat reflected in the evoked EFRs which accordingly also show a different structure of response peaks in one modulation cycle. For a lower modulation frequency, the number of structural peaks within one modulation period is of course higher than for a higher modulation frequency. At an early age (p8), no prominent waveform component is visible throughout the whole modulation

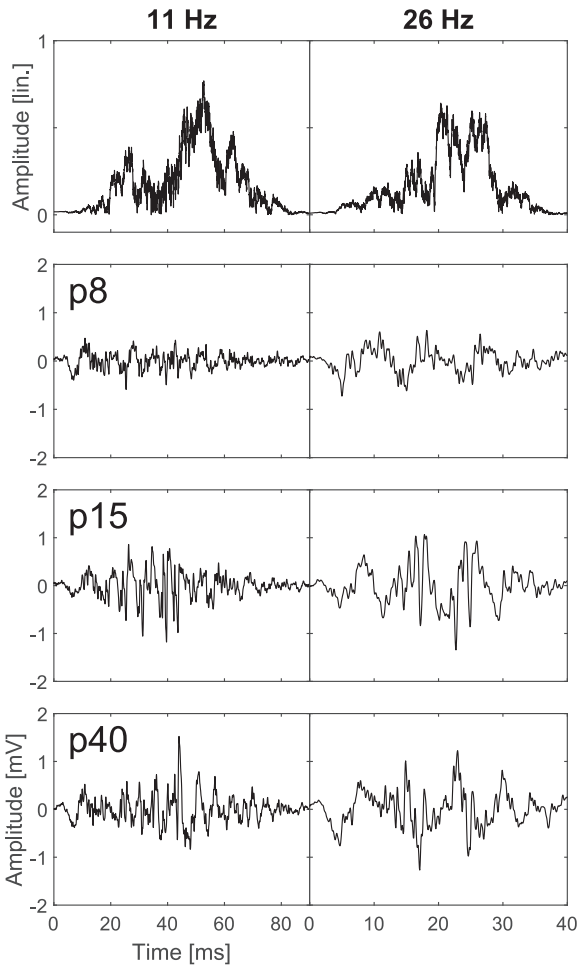

Fig. 2. Development of SAM noise evoked ABR waveforms for two MFs in Bat 1. In the top panel, the envelope of one modulation cycle of the respective stimulus is plotted. The waveforms corresponding to only one modulation cycle are shown in the lower three panels. Note different time scales of the abscissa of the left column and the right column.

cycle. For recordings on later days of juvenile development, large waveform components appear around the middle of the modulation cycle i.e. when the modulated stimulus reaches its peak-amplitude. The same can be observed for the SAM evoked ABR waveform for a modulation frequency of 26 Hz (Fig. 2, right column).

3.3. Development of the EFR

Fig. 3 illustrates the development of EFRs in Bat 1 for the seven different modulation frequencies. The ABR waveforms (Fig. 3, row 1 to 3) show changes in both shape and structure with increasing age of the juvenile bat. Typically, the waveforms show more distinct peaks in the responses to single modulation cycles and thus the envelope becomes more distinct for older bats. Additionally, RMS amplitude values of the waveform typically increase during post-natal development of the bats (Fig. 4) at least for higher MFs. Consecutively, these effects lead to an increase in the peak magnitude of the envelope modulation spectra in the frequency band corresponding to the modulation frequency (Fig. 5).

The development of the peak magnitude of the modulation frequency's envelope spectra in Bat 1 is shown in Fig. 3 (bottom row). Although peak magnitudes show some degree of fluctuations, for most modulation frequencies, the peak magnitude increases with age until it reaches a plateau. An exception to this trend can be seen for the modulation frequencies of 17 and 26 Hz, where the peak magnitude constantly decreases until p69 after a preliminary increase between p11 and p15. The peak magnitude values reached during the plateau-phase are in the same range for all MFs while the peak magnitude at p8 is lower for the highest MF (130 Hz).

The same developmental, age-dependent EFR pattern can be seen in the ABR measurements for Bat 2 (Fig. S2), with the exception, that for the MF of 130 Hz, peak magnitude values do not reach the same level reached for other MFs. In Bat 3, peak magnitudes of envelope modulation spectra for MF below 87 Hz remain at about the same level over the whole period of measurements (Fig. S3). Only for the MFs of 87 and 130 Hz an increase in peak magnitude is seen during juvenile development, which is strong for 87 Hz but only weak for 130 Hz.

In some cases, the ABR RMS amplitude displayed fluctuations over developmental time (see Fig. 4). We analyzed the EFR based on RMS-normalized averaged waveforms in order to guarantee that the nature of above-mentioned changes in the EFR were due to differences in its temporal fine structure and not only due to an increased ABR RMS amplitude.

The results show that the above-described age-dependent EFR pattern is also observable for normalized waveforms (Fig. 6 and Supplement S4). Thus, the fine structure of the SAM-noise evoked ABR waveform contributes substantially to the peak magnitude of envelope modulation spectra and to the maturation of the EFR, consequently.

3.4. Time course and amount of EFR maturation

As can be seen in Fig. 3, the chronological progression of the ERF maturation was different for the various MFs. In Bat 1, the increase of the peak magnitude of envelope modulation spectra reached a plateau on p15 for MFs up to 58 Hz. For higher MFs (87 and 130 Hz), the plateau-phase was reached later in time on p33. Differences between the different MFs can also been seen when comparing the range by which the peak magnitudes of envelope modulation spectra increased from the first measurement to the last recording day (Fig. 7, dark grey bars). For high MFs (87 and 130 Hz) an overall increase of 24 and 30 dB, respectively, was observed, whereas for lower MFs (11–58 Hz) peak magnitudes did not increase more than 18 dB. Therefore, the EFR in Bat 1 seems to be already stronger developed in early stages of the juvenile development for lower MFs compared to higher MFs.

In Bat 2, the same trend can be observed (Fig. 7, medium grey bars): Except for the MF of 38 Hz (16 dB peak magnitude), the peak magnitude changes for lower MFs was lower (range: −1 to 5 dB) than for the two highest MFs (25 and 10 dB, respectively). In Bat 2, the plateau-phase of peak magnitudes was reached at p20 for all MFs (Fig. S2).

The EFR to MFs up to 58 Hz showed little to no maturation in Bat 3 (Fig. 7, light grey bars). Consequently, the increase of peak magnitudes over time was low to non-existent and fluctuated in a range of −6 to +3 dB. Contrarily, MFs of 87 and 130 Hz showed an overall increase in the peak magnitude of the modulation spectrum (18 and 7 dB, respectively), which, however, was still less when compared to the increase observed in Bat 1 and Bat 2. In summary, at least in two animals, the maturation of the EFR was stronger and took longer for modulation frequencies above 87 Hz than for lower MFs, for which the EFR could be quite robust already at early stages of the post-natal development (from p8 on).

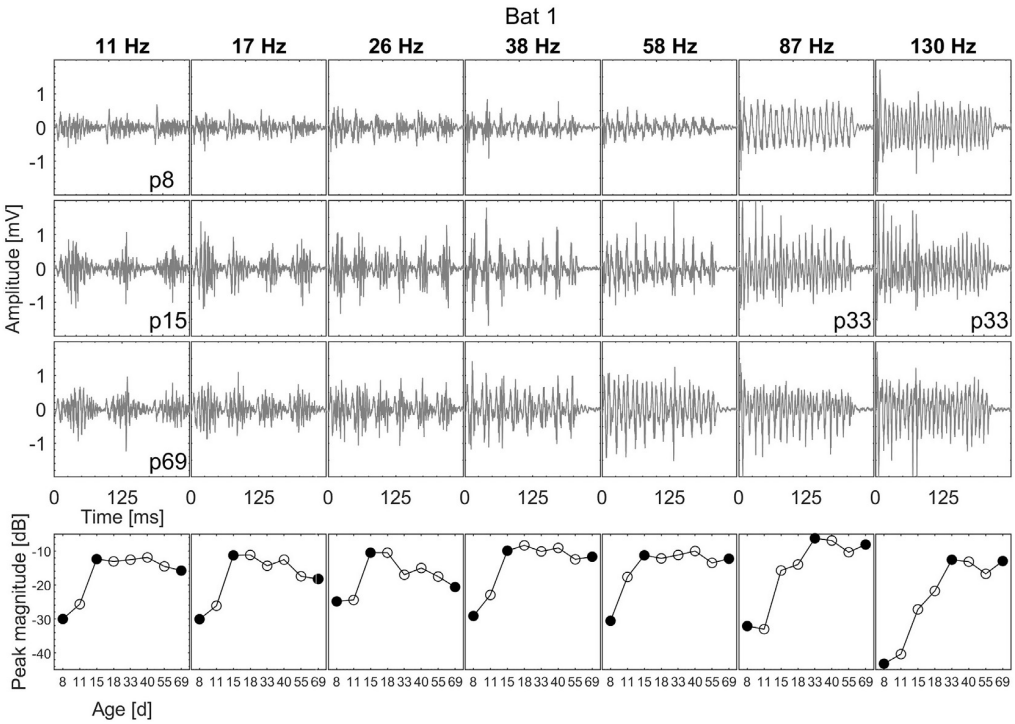

Fig. 3. Age-dependent development of the EFR in *P. discolor* (Bat 1) for seven different MFs. Row 1–3 show the SAM-noise evoked ABR waveforms over a duration of 250 ms. Row 4 shows the peak magnitude of the waveform-envelope modulation spectra. Black dots represent the postnatal days on which the waveforms shown in row1-3 were recorded.

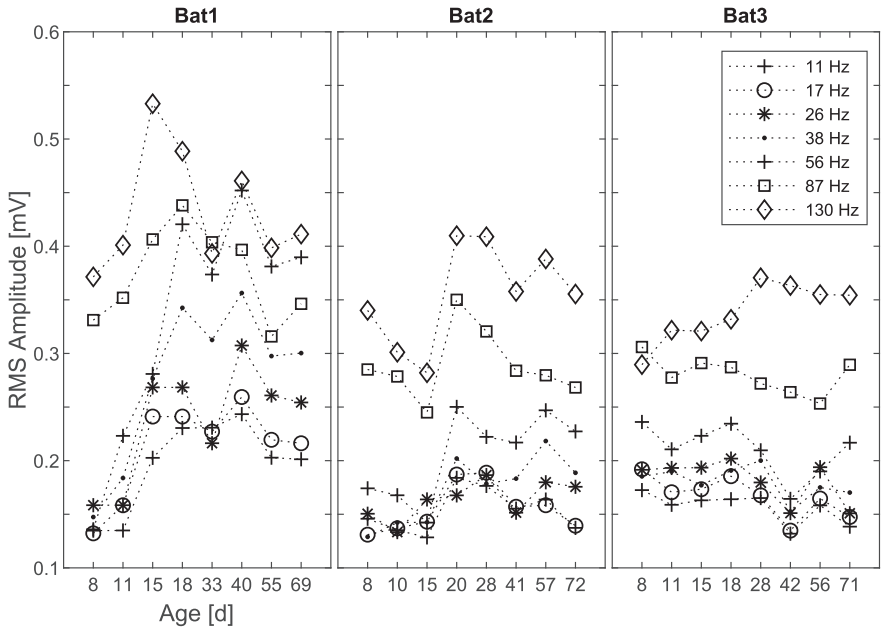

Fig. 4. Age-dependent development of the RMS amplitude of the SAM-noise evoked ABR waveforms.

4. Discussion

We measured EFRs during juvenile development of three *P. discolor* pups. EFRs were already present on p8. In two out of three animals, peak magnitude of envelope modulation spectra of SAM evoked ABRs increased consistently during development for most MFs, whereas the maturation of the EFR was slower for higher MFs.

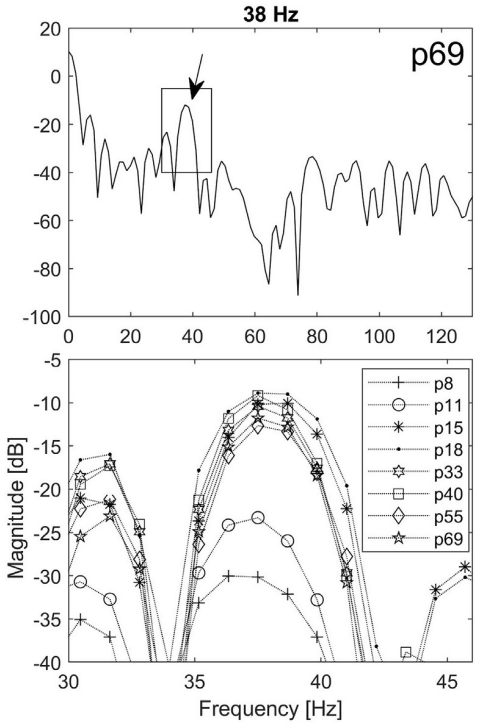

Fig. 5. Top: Modulation spectrum for the SAM (MF = 38Hz) evoked EFR recorded on p69 in Bat 1. The resulting spectral peak at 38 Hz is indicated by an arrow. Bottom: Age-dependent development of this spectral peak.

4.1. Waveform and development of click evoked ABRs

We measured click evoked ABRs to assess basic hearing abilities of the pups and as a quality check for recording conditions. The overall waveforms and duration of click evoked ABRs recorded in the present study were quite similar to those recorded by Linnenschmidt and Wiegrebe (2019) in the same species and up to seven waves were identifiable. Slight differences in the positioning of the electrodes might have contributed to the small differences observed in our recordings (e.g. ABR Wave II was as strong as Wave I) when compared with the results of Linnenschmidt and Wiegrebe (2019). Hearing thresholds established by click ABR fluctuated between 50 and 60 dB, which is 10–20 dB lower than measured by Linnenschmidt and Wiegrebe (2019), but still in a comparable range. Again, these differences might be due to slight differences in the recording set up e.g. in the positioning of the bats relative to the speaker. . Click ABR amplitudes typically decreased during juvenile development of the pups, however, as discussed in Linnenschmidt and Wiegrebe (2019), this effect is most probably due to growth of the head and attached muscles by which the electrodes become located in larger distance to the brain.

4.2. Development of the SAM-noise evoked ABR waveform and the EFR

As a trend, the RMS amplitude of the EFR increased with age at least for higher MFs. This finding falls in line with reported studies in rats and humans (e.g. Nodarse et al., 2012; Prado-Gutierrez et al., 2012) and can most likely be attributed to an increasing number of sensitive neurons and/or increasing neuronal temporal firing precision during post-natal development (Venkataraman and Bartlett, 2014).

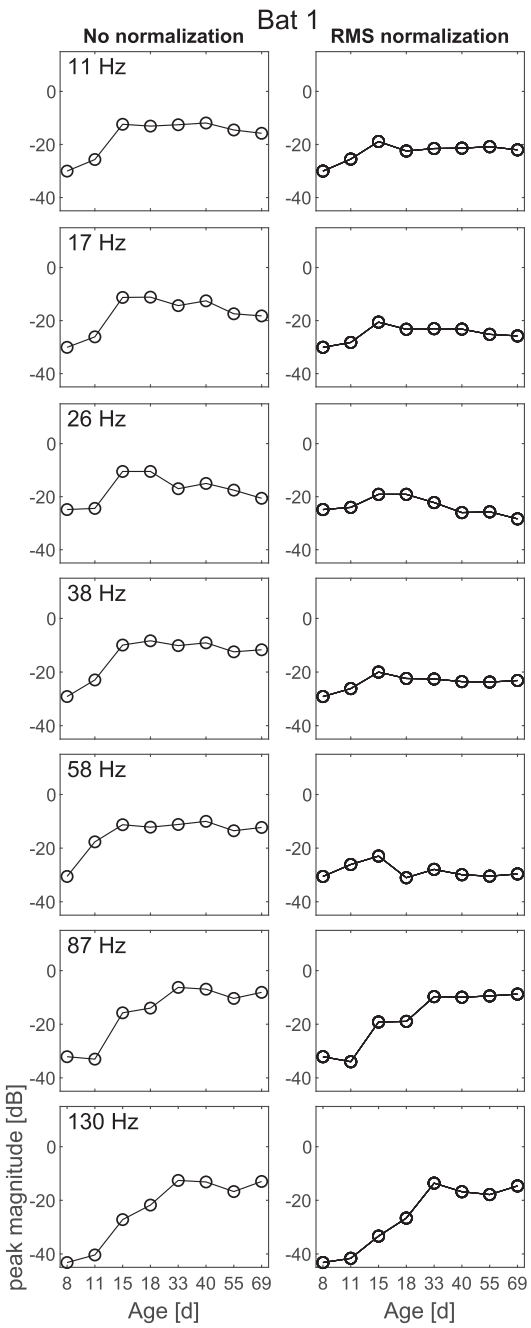

Fig. 6. Comparison of the age dependent development of the EFR in Bat 1 for non-normalized (left column, replotted from Fig. 3) and RMS-normalized SAM-noise evoked ABR waveforms (right column).

The increasing “peakyness” shown in Fig. 2 and described in 3.2 has also been shown in humans (Rance et al., 2006). Similar to our findings with click evoked ABRs, the threshold level of tone-burst evoked ABRs did not change and strong, “peaky” waves in the ABR responses emerged during maturation of the child.

In our study, the observed shape of SAM-noise evoked ABR waveforms to higher MFs corresponded to the waveforms shown in Venkataraman and Bartlett (2014). The observed changes in the ABR waveform shape might be explained by maturation of nuclei of

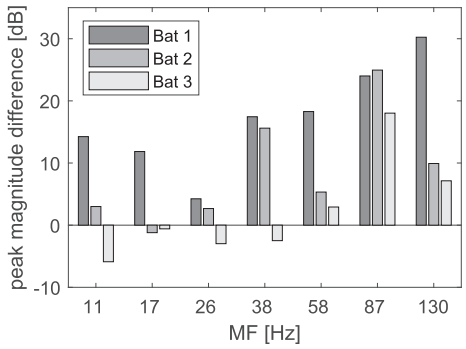

Fig. 7. Quantification of the MF dependent changes of the EFR during maturation for all three bats.
Changes in peak magnitude were calculated between the p8 and p69 (Bat 1), p72 (Bat 2) and p71 (Bat 3).

the ascending auditory pathway involved in amplitude modulation coding.

As a general trend, the fidelity by which ABR could follow noise envelope modulations increased during post-natal development in *P. discolor* pups. This was especially the case for the range of higher modulation frequencies tested in our study. Our findings corroborate earlier studies showing increasing best MFs to SAM stimuli (both tonal and noise carriers) and click-trains during the juvenile development of EFRs in rats (Prado-Gutierrez et al., 2012; Venkataraman and Bartlett, 2013) and for neuronal spike activity in the inferior colliculus (IC) of gerbils (Heil et al., 1995) and the auditory cortex of cats (Eggermont, 1993, 1991). Responsiveness to higher click-rates also increased in the cochlear nerve and the IC in mice (Sanes and Constantine-Paton, 1985).

The above-described development-dependent changes can be contributed to maturational processes of the cochlea (Johnson et al., 2005) and the ascending auditory pathway (e.g. increasing number of action potentials (AP) in stellate cells or decreasing AP duration in bushy cells (Müller et al., 2019)). Additionally, the myelination of axons and maturation of mechanisms underlying synaptic transmission also add to said changes (Brenowitz and Trussell, 2001; Müller et al., 2019; Prado-Gutierrez et al., 2012; Shu Hui Wu and Oertel, 1987; Venkataraman and Bartlett, 2013). In cats, the onset of myelination occurred at p5 and reached a rate of 70% by p10 (Ryugo et al., 2006). The endbulbs of Held undergo a reorganization into smaller compartments while increasing the volume fraction of the mitochondria and the synaptic vesicle density during the postnatal development of the animal. These changes ensure time-precise synaptic transmissions with short delay, which should be important for the encoding of high modulation frequencies (Ryugo et al., 2006).

The strong individual differences observed in the EFRs especially in Bat 3 might be contributed to differences in the electrode positioning, which is extremely intricate in bat pups of this young due to the small head size. This is supported by differences in the wave components of the click evoked ABRs (compare Figs. 1 and S1). Furthermore, we can of course not exclude developmental deficits of the auditory pathway in individual animals, although physically all three pups developed and behaved similarly.

In gerbils, a decrease of magnitude in the modulation spectrum with increasing modulation frequency has already been described (Dolphin and Mountain, 1992). In the range of 20–100 Hz modulation frequency, the peak magnitude fluctuated by ±3–4 dB, whereas for modulation frequencies greater than 100 Hz a decrease of 7–20 dB was observed. Similar findings have been reported for Fisher-344 rats, were strong decreases in the peak magnitude in the modulation spectrum were observed for modulation frequencies greater than 100 Hz (Parthasarathy et al., 2014). In our data, two out of three bats also displayed decreases in the peak magnitude of the modulation spectrum for frequencies larger than 100 Hz (compare Figs. S2 and S3, bottom row). However, in Bat 1 such a decrease was not observable. Therefore, it is not clear if this decrease might still be an effect of individual maturation, even though all three animals were of comparable age when measured.

As described by Dolphin et al. (1995), cetacean species do not show a drop-off in magnitude at such low modulation frequencies. The false killer whale *Pseudorca crassidens* showed no strong drop-off of the magnitude in the modulation spectrum for modulation frequencies of up to 1300 Hz, although a smaller drop-off occurred between 300 and 450 Hz. Similar findings were reported for the bottlenosed dolphin *Tursiops truncatus*, where the strong drop-off was shown for frequencies larger than 1500 Hz, with a slip dip in magnitude between 250 and 400 Hz modulation frequency. Therefore, there might be a preadaptation for high-fidelity temporal processing in echo locating animals, which might explain the differences in cut-off modulation frequency compared to rats and gerbils.

4.3. Functional implication for vocal development and species-specific communication

The here described developmental changes in the EFR (i.e. the improved responsiveness of the auditory brainstem to temporal modulation of sound envelope), although only observed in two of three juveniles of the bat *P. discolor*, might have (if generally applied) consequences on the development of vocal communication of this species. New born *P. discolor* pups reared without their mothers showed an altered structure (i.e. a reduced amount of temporal modulations) of the contact calls, typically used to communicate with their mothers (Esser and Schmidt, 1989). Other studies reported changes in fundamental frequency of the vocal communication repertoire of juvenile bats, which had been reared in isolation from adult conspecifics (Prat et al., 2015).

According to Esser and Schmidt (1989), communication between pups and mothers is, of course, bidirectional. The mother emit directive calls with resemble the contact/isolation calls emitted by the pups in their basic spectro-temporal structure. As described by Esser and Schmidt, the structure of the directive call influences the development of the isolation calls. Directive calls typically show frequency modulation, but also lesser degrees of amplitude modulation (Lattenkamp et al., 2019). However, in a natural social environment, pups also experience all other types of communication calls emitted by other group members. These include strongly amplitude modulated calls e.g. aggression calls (Hörpel and Firzlaff, 2019; Lattenkamp et al., 2019). Especially for vocal learning, auditory feedback is important to produce sounds that match a heard sound template (Brainard and Doupe, 2000; Nordeen and Nordeen, 1992; Tyack, 2016). The maturation period of the auditory system of *P. discolor*, and, regarding the prominent amount of temporal modulations in the communication calls of this species, especially the maturation of the EFR, therefore constitutes an important period during which the development of the vocal repertoire is accomplished. The fact, that at least for lower modulation frequencies the EFR can already be present (although not fully developed) at early ages of juvenile development (p8) would further support a possible role of processing of temporal modulation in mother infant communication.

Grants

This work was supported by Human Frontier Science Program (France)-Grant (RGP0058) to U. Firzlaff.

Declaration of competing interest

The authors declare no competing financial interests.

CRediT authorship contribution statement

Stephen Gareth Hörpel: Conceptualization, Methodology, Software, Investigation, Writing - original draft, Visualization. **Uwe Firzlaff:** Conceptualization, Methodology, Software, Writing - original draft, Visualization, Supervision, Funding acquisition.

Acknowledgements

We thank Lutz Wiegrebe for providing the experimental animals, his comments and input into the analysis. We would also like to thank Lutz Kettler for his comments on an earlier version of the manuscript.

Appendix A. Supplementary data

Supplementary data to this article can be found online at https://doi.org/10.1016/j.heares.2020.107904.

Abbreviations

ABR	auditory brainstem response
EFR	envelope following response
FFT	fast Fourier transformation
ITD	interaural time differences
RMS	root mean square
SAM	sinusoidally amplitude modulated
(pe)SPL	(peak equivalent) sound pressure level re 20 μPa

References

Bohn, K.M., Schmidt-French, B., Ma, S.T., Pollak, G.D., 2008. Syllable acoustics, temporal patterns, and call composition vary with behavioral context in Mexican free-tailed bats. J. Acoust. Soc. Am. 124, 1838–1848. https://doi.org/10.1121/1.2953314.

Boughman, J.W., 1998. Vocal learning by greater spear-nosed bats. Proc. R. Soc. B Biol. Sci. 265, 227–233. https://doi.org/10.1098/rspb.1998.0286.

Brainard, M.S., Doupe, A.J., 2000. Auditory feedback in learning and maintenance of vocal behaviour. Nat. Rev. Neurosci. 1, 31–40. https://doi.org/10.1038/35036205.

Brenowitz, S., Trussell, L.O., 2001. Maturation of synaptic transmission at end-bulb synapses of the cochlear nucleus. J. Neurosci. 21, 9487–9498.

Brown, P.E., Grinnell, A.D., Harrison, J.B., 1978. The development of hearing in the pallid bat, antrozous pallidus. J. Comp. Physiol. 126, 169–182. https://doi.org/10.1007/BF00666371.

Burkard, R.F., Eggermont, J.J., Don, M., 2007. Auditory Evoked Potentials: Basic Principles and Clinical Application. Lipincott Williams & Wilkins.

Dimitrijevic, A., Alsamri, J., John, M.S., Purcell, D., George, S., Zeng, F.-G., 2016. Human envelope following responses to amplitude modulation: effects of aging and modulation depth. Ear Hear. 37.

Dolphin, W.F., Mountain, D.C., 1992. The envelope following response: scalp potentials elicited in the Mongolian gerbil using sinusoidally AM acoustic signals. Hear. Res. 58, 70–78. https://doi.org/10.1016/0378-5955(92)90010-K.

Dolphin, W.F., Au, W.W.L., Nachtigall, P.E., Pawloski, J., 1995. Modulation rate transfer functions to low-frequency carriers in three species of cetaceans. J. Comp. Physiol. 177, 235–245. https://doi.org/10.1007/BF00225102.

Draganova, R., Schollbach, A., Schleger, F., Braendle, J., Brucker, S., Abele, H., Kagan, K.O., Wallwiener, D., Fritsche, A., Eswaran, H., Preissl, H., 2018. Fetal auditory evoked responses to onset of amplitude modulated sounds. A fetal magnetoencephalography (fMEG) study. Hear. Res. 363, 70–77. https://doi.org/10.1016/j.heares.2018.03.005.

Eggermont, J.J., 1991. Rate and synchronization measures of periodicity coding in cat primary auditory cortex. Hear. Res. 56, 153–167. https://doi.org/10.1016/0378-5955(91)90165-6.

Eggermont, J.J., 1993. Differential effects of age on click-rate and amplitude modulation-frequency coding in primary auditory cortex of the cat. Hear. Res. 65, 175–192. https://doi.org/10.1016/0378-5955(93)90212-J.

Esser, K.-H., Schmidt, U., 1989. Mother-infant communication in the lesser spear-nosed bat Phyllostomus discolor (chiroptera, phyllostomidae) — evidence for acoustic learning. Ethology 82, 156–168. https://doi.org/10.1111/j.1439-0310.1989.tb00496.x.

Esser, K.-H., Schmidt, U., 1990. Behavioral auditory thresholds in neonate lesser spear-nosed bats. Phyllostomus discolor. Sci. Nat. 77, 292–294. https://doi.org/10.1007/BF01131230.

Gaucher, Q., Huetz, C., Gourévitch, B., Laudanski, J., Occelli, F., Edeline, J.M., 2013. How do auditory cortex neurons represent communication sounds? Hear. Res. 305, 102–112. https://doi.org/10.1016/j.heares.2013.03.011.

Grinnell, A.D., 1963. The neurophysiology of audition in bats: resistance to interference. J. Physiol. 167, 114–127.

Heil, P., Schulze, H., Langner, G., 1995. Ontogenetic development of periodicity coding in the inferior colliculus of the Mongolian. Gerbil. Audit. Neurosci. 1, 363–383.

Hörpel, S.G., Firzlaff, U., 2019. Processing of fast amplitude modulations in bat auditory cortex matches communication call-specific sound features. J. Neurophysiol. 121 https://doi.org/10.1152/jn.00748.2018.

Johnson, S.L., Marcotti, W., Kros, C.J., 2005. Increase in efficiency and reduction in Ca2+ dependence of exocytosis during development of mouse inner hair cells. J. Physiol. 563, 177–191. https://doi.org/10.1113/jphysiol.2004.074740.

Khurana, S., Liu, Z., Lewis, A.S., Rosa, K., Chetkovich, D., Golding, N.L., 2012. An essential role for modulation of hyperpolarization-activated current in the development of binaural temporal precision. J. Neurosci. 32, 2814–2823. https://doi.org/10.1523/JNEUROSCI.3882-11.2012.

Knörnschild, M., 2014. Vocal production learning in bats. Curr. Opin. Neurobiol. 28, 80–85. https://doi.org/10.1016/j.conb.2014.06.014.

Knörnschild, M., Feifel, M., Kalko, E.K.V., 2014. Male courtship displays and vocal communication in the polygynous bat Carollia perspicillata. Behaviour 151, 781–798.

Kraus, H.J., Aulbach-Kraus, K., 1981. Morphological changes in the cochlea of the mouse after the onset of hearing. Hear. Res. 4, 89–102. https://doi.org/10.1016/0378-5955(81)90038-1.

Lattenkamp, E.Z., Shields, S.M., Schutte, M., Richter, J., Linnenschmidt, M., Vernes, S.C., Wiegrebe, L., 2019. The vocal repertoire of pale spear-nosed bats in a social roosting context. Front. Ecol. Evol. 7, 1–14. https://doi.org/10.3389/fevo.2019.00116.

Linnenschmidt, M., Wiegrebe, L., 2019. Ontogeny of auditory brainstem responses in the bat, Phyllostomus discolor. Hear. Res. 373, 85–95. https://doi.org/10.1016/j.heares.2018.12.010.

Linnenschmidt, M., Wahlberg, M., Damsgaard Hansen, J., 2013. The modulation rate transfer function of a harbour porpoise (Phocoena phocoena). J. Comp. Physiol. A 199, 115–126. https://doi.org/10.1007/s00359-012-0772-8. Neuroethol. Sensory, Neural, Behav. Physiol.

Lv, J., Simpson, D.M., Bell, S.L., 2007. Objective detection of evoked potentials using a bootstrap technique. Med. Eng. Phys. 29, 191–198. https://doi.org/10.1016/j.medengphy.2006.03.001.

Magnusson, A.K., Kapfer, C., Grothe, B., Koch, U., 2005. Maturation of glycinergic inhibition in the gerbil medial superior olive after hearing onset. J. Physiol. 568, 497–512. https://doi.org/10.1113/jphysiol.2005.094763.

Mikaelian, D., Ruben, R.J., 1965. Development of hearing in the normal cba-j mouse: Correlation of physiological observations with behavioral responses and with cochlear anatomy. Acta Oto- laryngologica.

Moore, D.R., 1982. Late onset of hearing in the ferret. Brain Res. 253, 309–311. https://doi.org/10.1016/0006-8993(82)90698-9.

Moushegian, G., Rupert, A.L., Stillman, R.D., 1973. Scalp-recorded early responses in man to frequencies in the speech range. Electroencephalogr. Clin. Neurophysiol. 35, 665–667. https://doi.org/10.1016/0013-4694(73)90223-X.

Müller, M.K., Jovanovic, S., Keine, C., Radulovic, T., Rübsamen, R., Milenkovic, I., 2019. Functional development of principal neurons in the anteroventral cochlear nucleus extends beyond hearing onset. Front. Cell. Neurosci. 13, 1–21. https://doi.org/10.3389/fncel.2019.00119.

Nodarse, E.M., Abalo, M.C.P., Fortuny, A.T., Hernández, M.V., Castellanos, A.L., 2012. Maturational changes in the human envelope-following responses. Acta Otorrinolaringol. 63, 258–264.

Nordeen, K.W., Nordeen, E.J., 1992. Auditory feedback is necessary for the maintenance of stereotyped song in adult zebra finches. Behav. Neural. Biol. 57, 58–66. https://doi.org/10.1016/0163-1047(92)90757-U.

Nourski, K.V., Brugge, J.F., 2011. Representation of temporal sound features in the human auditory cortex. Rev. Neurosci. 22, 187–203. https://doi.org/10.1515/RNS.2011.016.

Obrist, M.K., Wenstrup, J.J., 1998. Hearing and hunting in red bats (Lasiurus borealis, Vespertilionidae): audiogram and ear properties. J. Exp. Biol. 201, 143–154.

Parthasarathy, A., Datta, J., Torres, J.A.L., Hopkins, C., Bartlett, E.L., 2014. Age-related changes in the relationship between auditory brainstem responses and envelope-following responses. JARO J. Assoc. Res. Otolaryngol. 15, 649–661. https://doi.org/10.1007/s10162-014-0460-1.

Prado-Gutierrez, P., Mijares, E., Savio, G., Borrego, M., Martínez-Montes, E., Torres, A., 2012. Maturational time course of the envelope following response to amplitude-modulated acoustic signals in rats. Int. J. Audiol. 51, 309–316. https://doi.org/10.3109/14992027.2011.639812.

Prat, Y., Taub, M., Yovel, Y., 2015. Vocal learning in a social mammal: demonstrated by isolation and playback experiments in bats. Sci. Adv. 1, 1–6. https://doi.org/10.1126/sciadv.1500019.

Rance, G., Tomlin, D., Rickards, F.W., 2006. Comparison of auditory steady-state responses and tone-burst auditory brainstem responses in normal babies. Ear Hear. 27, 751–762. https://doi.org/10.1097/01.aud.0000240491.68218.

Razak, K.A., Fuzessery, Z.M., 2007. Development of functional organization of the pallid bat auditory cortex. Hear. Res. 228, 69–81. https://doi.org/10.1016/j.heares.2007.01.020.

Rübsamen, R., Neuweiler, G., Marimuthu, G., 1989. Ontogenesis of tonotopy in inferior colliculus of a hipposiderid bat reveals postnatal shift in frequency-place code. J. Comp. Physiol. 165, 755–769. https://doi.org/10.1007/BF00610874.

Ryugo, D.K., Montey, K.L., Wright, A.L., Bennett, M.L., Pongstaporn, T., 2006. Postnatal development of a large auditory nerve terminal: the endbulb of Held in cats. Hear. Res. 216–217, 100–115. https://doi.org/10.1016/j.heares.2006.01.007.

Sanes, D.H., Constantine-Paton, M., 1985. The development of stimulus following in the cochlear nerve and inferior colliculus of the mouse. Dev. Brain Res. 22, 255–267. https://doi.org/10.1016/0165-3806(85)90177-4.

Simmons, A.M., Boku, S., Riquimaroux, H., Simmons, J.A., 2015. Auditory brainstem responses of Japanese house bats (Pipistrellus abramus) after exposure to broadband ultrasonic noise. J. Acoust. Soc. Am. 138, 2430–2437. https://doi.org/10.1121/1.4931901.

Simmons, A.M., Hom, K.N., Warnecke, M., Simmons, J.A., 2016. Broadband noise exposure does not affect hearing sensitivity in big brown bats (Eptesicus fuscus). J. Exp. Biol. 219, 1031–1040. https://doi.org/10.1242/jeb.135319.

Smith, A.J., Owens, S., Forsythe, I.D., 2000. Characterisation of inhibitory and excitatory postsynaptic currents of the rat medial superior olive. J. Physiol. 529, 681–698. https://doi.org/10.1111/j.1469-7793.2000.00681.x.

Sonntag, M., Englitz, B., Kopp-Scheinpflug, C., Rübsamen, R., 2009. Early postnatal development of spontaneous and acoustically evoked discharge activity of principal cells of the medial nucleus of the trapezoid body: an in vivo study in mice. J. Neurosci. 29, 9510–9520. https://doi.org/10.1523/JNEUROSCI.1377-09.2009.

Sterbing, S.J., 2002. Postnatal development of vocalizations and hearing in the phyllostomid bat, Carollia perspicillata. J. Mammal. 83, 516–525. https://doi.org/10.1644/1545-1542(2002)083<0516:pdovah>2.0.co;2.

Tyack, P.L., 2016. Vocal learning and auditory-vocal feedback. In: Vertebrate Sound Production and Acoustic Communication. Springer, pp. 261–295.

Vater, M., Foeller, E., Mora, E.C., Coro, F., Russell, I.J., Kössl, M., 2010. Postnatal maturation of primary auditory cortex in the mustached bat, Pteronotus parnellii. J. Neurophysiol. 103, 2339–2354. https://doi.org/10.1152/jn.00517.2009.

Venkataraman, Y., Bartlett, E.L., 2013. Postnatal development of synaptic properties of the GABAergic projection from the inferior colliculus to the auditory thalamus. J. Neurophysiol. 109, 2866–2882. https://doi.org/10.1152/jn.00021.2013.

Venkataraman, Y., Bartlett, E.L., 2014. Postnatal development of auditory central evoked responses and thalamic cellular properties. Dev. Neurobiol. 74, 541–555. https://doi.org/10.1002/dneu.22148.

Walker, B.A., Gerhards, C.M., Werner, L.A., Horn, D.L., 2019. Amplitude modulation detection and temporal modulation cutoff frequency in normal hearing infants. J. Acoust. Soc. Am. 145, 3667–3674. https://doi.org/10.1121/1.5111757.

Walsh, E.J., McGee, J., Javel, E., 1986. Development of auditory-evoked potentials in the cat. III. Wave amplitudes. J. Acoust. Soc. Am. 79, 745–754. https://doi.org/10.1121/1.393463.

Wenstrup, J.J., 1984. Auditory sensitivity in the fish-catching bat, Noctilio leporinus. J. Comp. Physiol. 155, 91–101. https://doi.org/10.1007/BF00610934.

Wu, Shu Hui, Oertel, D., 1987. Maturation of synapses and electrical properties of cells in the cochlear nuclei. Hear. Res. 30, 99–110. https://doi.org/10.1016/0378-5955(87)90187-0.

5 The frontal auditory field: response properties and connectivity

The fifth chapter of the thesis covers an area in the frontal cortex of *Phyllostomus discolor*, which is responsive to auditory stimuli and which is called the frontal auditory field (FAF). The FAF receives not only inputs via the ascending auditory pathway, but also via an extralemniscal pathway and it has been hypothesised that it plays a role in linking both auditory and motor-systems. However, the neuronal response properties of the FAF are unknown for *Phyllostomus discolor*, so I recorded from 42 cortical neurons in two bats and analysed the results offline. Firstly, I measured the basic response properties of the neurons in the FAF by presenting pure-tone stimuli with varying frequency and sound pressure level. I could show that while the FAF neurons show a similar mean best frequency and mean threshold when compared to neurons in the auditory cortex, the temporal response properties differed strongly, with the FAF displaying a high response latency and longer, purely tonic responses. Furthermore, the tuning quality of the neurons in the FAF was broad, which is comparable to the tuning quality of neurons in the auditory cortex. Additionally and similar to Chapter 3, I also presented the same call library consisting of natural echolocation and social communication calls. Unlike the results from the auditory cortex of *Phyllostomus discolor*, the mean FAF response showed no preference for a specific call type. After conclusion of the electrophysiological experiments, the position of the recording sites was reconstructed, therefore pinpointing the location of the FAF in *Phyllostomus discolor*, which had not been done before. In a final set of experiments, a neuronal tracer was injected into the FAF of two bats in order to determine the neurocircuitry innervating it. Labelling was found in the auditory cortex, the thalamus and the amygdala, however, due to experimental constraints, these tentative findings are to be taken with reservations.

Both my supervisor and I were involved in the conceptualisation of the experiments, the methodology and software required and the visualisation of the results. Additionally, I performed all the experiments, while my supervisor contributed both the project supervision and project funding. The brain areas targeted by the neuronal tracing studies were identified with help from Susanne Radtke-Schuller. Although this chapter is unpublished at the date of thesis submission, it is in preparation for peer-reviewed submission and publication.

5.1 Introduction

The frontal cortex of the mammalian brain is typically considered to be involved in cognitive processes as stimulus selection and decision making (Rogers et al. [1999], Daw et al. [2006], Fritz et al. [2010], Rushworth et al. [2011]). The cognitive control of vocalisation in particular has become a major focus in research over the last decades (Loh et al. [2017], Gavrilov et al. [2017]). The prefrontal cortex (PFC) is now considered to be an important region in the network, enabling volitional control of vocalisations in primate and non-primate mammals (Paus [2001], Simões et al. [2010]). Consequently, the frontal/prefrontal cortex is also considered to be an important substrate for vocal learning in mammals (Arriaga et al. [2012]). The ventrolateral PFC in non-human primates receives input from physiologically and anatomically defined auditory cortex (Rauschecker et al. [1995], Hackett et al. [1998], Romanski et al. [1999a], Romanski et al. [1999b]) and Romanski and Goldman-Rakic [2002] reported neurons in the macaque ventrolateral PFC responding to complex sounds like animal vocalisations. In awake and trained rhesus monkeys, activity of neurons in the ventrolateral PFC predicted the preparation of instructed vocalisations (Hage and Nieder [2013]).

Bats are known to express a rich repertoire of sounds for social communication (Bohn et al. [2008], Lattenkamp et al. [2019]), and are supposed to be among the few mammalian species capable of vocal learning (Esser and Schubert [1998], Knörnschild [2014], Prat et al. [2015], Lattenkamp et al. [2018]). Besides extensive work on the ascending auditory pathway in bats which mostly investigated bio-sonar related functions (Pollak and Casseday [1989], Olsen and Suga [1991], Casseday and Covey [1992], Park and Pollak [1993], Ohlemiller et al. [1996], Portfors and Wenstrup [2002]), considerably less research has investigated frontal cortical areas which might be involved in control of vocalisations, relying on auditory input as feedback for fine-tuned motor control. Besides one study highlighting the role of the anterior cingulate cortex (ACC) for vocal control (Gooler and O'Neill [1987]), most work focused on an area responsive to auditory stimulation, the frontal auditory field (FAF) in two bat species (*Pteronotus parnellii*: Kobler et al. [1987], Casseday et al. [1989], Kanwal et al. [2000]; *Carollia perspicillata*: Eiermann and Esser [2000], López-Jury et al. [2019]). Neuroanatomical tracer studies in *P. parnellii* demonstrated direct projections from a division of the auditory thalamus, the suprageniculate nucleus to the FAF (Kobler et al. [1987]), therefore labelling the FAF as a target region of the extralemniscal pathway (Casseday et al. [1989]). However, the FAF also receives direct input from the auditory cortex (Kobler et al. [1987]). In *C. perspicillata*, studies on anatomical projections are sparse (Eiermann [2000]). Electrophysiological studies on neuronal response properties in the FAF show a common feature in both *P. parnellii* and *C. perspicillata*: Neurons often display only loosely time locked firing patterns with long latencies (Kanwal et al. [2000], Eiermann and Esser [2000], López-Jury et al. [2019]), although local field-potential evoked by acoustic stimuli could have shorter latencies (García-Rosales et al. [2020]). Furthermore, García-Rosales et al. [2020] demonstrated coherent, sound-onset evoked gamma-oscillations in the FAF and the AC, suggesting functional coupling between these two auditory brain regions. In general, the FAF may broadly serve to link auditory and motor-systems, as it also projects

to the superior colliculus, which is a major hub for sensory-motor-integration (Kobler et al. [1987], Valentine et al. [2002]). I used extracellular recordings under stereotaxic-control to demonstrate an area responsive to acoustic stimulation in the frontal cortex of the bat *Phyllostomus discolor*. Neuroanatomical tracing techniques indicated connections of this area to the thalamus, the auditory cortex, the striatum and the amygdala, however, these preliminary findings need to be validated in additional experiments.

5.2 Methods

5.2.1 Surgery

All the experiments complied with the principles of laboratory animal care and were conducted following the regulations of the current version of the German Law on Animal Protection (approval ROB-55.2-2532.Vet_02-13-147, Regierung von Oberbayern). The bats (*Phyllostomus discolor*; 3 adult females, one adult male) originated from a breeding colony situated in the Department Biology II of the Ludwig-Maximilian University of Munich. For experiments, animals were kept separated from other bats under semi-natural conditions (12 h day/12 h night cycle, 65%–70% relative humidity,28 °C) with free access to food and water. The surgical procedures are described in detail in previous publications (Hoffmann et al. [2008], Hörpel and Firzlaff [2019], see Chapter 3). Details of the stereotaxic device and the procedure used to reconstruct the recording sites are described elsewhere (Schuller et al. [1986]). Briefly, the alignment of the animal's skull and the underlying brain within the stereotaxic coordinate system was measured by scanning the characteristic profile lines of the skull in the parasagittal and frontal planes. These profiles were then digitally fitted to a standardized skull profile in a standardized coordinate system. To alleviate postoperative pain, an analgesic (0.2 μg/g body weight; Meloxicam, Metacam, Boehringer-Ingelheim) was administered after the surgery for four postoperative days. The anaesthesia was antagonized with a mixture of atipamezole (Alzane®, Novartis), flumazenil (Flumazenil, Hexal) and naloxone (Naloxon-ratiopharm®, Ratiopharm), which was injected subcutaneously (2.5, 0.5 and 1.2 μg/g body weight, respectively). The bats were treated with antibiotics (0.5 μg/g body weight; enrofloxacin, Baytril®, Bayer AG) for four postoperative days.

5.2.2 Acoustic stimulation

The acoustic stimulation has been described in great detail in Chapter 3 and in Hörpel and Firzlaff [2019], however, the stimuli were presented and the data were plotted using AudioSpike (HörTech gGmbH, Oldenburg, Germany). To summarise, a frequency response curve of the neuron under test was established by presenting pure tone stimuli with a frequency range from 5 to 80 kHz (logarithmically spaced in 1/8 octave steps) and SPL from 80 dB to 15 dB re 20 μPa (20 ms duration of each pure tone preceded by 50 ms silence, 2 Hz repetition rate, stimuli presented in random order and repeated 10 times). Additionally, each neuron was presented with a extensive library of *Phyllostomus discolor* communication calls (described below in great detail), with 20 repetitions per

call in random order at at a level of approximately 15 to 20 dB above CF threshold. Since *Phyllostomus discolor* has a rich vocal repertoire (Lattenkamp et al. [2019]), I used an extensive call library consisting of 25 different vocalisations grouped into 5 classes. Classes 1 and 2 were typical echolocation calls, therefore short in duration and multi-harmonic. Class 1 calls differed from class 2 calls by lacking the lowest harmonic at roughly 20 kHz (see Figure 5.1). Call class 3 consisted of long amplitude and frequency modulated calls with relatively low fundamental frequency of approximately 13 kHz (see Figure 5.1). These calls are usually associated with aggressive behaviour towards conspecifics. Class 4 calls showed no amplitude modulations, were shorter in duration and had a higher fundamental frequency of about 17 kHz (see Figure 5.1). The calls were very similar to mother-pup contact or appeasement calls, as shown by Esser and Schubert [1998]. Class 5 calls consisted of a varying number of short broadband sound elements separated by approximately 8 ms and thus giving rise to strong amplitude modulations (see Figure 5.1). In contrast to class 3, class 5 calls showed no frequency modulations and had a significantly lower fundamental frequency of approximately 7.5 kHz. The stimuli assigned to call classes 3 to 5 were previously used in Hörpel and Firzlaff [2019] (see Chapter 3, Call class 3 = call category 1 in the publication, class 4 = category 2 and class 5 =category 3). Due to changes in the stimulus presentation hardware, the stimuli had to be resampled to 192 kHz sampling rate (unlike the 195.312 kHz sampling rate used in Hörpel and Firzlaff [2019]).

5.2.3 Electrophysiological recordings

The recording procedure was similar to the one described in Chapter 3 and in Hörpel and Firzlaff [2019]. Changes were made to the hardware used in the experiments. The electrode signal was recorded using a AD-Converter (Fireface 400, RME, Haimhausen, Germany; sampling rate 25 kHz, band-pass filter 400-3000 Hz) and AudioSpike (HörTech gGmbH, Oldenburg, Germany). All acoustic stimuli were computer-generated (Matlab 2018b; Mathworks, Natick, MA, USA), digital–analogue converted (Fireface 400, RME, Haimhausen, Germany; sampling rate 192 kHz), amplified (AX-396, Yamaha Music Foundation, Tokyo, Japan) and presented via free-field loudspeaker (R2904/700000, Scan-Speak, Videbæk, Denmark). The loudspeaker had been calibrated for linear frequency response between 1 kHz to 96 kHz.

5.2.4 Tracing experiments

In order to determine the neurocircuitry innervating the frontal auditory field, I pressure-injected (Nanoliter 2010 injector, World Precision Instruments, Sarasota, FL, USA) a neuronal tracer (18.2 nl of 10% Alexa Fluor 488, 10.000 MW, Thermo Fisher Scientific, Waltham, MA, USA) into the FAF. The injection site was electrophysiologically validated. After a survival time of 5 days, the animals were sedated with MMF (medetomidine (Dorbene®, Zoetis), midazolam (Dormicum®, Hoffmann-La Roche) and fentanyl (Fentadon®, Albrecht) at a dosage of 0.4, 4.0 and 0.04 μg/g body weight, respectively), euthanised with an injection of pentobarbital (Narcore,®, Boehringer

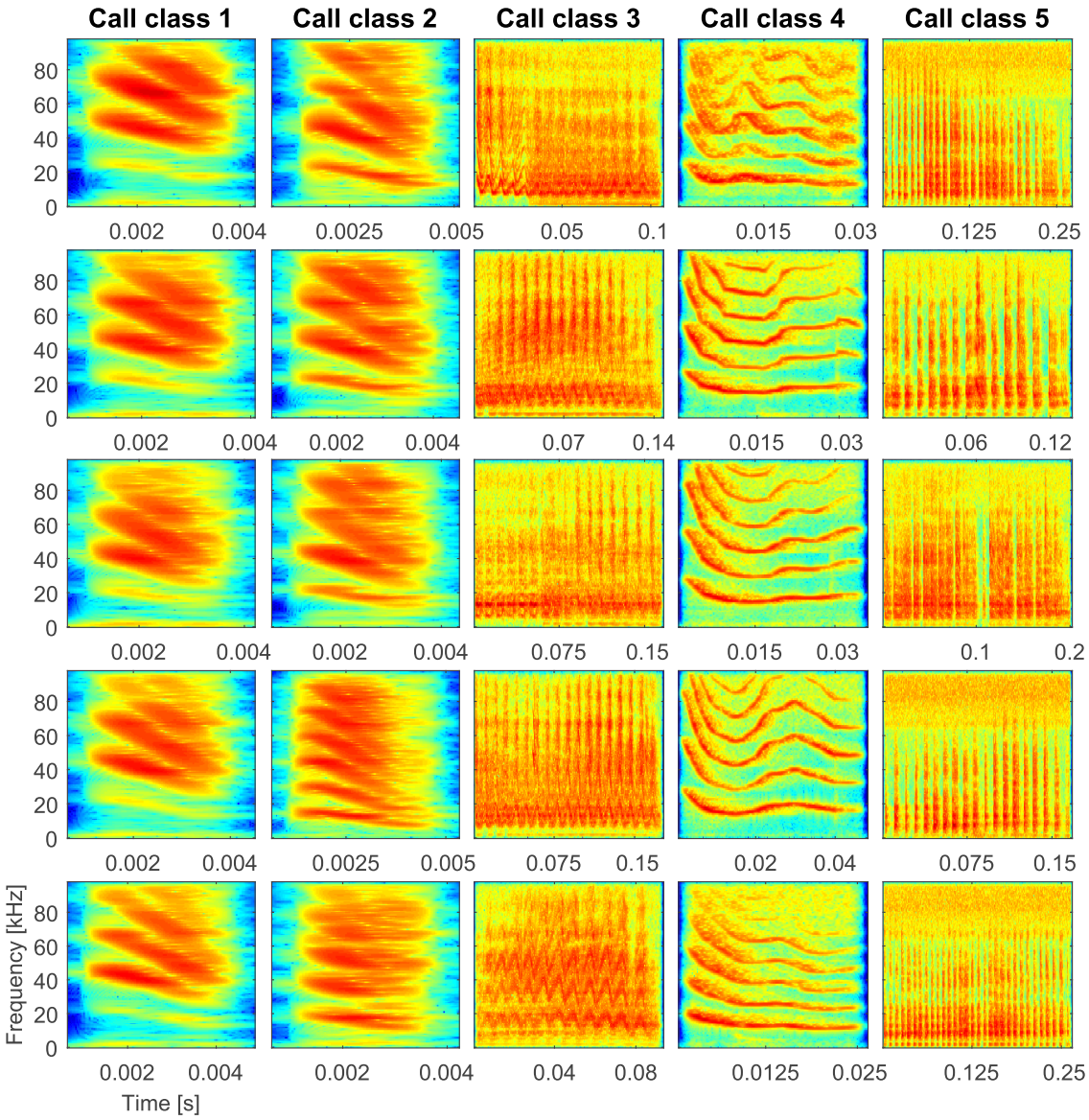

Figure 5.1: Call library used in the recordings from the frontal auditory field in *Phyllostomus discolor:* 25 calls grouped into 5 different call classes, class 1 and 2 are echolocation calls with (class 2) or without a ∼20 kHz harmonic. Class 3 and 5 are amplitude modulated aggression calls with (class 3) or without (class 5) sinusoidal frequency modulations. Class 4 calls are sinusoidally frequency modulated appeasement or contact calls used in mother-pup interactions. The colour coding shows the distribution of sound energy within the individual stimuli and ranges from dark blue (low energy) to bright red (high energy)

Ingelheim Vetmedica GmbH, 0.16 mg/g bodyweight) and perfused transcardially (4%

paraformaldehyde). The animals were dissected and the brains cryoprotected in 30% sucrose solution. They were then embedded (Schuller et al. [1986]) and sliced to 40 μm thickness using a sliding microtome (Microm HM440E, Thermo Fisher Scientific). The slices were mounted (VECTASHIELD® HardSet™ Antifade Mounting Medium H-1400) and digitised (10 times magnification, 20 layer Z-stack, Axio Scan.Z1, Carl Zeiss Microscopy GmbH, Jena, Germany). Successfully labelled fibres and neurons were identified manually by observation of the images and their position was determined by comparing the results to a brain atlas of *Phyllostomus discolor* (Radtke-Schuller et al., in prep.).

5.3 Data analysis

Spike responses from the pure-tone and 25 natural stimuli were displayed as PSTHs (peristimulus time histogram, bin width 1 ms) and raster plots. Generally, the neuronal firing was quantified in a response window starting at the beginning of the neuronal discharge and spanning the duration of said discharge (end of response window). The neuronal latency was also quantified using the PSTH of a neuron, it describes the time from stimulus onset to an increase of neuronal activity of the neuron under investigation. The characteristic frequency (CF; frequency at which a given neuron responds to the lowest sound intensity) and its corresponding threshold SPL as well as the best frequency (BF, frequency and SPL at which a given neuron shows a maximum response) of the neurons under investigation were measured. Finally, the tuning quality (Q_{10dB}) of each neuron under investigation was calculated offline, with Q_{10dB} values greater than 10 indicating sharply tuned neurons, whereas lower values are characteristic for more broadly tuned neurons (Thomas et al. [2007]). For the natural stimuli, the mean spike rates of the neuronal responses to aggression (call classes 3 and 5, $R_{\text{agg.}}$) and appeasement/contact calls (call class 4, $R_{\text{cont.}}$) were calculated over a 400 ms response window, starting at the stimulus presentation. Using the following equation (*Equation (5.1)*; Wang et al. [1995], Wang and Kadia [2001], Schnupp et al. [2006]), the "selectivity index" d_{i} of each unit was calculated. This course of action was identical to the procedures described in Chapter 3 and published in Hörpel and Firzlaff [2019].

$$d_{\text{i}} = \frac{R_{\text{agg.}} - R_{\text{cont.}}}{R_{\text{agg.}} + R_{\text{cont.}}} \tag{5.1}$$

The d_{i} ranges from +1 to -1, indicating a neuron responding only to the aggression call (+1) or only to the contact call (-1), with a 50% difference between $R_{\text{agg.}}$ and $R_{\text{cont.}}$ resulting in a d_{i} of $\pm$ 0.3.

5.4 Results

In total, recordings were achieved from 42 cortical neurons in two bats and their position reconstructed (see Figure 5.2) as described by Schuller et al. [1986]. These reconstructed positions match the positions of lesions within the cortex, which were caused by the

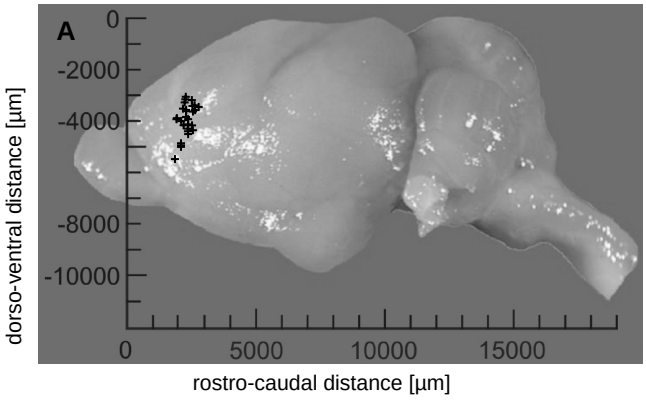

Figure 5.2: Position of cortical neurons in the frontal auditory field of *Phyllostomus discolor*: Reconstruction of the recorded neurons within the frontal cortex. Note low dispersion in rostro-caudal dimension.

penetration of the recording electrodes (See Figure 5.3). Additionally, the neurocircuitry innervating the frontal auditory field could be outlined by neuronal tracing in two bats.

5.4.1 Electrophysiology

Spike responses from the pure-tone and 25 natural stimuli were displayed as PSTHs (peri-stimulus time histogram, bin width 1 ms) and raster plots. Generally, the neuronal firing was quantified in a response window starting at the beginning of the neuronal discharge (green line) and spanning the duration of said discharge (end of response window indicated by red line, see Figure 5.4).

5.4.1.1 Basic neuronal response properties to pure-tone stimuli

The characteristic frequency (CF; frequency at which a given neuron responds to the lowest sound intensity) and its corresponding threshold SPL as well as the best frequency (BF, frequency and SPL at which a given neuron shows a maximum response) of the neurons under investigation were measured. This was achieved by calculating the median neuronal response rate (over 10 repetitions) for every frequency and SPL tested.

The neuronal latency was quantified using the PSTH of a neuron, which describes the time from stimulus onset (blue line) to an increase of neuronal activity of the neuron under investigation (green line), as indicated by the arrows in Figure 5.4.

As can be seen in Figure 5.5A, there is a clear inclination towards high frequency CFs, with the majority of the neurons showings CFs in the range of 55 to 75 kHz. The mean CF of all 42 units was 58.7 ± 18.2 kHz (median CF = 67 kHz). Additionally, the BFs of the neurons were also analysed . Similar to the CFs, there was also a inclination towards high frequency BFs in the range of 55 to 85 kHz (See Figure 5.5B). The mean BF of all

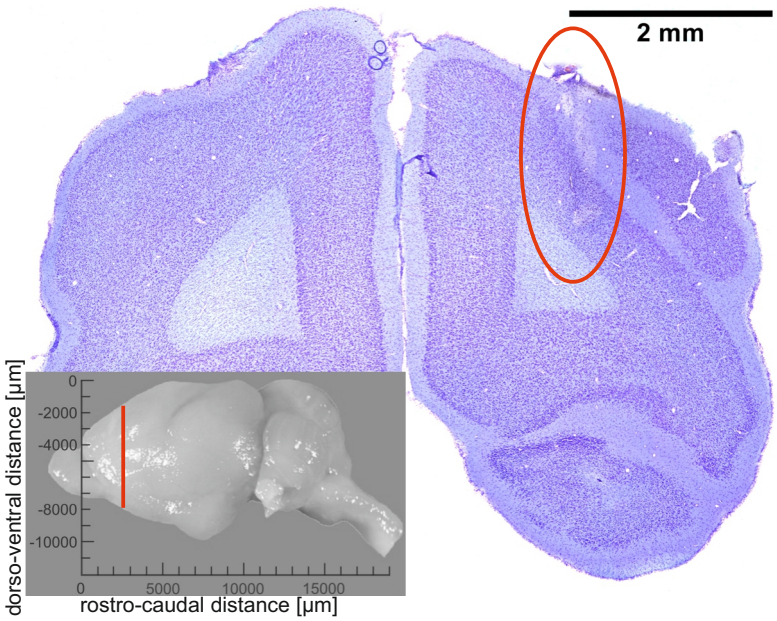

Figure 5.3: Bright field image of a Nissl stained slice containing the FAF and corresponding position in the brain: 40 μm thick slice of a *Phyllostomus discolor* brain containing the FAF, note penetration lesion from recording electrode in the dorsal part of the right hemisphere indicated by a red ellipse. The inlay (bottom left) shows the position of the section plane in the brain.

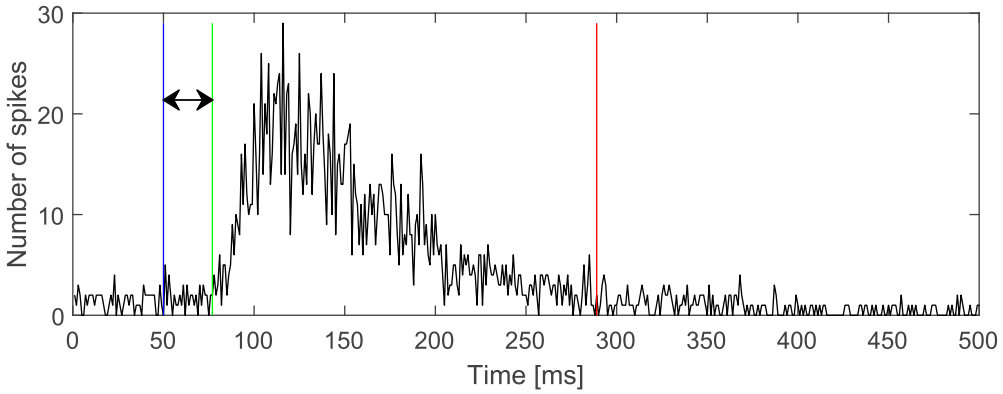

Figure 5.4: PSTH of a neuronal response in the FAF: Stimulus onset (blue line) was at 50 ms and the onset of neuronal activity is indicated by the green line. The neuronal latency is symbolised by the arrow. The return of the neuronal discharge to the background activity is marked with a red line.

42 units was 56.2 ± 24.8 kHz (median BF: 65 kHz; interquartile range (IQR): 30 kHz). As can be seen in Figure 5.5C, the sound pressure thresholds for neuronal responses are broadly distributed, with a majority of the neurons requiring sound pressure levels in the range of 55 to 65 dB to elicit responses at their BFs. The mean SPL required to elicit neuronal responses at the BFs of the neurons was 50 ± 19.2 dB (median SPL: 56.5 dB, IQR: 35 dB). The latencies of the neuronal responses (i.e. the time from stimulus onset to onset of neuronal discharge) were also measured. As can be seen in Figure 5.5D, the majority of neurons displayed latencies between 15 and 35 ms, with the mean latency being 32.7 ± 13.0 ms (median latency: 33 ms; IQR: 11 ms). Additionally, the duration of the neuronal discharge after stimulus presentation was determined . As can be seen in Figure 5.5E, the duration is more spread out with no clear preference, although two larger groups (37.5 to 62.5 ms and 87.5 to 112.5 ms, respectively) are noticeable. The mean duration of the neuronal discharge was 91.0 ± 24.8 ms (median duration: 92.5 ms, IQR :60 ms). As a final step, I analysed the tuning quality (Q_{10db}) of the neurons under investigation. Generally speaking, the neurons in the FAF showed almost exclusively broad tuning properties with a mean Q_{10db} of 3.5 ± 2.3748 (median Q_{10db}: 4; IQR: 2.6) with only a single neuron (2.38%) displaying a Q_{10db} value exceeding 10 (see Figure 5.5F). The regression line plotted in Figure 5.5G shows only a small increase in Q_{10db} with increasing BFs.

5.4.1.2 Call selectivity

As previously mentioned, it was also analysed whether the neurons under investigation showed preferences towards the different call types in their response behaviour, this was done for a total of 33 neurons. Generally speaking, the results from the FAF show greater variability when compared to the findings from the AC (Chapter 3 and Hörpel and Firzlaff [2019]). I found 3 major response categories, with multiple units showing strong responses to echolocation and contact calls (Category I, see Figure 5.6). Additionally, there were also units which responded stronger to aggression calls (Category II, see Figure 5.7) and finally, a large number of units showed no preferential response pattern whatsoever (Category III, see Figure 5.8). However, all units responded in a purely tonic firing pattern, resulting in a lack of a strong temporal response pattern in the raster plots of Figures 5.6 - 5.8.

To enable the comparison of the results from the FAF with the results from the AC of *Phyllostomus discolor*, I calculated the d_i for the call classes 3 to 5, i.e. the aggression and contact calls, as the d_i values obtained in the AC were calculated for these call classes, only. Of the 33 units recorded, a total of 6 units (18.2%) had a strong preference for the contact/appeasement calls ($d_i < -0.3$), whereas 5 units (15.2%) showed a strong preference towards the aggression calls ($d_i > 0.3$). A majority of 22 units (66.7%) had d_i values between -0.3 and 0.3 and therefore showed no strong preference to either the contact/appeasement or aggression calls, respectively. The mean d_i of all 33 recorded units was 0.0486 ± 0.3606 (median $d_i = 0.0848$), further emphasising the broader variability in the neuronal responses and preferences, especially when compared to the data from the AC (see Chapter 3 and Hörpel and Firzlaff [2019]), where a total of

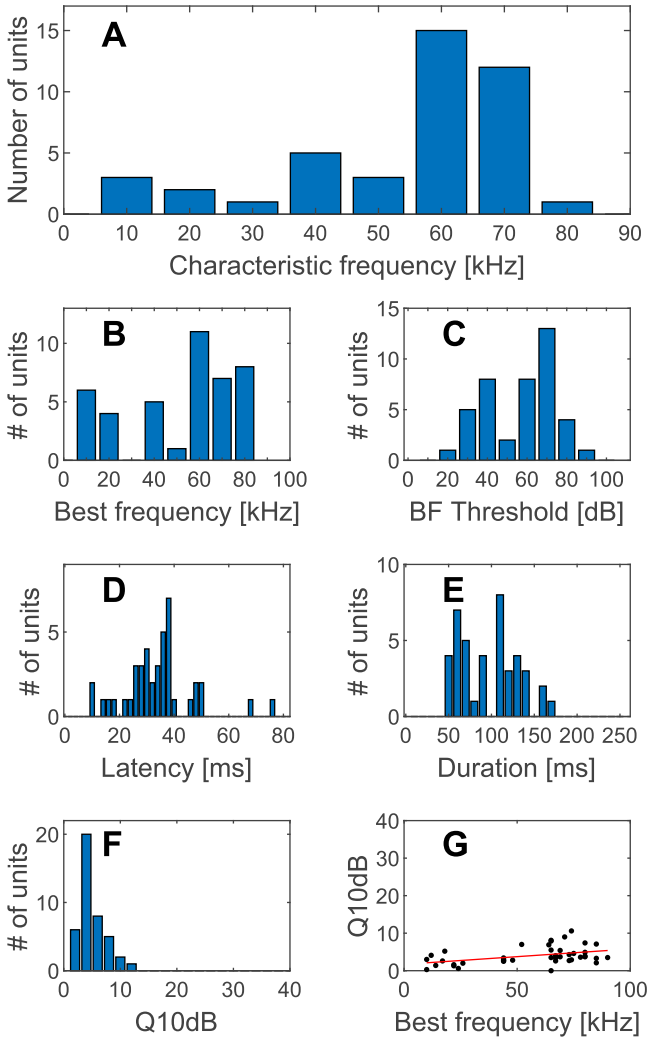

Figure 5.5: Distribution of response properties of 42 cortical units in the FAF of *Phyllostomus discolor*: The frequency distribution of neuronal response properties evoked by pure-tone stimulation is shown for: (A) Characteristic frequency, (B) Best frequency, (C) Response threshold, (D) First spike latency, (E) Response duration (F) Q_{10dB} values and (G) Q_{10dB} values as a function of best frequency with a linear regression line plotted in red.

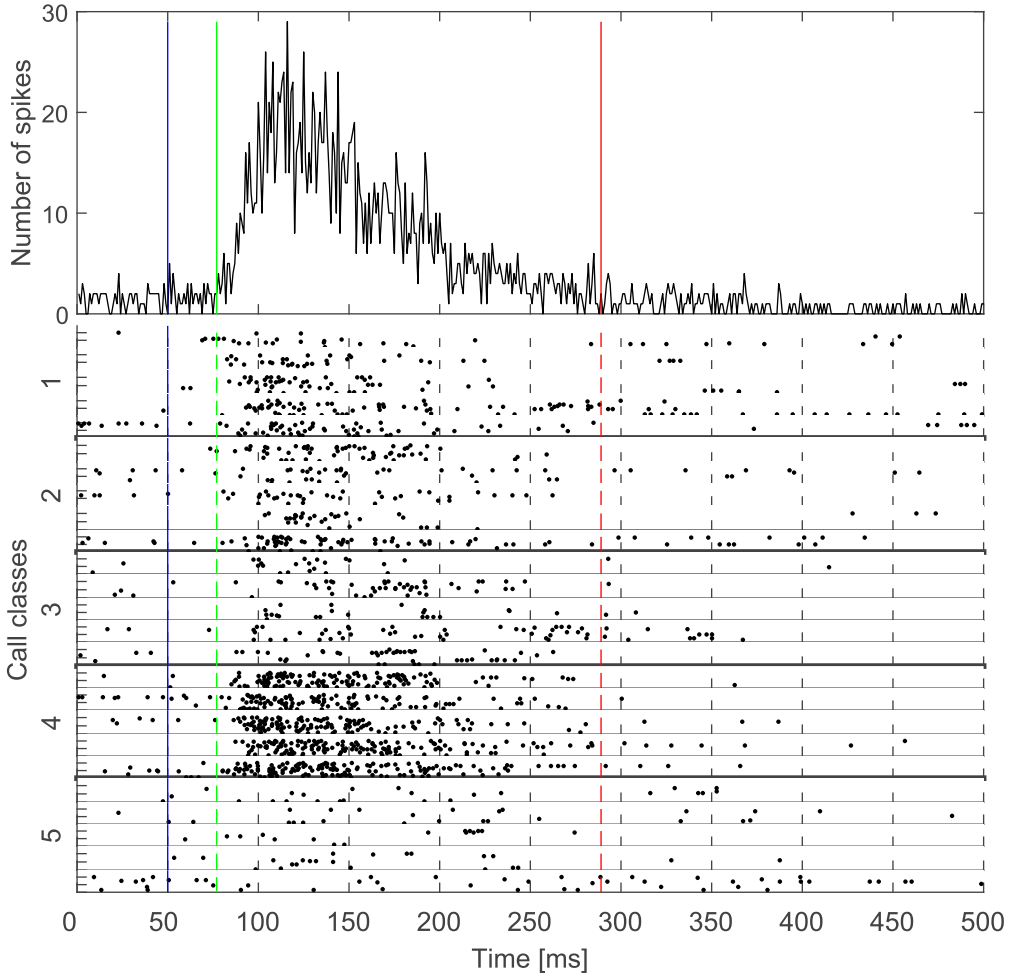

Figure 5.6: PSTH and raster plot of neuronal responses in the FAF preferring echolocation and contact calls: This neuron displayed preferential behaviour towards echolocation (Call classes 1 and 2) and contact/appeasement calls(Call class 4) by an increased firing rate, when presented with these stimuli.

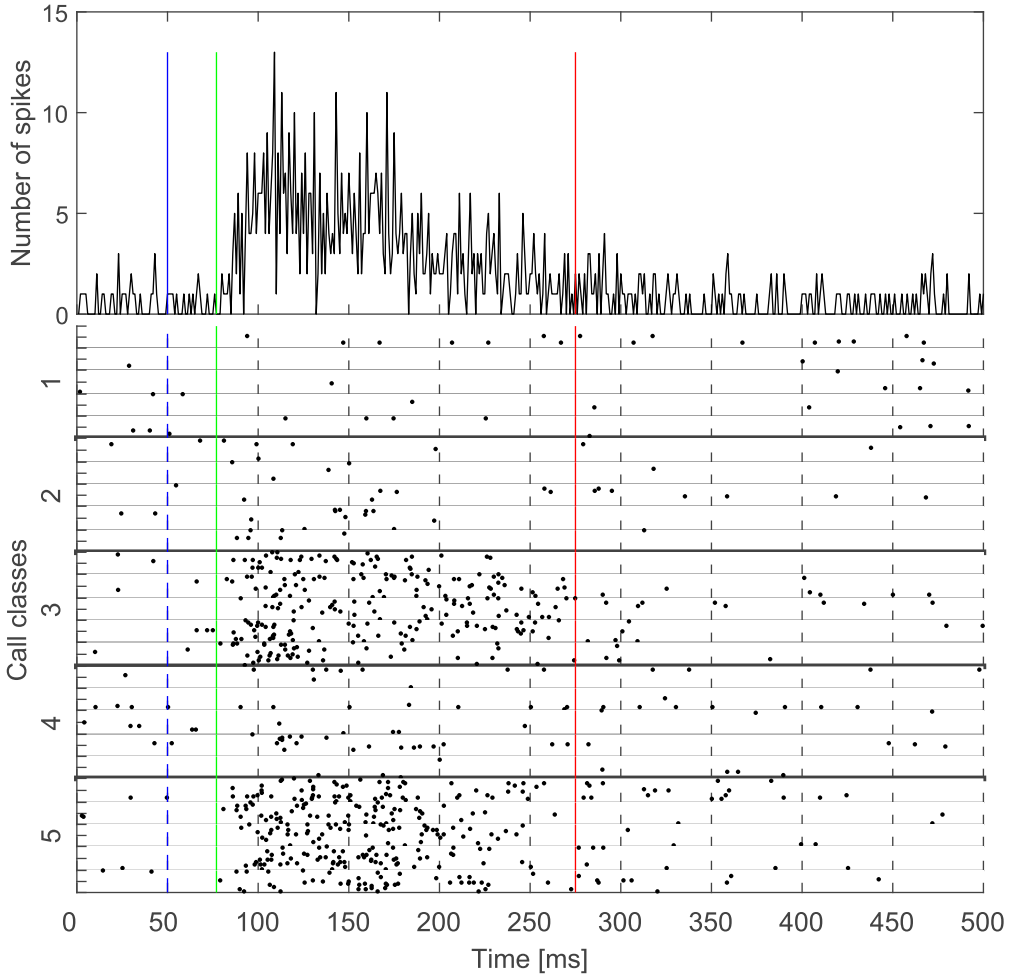

Figure 5.7: PSTH and raster plot of neuronal responses in the FAF showing a strong preference for aggression calls: This neuron displayed preferential behaviour towards aggression calls (Call class 3 and 5) by an increased firing rate, when presented with these stimuli. Substantially less neuronal discharge occurred when presented with the other call classes.

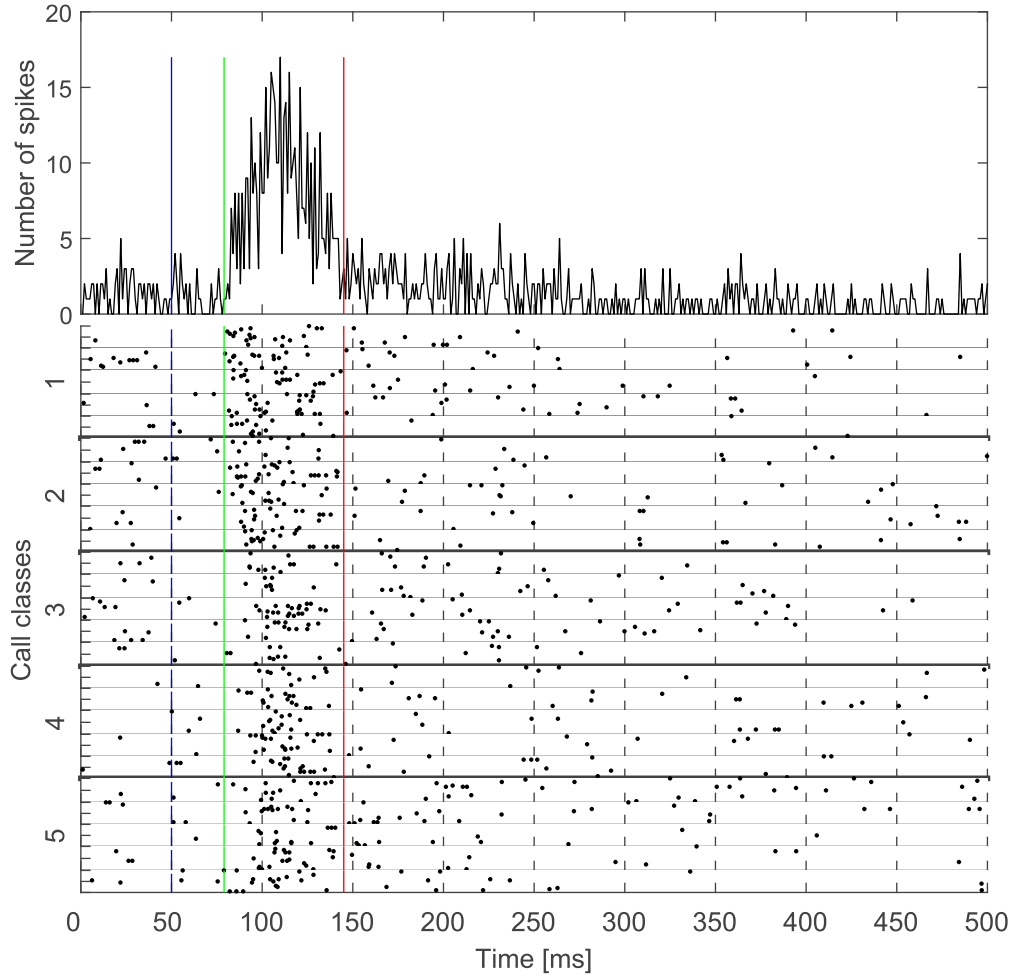

Figure 5.8: PSTH and raster plot of neuronal responses in the FAF showing no preference: This neuron displayed no preferences towards any of the call classes. Additionally note, that the duration of the neuronal discharge is short when compared to neurons in Figures 5.6 and 5.7.

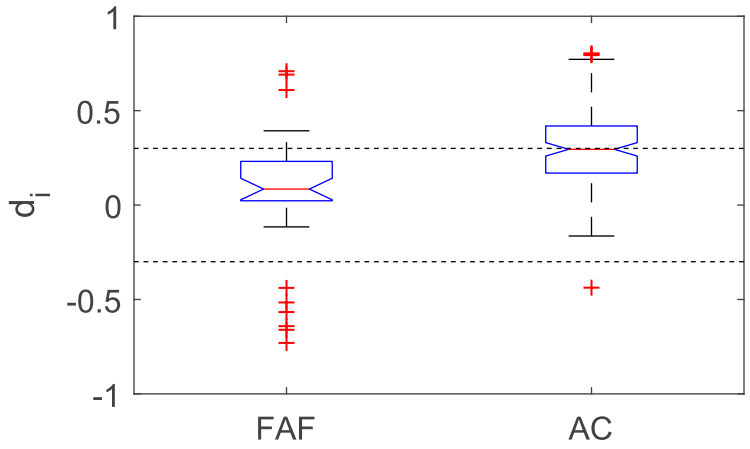

Figure 5.9: Comparison of call selectivity in neurons of the FAF and AC: box plots of the directionality index d_i of 33 FAF neurons and 121 AC neurons. The dotted lines indicate the d_i of ± 0.3, where the difference in firing rates between aggression and contact/appeasement calls exceeds 50%

61 units (50%) had a strong preference for the aggression calls ($d_i > 0.3$) and only 4 units (3.3%) had a negative d_i and thus showed preference towards the contact/appeasement calls. Furthermore, 57 units (46.7%) showed no selectivity or only a small preference towards the aggression calls ($0 \leq d_i < 0.3$). The mean d_i of all recorded units was 0.3153 ± 0.2055 (median $d_i = 0.3011$). For easier comparability, I plotted all values obtained from both the FAF and the AC of *Phyllostomus discolor* in the following Figure 5.9. When compared to the values from the AC (right box plot), the greater variability in neuronal call preference of FAF units is easily distinguishable. While the mean AC response displayed a preference for aggression calls, the mean FAF response was indifferent to the presented stimulus and only a subpopulation of 11 units showed preferential behaviour (left box plot, indicated by the red crosses as outliers).

5.4.2 Tracing experiments

Tracing studies of the neurocircuitry innervating the frontal auditory field of *Phyllostomus discolor* were performed in 2 bats (an overview of the corresponding section planes in the brain can be seen in Figure 5.10, while the injection site in one animal can be seen in Figure 5.11). After histological preparation of the brain, fluorescent labelling of fibres and neurons could be observed throughout the brain with an accumulation in several nuclei. Faint labelling of neurons could be observed in the AC (see Figure 5.12) and the suprageniculate nucleus of the thalamus. Stronger neuronal labelling was found in ventral lateral nucleus and the medial dorsal nucleus of the thalamus (See Figure 5.14). Furthermore, strongly labelled neurons could be seen in the amygdala (see Figure 5.13), but the subregion was not identifiable. However, the injection site varied between the

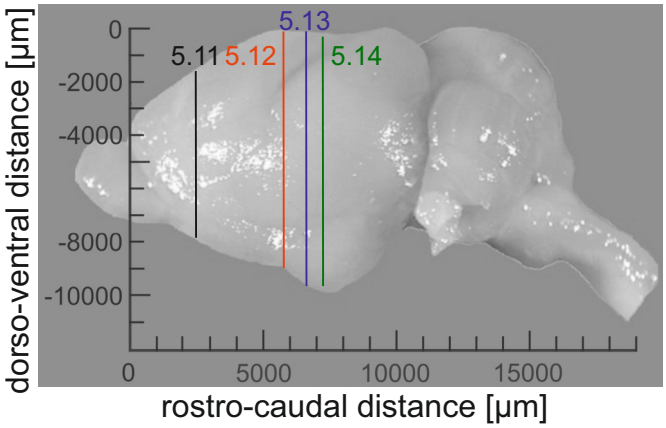

Figure 5.10: Corresponding section planes of the tracing results: Each section plane is labelled with the respective figure number.

two animals, with one injection being particularly more caudal than the other, while the tissue of the other brain had been severely lesioned at the injection site.

5.5 Discussion

This chapter investigated the basic response properties of neurons to acoustic stimuli within the frontal auditory field in *Phyllostomus discolor*, its call selectivity and the neurocircuitry involved in connecting it to other cortical and subcortical brain regions. Stimulation with pure-tones revealed exclusively tonic neuronal responses with longer response latencies when compared to data recorded from the auditory cortex using the identical stimulation scheme (see Hoffmann et al. [2008]). Responses to 25 natural echolocation and communication calls revealed an ambivalent response behaviour with some neurons showing strong responses to either aggression of contact/appeasement calls, however, roughly 67% of the units presented with said stimuli where indifferent to these and showed no preferences in their neuronal discharge pattern. As a result of dextran-based tracer injection into the area of FAF, strong neuronal labelling occurred in both the ventral lateral nucleus and the medial dorsal nucleus of the thalamus and also in the amygdala, while fainter labelling was observed in the auditory cortex and the suprageniculate nucleus of the thalamus.

5.5.1 Electrophysiological recordings from the FAF

As previously mentioned and similar to the results found in both *Pteronotus parnellii* and *Carollia perspicillata*, the neurons in the FAF responded to pure-tones in a tonic fashion with a higher latency when compared to results from the auditory cortex (Kanwal et al. [2000], Eiermann [2000]). This longer latency is somewhat to be expected, considering that the FAF is located rostrally of the auditory cortex, thus the neuronal input to the FAF covers a greater distance before reaching the FAF, however, the increased distance

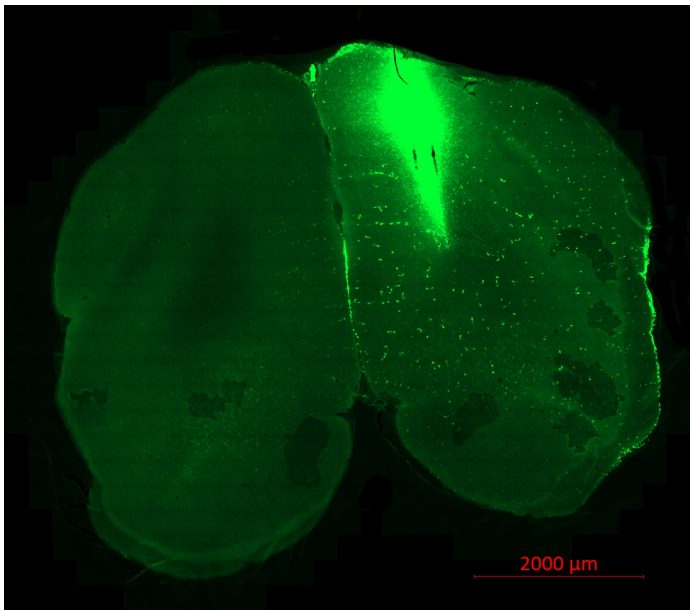

Figure 5.11: Tracer injection site in the FAF: Self-provided image of the tracer dispersion at the injection site. Lesions (vertical black slits) can be seen left and right of the penetration site.

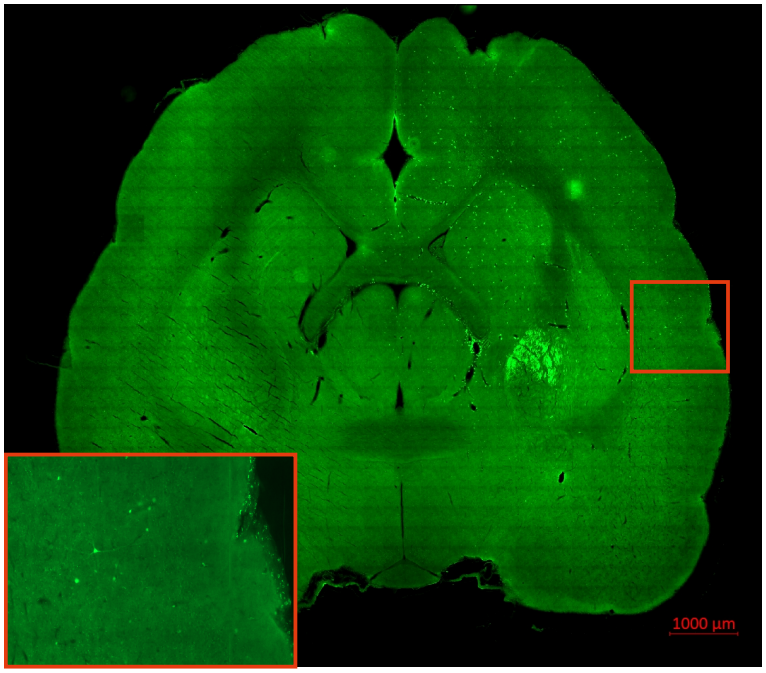

Figure 5.12: Faintly labelled neurons in the auditory cortex: Self-provided image of labelling in the ipsilateral auditory cortex of *Phyllostomus discolor*.

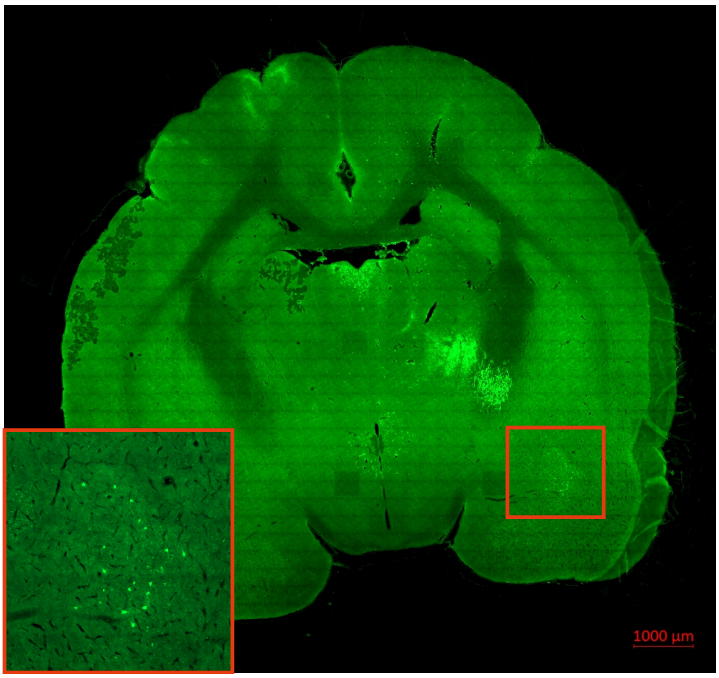

Figure 5.13: Strongly labelled neurons in the amygdala: Self-provided image of strong labelling in the ipsilateral amygdala of *Phyllostomus discolor*.

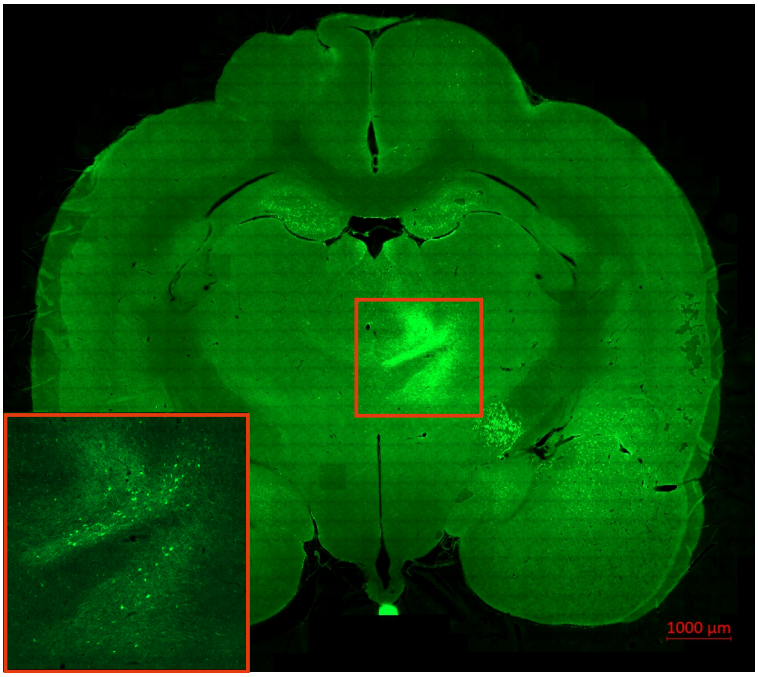

Figure 5.14: Strongly labelled neurons in the thalamus: Self-provided image of strong labelling in the ipsilateral thalamus of *Phyllostomus discolor*.

would not cause an increase of several tens of milliseconds. Therefore, it has been hypothesised that the FAF performs signal integration, as spikes show greater latency when compared to local field potentials (LFP) evoked by the same stimulus and recorded simultaneously to the spikes (García-Rosales et al. [2020]). The median latency was 32.7 ± 13.0 ms, which is comparable to the results reported for *C. perspicillata* (23.1 ± 7.3 ms, Eiermann [2000]), but significantly shorter than the values reported by López-Jury et al. [2019], where the average response latency was 93.4 ± 66 ms. Furthermore, LFPs recorded in the FAF of *C. perspicillata* actually preceded cortical LFPs recorded simultaneously (García-Rosales et al. [2020]), however, these discrepancies in neuronal response latencies can be attributed to the different pathways innervating the FAF, with the extralemniscal pathway (Casseday et al. [1989]) being associated with the faster inputs and the pathway via the auditory cortex (Kobler et al. [1987]) usually showing larger response latencies. The units in the FAF of *P. parnellii* also responded with a similarly tonic discharge pattern, with a median latency of 18.7 ± 15.3 ms when presented with pure tone stimuli (Kanwal et al. [2000]). Likewise, the BFs and CFs of the FAF neurons were mainly in the high frequency range, but while this means the 55 to 75 kHz range in *Phyllostomus discolor* (see Figure 5.15A&B), the BFs and CFs reported for *C. perspicillata* were in the 80 to 100 kHz range (Eiermann [2000]) or had BF and CF maxima in both the low and high-frequency domain (López-Jury et al. [2019]). To summarise, the FAF of 3 different bat species share the same basic response properties, although inter-species and intra-species variations do occur. As these bat species are closely related within the superfamily of the Noctilionoidea (Jones et al. [2002]), this similarity is not entirely unexpected, however, it does allow for some speculation of a similar functionality of the FAF (beyond its basic response properties) across these bat species.

When compared to the results from the AC of *Phyllostomus discolor*, some of the basic response properties of the FAF show only little differences, whereas some properties deviate strongly (see Figure 5.15 and Hoffmann et al. [2008] for the AC values used in this comparison). In the AC, the median BF was 60 kHz, which is close to the 65 kHz median BF in the FAF, however, the histogram shows a more distinct distribution in the AC than in the FAF (compare Figure 5.15A and 5.5B). Furthermore, the threshold to evoke neuronal responses at BF was also similar in both the FAF (mean SPL: 50 ± 19.2 dB) and AC (45 ± 16 dB) with a relatively uniform distribution (compare Figure 5.15B and 5.5C). Greater deviations can be seen when measuring the response latencies of the AC and the FAF. While the AC usually displays low response latencies (median latency: 9 ms), units in the FAF responded nearly four times slower to a stimulus with a median latency of 33 ms. Additionally, the units in the AC show a very strong bias towards low latency responses (see Figure 5.15C), whereas the units in the FAF showed more evenly distributed response latencies (see Figure 5.5D). A similar pattern can be observed in the response duration, as the AC produces shorter neuronal responses than the FAF (median duration of 25 ms in the AC vs. 92.5 ms in the FAF), which is also reflected in the duration distribution, where a strong bias towards short durations can be observed for the AC (see Figure 5.15D), while the FAF values were yet again more evenly distributed (see Figure 5.5E; note the lack of short duration values). Finally,

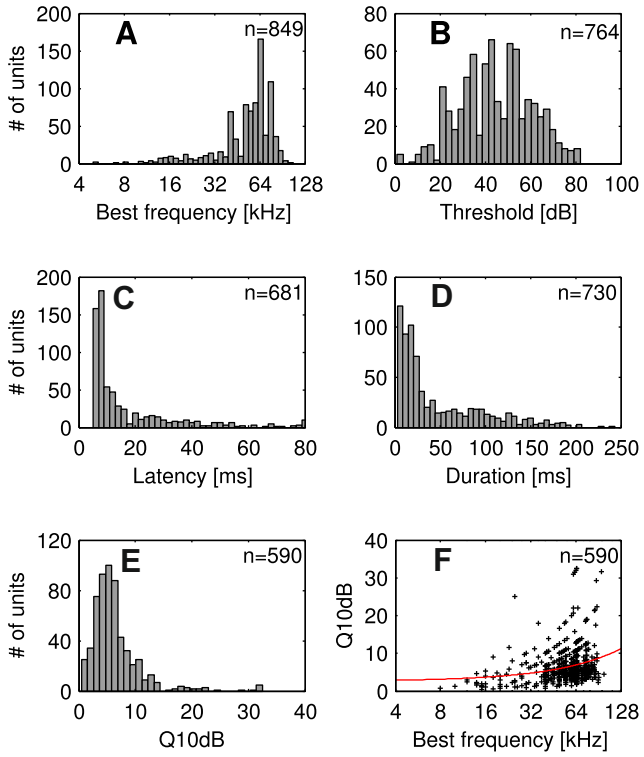

Figure 5.15: Distribution of response properties of cortical units in the AC of *Phyllostomus discolor*: The frequency distribution of neuronal response properties evoked by pure-tone stimulation is shown for: (A) Best frequency, (B) Response threshold, (C) First spike latency, (D) Response duration (E) Q_{10dB} values and (F) Q_{10dB} values as a function of best frequency with a regression line plotted in red ([Hoffmann et al., 2008, modified under CC BY 2.0])

the units in both the AC and FAF showed similar tuning properties (median AC Q_{10db}: 3.1 and median FAF Q_{10db}: 4), indicating that both regions rarely display any sharp frequency tuning (i.e. Q_{10db} greater than 10; Thomas et al. [2007], see Figures 5.5F and 5.15E). In both the AC and the FAF, the Q_{10dB} values only showed small changes with increasing BFs (indicated by the red regression lines in Figures 5.15F and 5.5G) and mostly remained below the threshold value of 10 for sharper frequency tuning (Thomas et al. [2007]). Considering the variability of *Phyllostomus discolor* vocalisations, these findings show a somewhat expected lack of auditory specialisation on a certain frequency range, unlike neurons of the auditory pathway in *P. parnellii*, a bat species with an acoustic fovea (see Chapter 1), where the Q_{10dB} values changed dramatically depending on the BF of the peripheral auditory neuron (Suga and Jen [1977]) and where a majority of neurons in the FAF displayed Q_{10dB} values greater than 180 (Kanwal et al. [2000]). To summarise, both the AC and the FAF of *Phyllostomus discolor* show similar basic response properties in BF distribution, threshold and frequency tuning. However, the temporal response properties differ strongly between these two cortical areas, with the AC showing a greater emphasis on low latency and short duration, unlike the FAF with its high response latency and longer, purely tonic responses.

Recently, it has been supposed that the FAF is part of a functional fronto-striatal network, which is involved in control of vocal production (Weineck et al. [2020]). The experiments in *C. perspicillata* revealed a distinct change in neuronal oscillations in both the FAF and the dorsal striatum prior to vocalisation and it was suggested, that the fronto-striatal network is involved in neuronal processing for selecting and producing different types of vocalisations. In *P. parnellii*, neurons in the FAF projected directly to the anterior cingulate cortex (Gooler and O'Neill [1987]), a cortical region where electro-stimulation evokes either echolocation or communication calls, depending on the stimulation location (Eiermann and Esser [2000]). Additionally, there have been reports of a functional coupling between the AC and the FAF in *C. perspicillata*, where synchronised gamma-band oscillations were recorded in both brain regions after stimulus presentation (García-Rosales et al. [2020]), further contributing to the hypothesis that the FAF is part of a pre-motor network contributing to vocalisation.

However, due to the lack of temporal precision in the FAF, the hypothesised involvement of the FAF in template matching (i.e. auditory feedback) or in the initiation of vocal motor patterns is debatable, as one would expect to see greater temporal precision in an area supposedly involved in vocal production. This is supported by my electrophysiology data, considering, unlike my results from the AC (see Chapter 3 and Hörpel and Firzlaff [2019]), where a subpopulation of cortical units displayed both a strong preference for the heavily amplitude modulated aggression calls and showed extensive phase-locking capabilities, the units in the FAF seem to lack these features and show no temporal precision in their firing behaviour, therefore making precise template matching highly unlikely. Furthermore, the selectivity indices of the recorded units in our study (mean d_i 0.0486) were substantially lower than the values reported for the AC of *Phyllostomus discolor* (mean d_i 0.3153, see Chapter 3 and Hörpel and Firzlaff [2019]). Some FAF units showed preferential responses towards either aggression or appeasement/contact calls, yet, the average FAF neuron in *Phyllostomus discolor* showed no preferential

discharge pattern when presented with a variety of *Phyllostomus discolor* calls and all recorded neurons only showed tonic responses, irrespective of the stimulus.

5.5.2 Tracing experiments

In *Pteronotus parnellii*, injections of WGA-HRP (wheat germ agglutinin conjugated to horseradish peroxidase) into the FAF revealed connections with the auditory cortex, the superior colliculus, the mediodorsal and ventrolateral thalamus and the suprageniculate nucleus of the posterior thalamus (Kobler et al. [1987]). They therefore concluded that the FAF was an extension of the central acoustic tract and that it possibly plays a role in behaviour guided by auditory information, basing their hypothesis on the fact that the FAF is directly connected to the SC. Seeing as the FAF receives multiple inputs from auditory nuclei and projects to areas within the SC which are the source for head and pinna movements, Kobler et al. [1987] speculated that the FAF plays a vital role in acoustic orientation, similar to the frontal eye fields in animals that utilise mainly optical orientation. This theory is supported by recordings from the prefrontal cortex of monkeys, where neurons showed involvement in temporal organisation of behaviour by integrating both acoustic and visual stimuli (Fuster et al. [2000]). This is something that has not been investigated in the bat FAF or prefrontal cortex and while the SC of *Phyllostomus discolor* represents both visual and acoustic information, there was no evidence of multi-modal integration on cellular level (Hoffmann et al. [2016]). Similar to the findings in *Pteronotus parnellii*, an injection of the retrograde tracer FluoroGold™ into the FAF of *Carollia perspicillata* led to strong labelling of neurons in the ipsilateral auditory cortex and fainter labelling in the contralateral auditory cortex (Eiermann [2000] and it was postulated that there was a strong connection between ipsilateral cortical layer II and III and the FAF. Additionally and similar to the findings in *P. parnellii*, labelling also occurred in the thalamus (suprageniculate body of the thalamus (SG, see Figure 1.4), mediodorsal thalamic nucleus, rostral parts of the ventral thalamic nuclei) and additional, not further identified nuclei of the pons (due to their position, they were speculated to be part of the central acoustic tract, however, no identification occurred). Eiermann [2000] also reported a "massive" connection between the FAF, the cingulate cortex and the claustrum.

Furthermore, injections of *Phaseolus vulgaris* leucoagglutinin into the PFC of rats showed a strong connection of the PFC with the various subregions of the amygdala (McDonald et al. [1996]).

These findings are somewhat similar to the results of my study, as I could show strong labelling not only in the ipsilateral thalamus (see Figure 5.14), but also in the ipsilateral amygdala (see Figure 5.13). I could also show faint labelling in the ipsilateral auditory cortex (see Figure 5.12) like Eiermann [2000] in *Carollia perspicillata*, yet his labelling was much stronger. However, the overall results of the tracing studies are to be taken with reservations. The injection volume was too large, resulting in tracer diffusion into the tissue surrounding the FAF and therefore limiting the value of these tracing experiments. Furthermore, the injection site varied between the animals, with one injection being more caudal than the other and with the brain tissue of the other brain showing

severe lesions at the injection site. Additionally, there was an unexpected lack of labelled neurons in the SC, which contradicts the findings by Kobler et al. [1987] and unpublished data from Hoffmann in *Phyllostomus discolor*, where an injection into the SC resulted in strong neuronal labelling in the frontal cortex. This lack of labelling in the SC could be explained by the faulty injection (i.e. wrong location, lesioned tissue), seeing as the tracer performed well otherwise and labelled both neurons and fibres clearly.
Conclusively, taking the lack of temporal precision, the high response latency and the mainly non-preferential discharge pattern of the FAF units into consideration, I am inclined to follow the hypothesis suggested by Eiermann [2000], where the FAF was associated with attentive behaviour (i.e. the bat turning its head and/or pinnae towards a sound source) and that it may broadly serve to link auditory and motor-systems, as it also projects to the superior colliculus, which is a major hub for sensory-motor-integration (Kobler et al. [1987], Valentine et al. [2002]). Seeing as the connection between the SC and FAF has been shown in *Phyllostomus discolor* in unpublished work by Hoffmann, I consider part of my tracing studies to have failed for the reasons discussed above and I am strongly in favour of the direct FAF-SC connection. Furthermore, the FAF of *Phyllostomus discolor* projects to the amygdala, which has also been reported for rats (prefrontal cortex projects to basolateral amygdala; McDonald et al. [1996]) and the moustached bat *P. parnellii* (Naumann and Kanwal [2011]). It has been proposed that social calls can selectively influence emotion, motivation, and behaviour via the amygdala (Naumann and Kanwal [2011], Gadziola et al. [2016]), which therefore may lead to an increased attentive behaviour of the bat via the FAF.

6 Conclusion & Outlook

This thesis focussed on the neural representation of amplitude modulated sounds in both juvenile and adults bats and how it relates to vocal communication. Traditionally, most acoustic studies in bats focussed mainly on echolocation (e.g. Pollak and Casseday [1989], Olsen and Suga [1991], Casseday and Covey [1992], Park and Pollak [1993], Ohlemiller et al. [1996], Portfors and Wenstrup [2002]) and purely a few (e.g. Kanwal et al. [1994], Medvedev and Kanwal [2004], DiMattina and Wang [2005]) covered vocal communication and its social relevance for the animals. Even less studies investigated vocal learning in bats (e.g. Boughman [1998], Esser and Schubert [1998]) and it was only during the last decade, that the scientific focus on bats shifted from mainly echolocation based studies to studies investigating the vocal learning capabilities of bats (Knörnschild [2014], Prat et al. [2015], Lattenkamp et al. [2018] and Lattenkamp et al. [2020]).

In my thesis, I investigated the neuronal representation of amplitude modulated sounds by using a variety of natural calls used by *Phyllostomus discolor* for echolocation, prosocial interaction and aggressive behaviour (Esser and Schmidt [1989], Lattenkamp et al. [2019]). I presented these calls via free-field loudspeaker, eliminating the drawbacks of free-field stimulation (mainly unwanted reverb) by heavily sound insulating the anechoic sound chambers used for the experiments. In the first part of my thesis, I recorded from the dorsal fields of the auditory cortex in *Phyllostomus discolor* and was able to show a predisposition of the neurons towards heavily amplitude calls used mainly for aggressive interaction. Furthermore, I also recorded while presenting artificial sinusoidally amplitude modulated sounds with a modulation frequency range between 5 and 1500 Hz. Strikingly, the neurons in the auditory cortex were capable of phase-locking to the stimulus envelope well into frequency ranges normally not seen in the mammalian auditory cortex (Joris et al. [2004], Martin et al. [2017]) and the neurons displayed their best firing rate at the modulation frequency most common to the aggression calls of the bat. The neuronal preference for aggression calls along with the capability of precisely encoding fast amplitude modulations hints at the important role the auditory cortex of *Phyllostomus discolor* might play in vocal communication among conspecifics.

In the following part of my thesis, I focussed exclusively on the development of this amplitude modulation encoding in the bat brain and could show that the neural representation of amplitude modulated stimuli underwent a maturation period. Over a period of eight weeks I recorded the envelope following responses from juvenile bats while presenting artificial amplitude modulated stimuli, uncovering that the neural representation of low frequency (5-58 Hz modulation frequency) amplitude modulation matured quicker than the higher frequency (87-130 Hz) representation, however, both were basically developed at an early age (postnatal day 8), supporting a possible involvement in the processing mother-infant communication. A maturation period has also been seen for the vocalisations uttered by juvenile bats, during which the juvenile bats imitated the calls used by their mothers (Esser and Schmidt [1989]), hinting at vocal learning and requiring at least a rudimentary envelope following capability in order to modify their calls (e.g. template matching through auditory feedback).

Finally, my focus shifted to the frontal auditory field, a small region in the frontal cortex, which is acoustically driven. Its existence in bats has been know for quite some time (Kobler et al. [1987], Eiermann [2000]), yet only recently has it been increasingly

investigated (López-Jury et al. [2019], García-Rosales et al. [2020]). I could establish the basic neuronal response properties of this region and could show, that some of these properties were similar to findings from the auditory cortex (e.g. median BF and SPL threshold at BF), while especially the temporal properties (i.e. response latency and duration) differed dramatically (Hoffmann et al. [2008]). Furthermore, there seemed to be greater variation in said properties when compared with other bat species (Eiermann [2000], Kanwal et al. [2000], López-Jury et al. [2019], García-Rosales et al. [2020]). Additionally, I could histologically pinpoint the location of the frontal auditory field in *Phyllostomus discolor*, which had not been done before. In a final step, I managed to partially reveal the neurocircuitry innervating the frontal auditory field, however, the results from the tracing experiments were not entirely satisfactory and require further attention in the future.

Speaking of the future, the results from my thesis have created additional interesting research questions. The most straightforward project would concern the frontal auditory field and its neurocircuitry, as preliminary results already exist and its precise location in *Phyllostomus discolor* has finally been established. Eiermann [2000] speculated, that the FAF might be involved in the initiation of motor responses after sound presentation, which I want to investigate further. Initially, I will be exploring a connection from the frontal auditory field to the laryngeal motor cortex. Additionally, I want to investigate the involvement of the FAF in the initiation of motor responses and in vocal learning. I will be comparing the results from extracellular recordings from the FAF in both control animals and animals with an induced knockdown of the "speech gene" FOXP2 in the auditory cortex.

References

G. Arriaga, E. P. Zhou, and E. D. Jarvis. Of Mice, Birds, and Men: The Mouse Ultrasonic Song System Has Some Features Similar to Humans and Song-Learning Birds. *PLoS ONE*, 7(10), 2012. ISSN 19326203. 10.1371/journal.pone.0046610.

M. Aytekin, E. Grassi, M. Sahota, and C. F. Moss. The bat head-related transfer function reveals binaural cues for sound localization in azimuth and elevation. *The Journal of the Acoustical Society of America*, 116(6):3594–3605, 2004. ISSN 0001-4966. 10.1121/1.1811412.

Kirsten M Bohn, Barbara Schmidt-French, Sean T Ma, and George D Pollak. Syllable acoustics, temporal patterns, and call composition vary with behavioral context in Mexican free-tailed bats. *The Journal of the Acoustical Society of America*, 124(3): 1838–1848, 2008. ISSN 0001-4966. 10.1121/1.2953314.

J. W. Boughman. Vocal learning by greater spear-nosed bats. *Proceedings of the Royal Society B: Biological Sciences*, 265(1392):227–233, 1998. ISSN 14712970. 10.1098/rspb.1998.0286.

J. W. Bradbury. Social organization and communication. *Biology of bats*, 3:1–72, 1977.

V. Bruns. Peripheral auditory tuning for fine frequency analysis by the CF-FM bat, Rhinolophus ferrumequinum - I. Mechanical specializations of the cochlea. *Journal of Comparative Physiology A*, 106(1):77–86, 1976. ISSN 03407594. 10.1007/BF00606573.

J. H. Casseday and E. Covey. Frequency tuning properties of neurons in the inferior colliculus of an FM bat. *Journal of Comparative Neurology*, 319(1):34–50, 1992. ISSN 10969861. 10.1002/cne.903190106.

J. H. Casseday, J. B. Kobler, S. F. Isbey, and E. Covey. Central acoustic tract in an echolocating bat: An extralemniscal auditory pathway to the thalamus. *Journal of Comparative Neurology*, 287(2):247–259, 1989. ISSN 10969861. 10.1002/cne.902870208.

A. Corti. *Recherches sur l'organe de l'ouie des mammifères*. 1851.

A. Costa-Pinto. First Record of Natural Predation on Bats By Domestic Cat in Brazil, With Distribution Extension for Phyllostomus Discolor. *Oecologia Australis*, 24(01): 242–248, 2020. ISSN 2177-6199. 10.4257/oeco.2020.2401.24.

N. D. Daw, J. P. O'Doherty, P. Dayan, B. Seymour, and R. J. Dolan. Cortical substrates for exploratory decisions in humans. *Nature*, 441(7095):876–879, 2006. ISSN 14764687. 10.1038/nature04766.

F. De Mey, J. Reijniers, H. Peremans, M. Otani, and U. Firzlaff. Simulated head related transfer function of the phyllostomid bat Phyllostomus discolor. *The Journal of the Acoustical Society of America*, 124(4):2123–2132, 2008. ISSN 0001-4966. 10.1121/1.2968703.

C. DiMattina and X. Wang. Virtual Vocalization Stimuli for Investigating Neural Representations of Species-Specific Vocalizations. *Journal of Neurophysiology*, 95(2):1244–1262, 2005. ISSN 0022-3077. 10.1152/jn.00818.2005.

J. J. Eggermont. Representation of spectral and temporal sound features in three cortical fields of the cat. Similarities outweigh differences. *Journal of Neurophysiology*, 80(5):2743–2764, 1998. ISSN 0022-3077. 10.1152/jn.1998.80.5.2743.

A. Eiermann. Kolokalisation auditorischer und (prä-) motorischer Funktionen im präfrontalen Cortex der Brillenplattnase, Carollia perspicillata, 2000.

A. Eiermann and K.-H. Esser. Auditory responses from the frontal cortex in the short-tailed fruit bat Carollia perspicillata. *NeuroReport*, 11(2), 2000. ISSN 0959-4965. URL `https://journals.lww.com/neuroreport/Fulltext/2000/02070/Auditory{_}responses{_}from{_}the{_}frontal{_}cortex{_}in{_}the.40.aspx`.

K.-H. Esser and U. Schmidt. Mother-Infant Communication in the Lesser Spear-nosed Bat Phyllostomus discolor (Chiroptera, Phyllostomidae) — Evidence for Acoustic Learning. *Ethology*, 82(2):156–168, 1989. ISSN 14390310. 10.1111/j.1439-0310.1989.tb00496.x.

K.-H. Esser and J. Schubert. Vocal dialects in the lesser spear-nosed bat Phyllostomus discolor. *Naturwissenschaften*, 85(7):347–349, 1998. ISSN 00281042. 10.1007/s001140050513.

U. Firzlaff, S. Schörnich, S. Hoffmann, G. Schuller, and L. Wiegrebe. A Neural Correlate of Stochastic Echo Imaging. *Journal of Neuroscience*, 26(3):785–791, 2006. ISSN 0270-6474. 10.1523/JNEUROSCI.3478-05.2006.

J. B. Fritz, S. V. David, S. Radtke-Schuller, P. Yin, and S. A. Shamma. Adaptive, behaviorally gated, persistent encoding of task-relevant auditory information in ferret frontal cortex. *Nature Neuroscience*, 13(8):1011–1019, 2010. ISSN 10976256. 10.1038/nn.2598. URL `http://dx.doi.org/10.1038/nn.2598`.

J. M. Fuster, M. Bodner, and J. K. Kroger. Cross-modal and cross-temporal association in neurons of frontal cortex. *Nature*, 405(6784):347–351, 2000. ISSN 00280836. 10.1038/35012613.

M. A. Gadziola, S. J. Shanbhag, and J. J. Wenstrup. Two distinct representations of social vocalizations in the basolateral amygdala. *Journal of Neurophysiology*, 115(2): 868–886, 2016. ISSN 0022-3077. 10.1152/jn.00953.2015.

B. H. Gaese and J. Ostwald. Temporal coding of amplitude and frequency modulation in the rat auditory cortex. *European Journal of Neuroscience*, 7:438–450, 1995.

F. García-Rosales, M. J. Beetz, Y. Cabral-Calderin, M. Kössl, and J. C. Hechavarria. Neuronal coding of multiscale temporal features in communication sequences within the bat auditory cortex. *Communications Biology*, 1(1):200, 2018. ISSN 2399-3642. 10.1038/s42003-018-0205-5.

F. García-Rosales, L. López-Jury, E. González-Palomares, Y. Cabral-Calderín, and J. C. Hechavarría. Fronto-Temporal Coupling Dynamics During Spontaneous Activity and Auditory Processing in the Bat Carollia perspicillata, 2020. URL `https://www.frontiersin.org/article/10.3389/fnsys.2020.00014`.

N. Gavrilov, S. R. Hage, and A. Nieder. Functional Specialization of the Primate Frontal Lobe during Cognitive Control of Vocalizations. *Cell Reports*, 21(9):2393–2406, 2017. ISSN 22111247. 10.1016/j.celrep.2017.10.107. URL `https://doi.org/10.1016/j.celrep.2017.10.107`.

E. Gillam and M. B. Fenton. *Roles of Acoustic Social Communication in the Lives of Bats*, pages 117–139. Springer New York, New York, NY, 2016. ISBN 978-1-4939-3527-7. 10.1007/978-1-4939-3527-7_5. URL `https://doi.org/10.1007/978-1-4939-3527-7{_}5`.

D. M. Gooler and W. E. O'Neill. Topographic representation of vocal frequency demonstrated by microstimulation of anterior cingulate cortex in the echolocating bat, Pteronotus parnelli parnelli. *Journal of Comparative Physiology A*, 161(2):283–294, 1987. ISSN 03407594. 10.1007/BF00615248.

B. Grothe. Interaction of excitation and inhibition in processing of pure tone and amplitude-modulated stimuli in the medial superior olive of the mustached bat. *Journal of Neurophysiology*, 71(2):706–721, 1994. ISSN 0022-3077. 10.1152/jn.1994.71.2.706.

B. Grothe and T. J. Park. Structure and function of the bat superior olivary complex. *Microscopy Research and Technique*, 51(4):382–402, 2000. ISSN 1059910X. 10.1002/1097-0029(20001115)51:4⟨382::AID-JEMT7⟩3.0.CO;2-7.

T. A. Hackett, I. Stepniewska, and J. H. Kaas. Thalamocortical connections of the parabelt auditory cortex in macaque monkeys. *Journal of Comparative Neurology*, 400(2):271–286, 1998. ISSN 00219967. 10.1002/(SICI)1096-9861(19981019)400:2⟨271::AID-CNE8⟩3.0.CO;2-6.

S. R. Hage and A. Nieder. Single neurons in monkey prefrontal cortex encode volitional initiation of vocalizations. *Nature Communications*, 4(1):2409, 2013. ISSN 2041-1723. 10.1038/ncomms3409. URL `https://doi.org/10.1038/ncomms3409`.

E. R. Heithaus, T. H. Fleming, and P. A. Opler. Foraging Patterns and Resource Utilization in Seven Species of Bats in a Seasonal Tropical Forest. *Ecology*, 56(4): 841–854, 1975. ISSN 0012-9658. 10.2307/1936295.

O. W. Henson. Some morphological and functional aspects of certain structures of the middle ear in bats and insectivores, 1960.

S. Hoffmann, U. Firzlaff, S. Radtke-Schuller, B. Schwellnus, and G. Schuller. The auditory cortex of the bat Phyllostomus discolor: Localization and organization of basic response properties. *BMC Neuroscience*, 9:1–17, 2008. ISSN 14712202. 10.1186/1471-2202-9-65.

S. Hoffmann, T. Vega-Zuniga, W. Greiter, Q. Krabichler, A. Bley, M. Matthes, C. Zimmer, U. Firzlaff, and H. Luksch. Congruent representation of visual and acoustic space in the superior colliculus of the echolocating bat Phyllostomus discolor. *European Journal of Neuroscience*, 44(9):2685–2697, 2016. ISSN 14609568. 10.1111/ejn.13394.

S. G. Hörpel and U. Firzlaff. Processing of fast amplitude modulations in bat auditory cortex matches communication call-specific sound features. *Journal of Neurophysiology*, 121(4), 2019. ISSN 15221598. 10.1152/jn.00748.2018.

S. G. Hörpel and U. Firzlaff. Post-natal development of the envelope following response to amplitude modulated sounds in the bat Phyllostomus discolor. *Hearing Research*, 388: 107904, 2020. ISSN 0378-5955. https://doi.org/10.1016/j.heares.2020.107904. URL `http://www.sciencedirect.com/science/article/pii/S0378595519305076`.

K. E. Jones, A. Purvis, A. MacLarnon, O. R. P. Bininda-Emonds, and N. B. Simmons. A phylogenetic supertree of the bats (Mammalia: Chiroptera). *Biological Reviews of the Cambridge Philosophical Society*, 77(2):223–259, 2002. ISSN 14647931. 10.1017/S1464793101005899.

P. X. Joris and T. C. T. Yin. Responses to amplitude-modulated tones in the auditory nerve of the cat. *Journal of the Acoustical Society of America*, 91(1):215–232, 1992.

P. X. Joris, C. E. Schreiner, and A. Rees. Neural Processing of Amplitude-Modulated Sounds. *Physiological Reviews*, 84(2):541–577, 2004. ISSN 0031-9333. 10.1152/physrev.00029.2003.

J. S. Kanwal, S. Matsumura, K. Ohlemiller, and N. Suga. Analysis of acoustic elements and syntax in communication sounds emitted by mustached bats. *The Journal of the Acoustical Society of America*, 96(3):1229–1254, 1994. ISSN 0001-4966. 10.1121/1.410273.

J. S. Kanwal, M. Gordon, J. P. Peng, and K.-H. Esser. Auditory responses from the frontal cortex in the mustached bat, Pteronotus parnellii. *NeuroReport*, 11(2):367–372, 2000. ISSN 09594965. 10.1097/00001756-200002070-00029.

M. Knörnschild. Vocal production learning in bats. *Current Opinion in Neurobiology*, 28:80–85, 2014. ISSN 18736882. 10.1016/j.conb.2014.06.014.

J. B. Kobler, S. F. Isbey, and J. H. Casseday. Auditory pathways to the frontal cortex of the mustache bat, Pteronotus parnellii. *Science*, 236(4803):824–826, 1987. ISSN 00368075. 10.1126/science.2437655.

L. Köles, J. Szepesy, E. Berekméri, and T. Zelles. Purinergic signaling and cochlear injury-targeting the immune system? *International Journal of Molecular Sciences*, 20 (12):125–150, 2019. ISSN 14220067. 10.3390/ijms20122979.

M. Kössl and M. Vater. *Cochlear Structure and Function in Bats*, pages 191–234. Springer New York, New York, NY, 1995. ISBN 978-1-4612-2556-0. 10.1007/978-1-4612-2556-0_5. URL `https://doi.org/10.1007/978-1-4612-2556-0{_}5`.

B. Suresh Krishna and Malcolm N. Semple. Auditory temporal processing: responses to sinusoidally amplitude-modulated tones in the inferior colliculus. *Journal of Neurophysiology*, 84(1):255–273, 2000. ISSN 15221598. 10.1152/jn.2000.84.1.255.

G. G. Kwiecinski. Phyllostomus discolor. *Mammalian Species*, 0(801):1–11, 2006. ISSN 00763519. 10.1644/801.1.

E. Z. Lattenkamp, S. C. Vernes, and L. Wiegrebe. Volitional control of social vocalisations and vocal usage learning in bats. *The Journal of experimental biology*, 221:1–8, 2018. ISSN 14779145. 10.1242/jeb.180729.

E. Z. Lattenkamp, S. M. Shields, M. Schutte, J. Richter, M. Linnenschmidt, S. C. Vernes, and L. Wiegrebe. The Vocal Repertoire of Pale Spear-Nosed Bats in a Social Roosting Context. *Frontiers in Ecology and Evolution*, 7(April):1–14, 2019. 10.3389/fevo.2019.00116.

E. Z. Lattenkamp, S. C. Vernes, and L. Wiegrebe. Vocal production learning in the pale spear-nosed bat, Phyllostomus discolor. *Biology letters*, 16(4):20190928, 2020. ISSN 1744957X. 10.1098/rsbl.2019.0928.

M. Linnenschmidt and L. Wiegrebe. Ontogeny of auditory brainstem responses in the bat, Phyllostomus discolor. *Hearing research*, 373:85–95, 2019. ISSN 1878-5891. 10.1016/j.heares.2018.12.010.

K. K. Loh, M. Petrides, W. D. Hopkins, E. Procyk, and C. Amiez. Cognitive control of vocalizations in the primate ventrolateral-dorsomedial frontal (VLF-DMF) brain network. *Neuroscience and Biobehavioral Reviews*, 82:32–44, 2017. ISSN 18737528. 10.1016/j.neubiorev.2016.12.001. URL `http://dx.doi.org/10.1016/j.neubiorev.2016.12.001`.

L. López-Jury, A. Mannel, F. García-Rosales, and J. C. Hechavarria. Modified synaptic dynamics predict neural activity patterns in an auditory field within the frontal cortex. *European Journal of Neuroscience*, (June):1–15, 2019. ISSN 14609568. 10.1111/ejn .14600.

L. M. Martin, F. García-Rosales, M. J. Beetz, and J. C. Hechavarría. Processing of temporally patterned sounds in the auditory cortex of Seba's short-tailed bat, Carollia perspicillata. *European Journal of Neuroscience*, 46(8):2365–2379, 2017. ISSN 14609568. 10.1111/ejn.13702.

A. J. McDonald, F. Mascagni, and L. Guo. Projections of the medial and lateral prefrontal cortices to the amygdala: a Phaseolus vulgaris leucoagglutinin study in the rat. *Neuroscience*, 71(1):55–75, 1996. ISSN 0306-4522.

A. V. Medvedev and J. S. Kanwal. Local Field Potentials and Spiking Activity in the Primary Auditory Cortex in Response to Social Calls. *Journal of Neurophysiology*, 92 (1):52–65, 2004. ISSN 0022-3077. 10.1152/jn.01253.2003.

J. Mogdans, J. Ostwald, and H.-U. Schnitzler. The role of pinna movement for the localization of vertical and horizontal wire obstacles in the greater horseshoe bat, Rhinolopus ferrumequinum. *Journal of the Acoustical Society of America*, 84(5):1676–1679, 1988. ISSN NA. 10.1121/1.397183.

R. T. Naumann and J. S. Kanwal. Basolateral amygdala responds robustly to social calls: spiking characteristics of single unit activity. *Journal of Neurophysiology*, 105 (5):2389–2404, 2011. ISSN 0022-3077. 10.1152/jn.00580.2010.

G. Neuweiler. *Biologie der Fledermäuse*. Flexible Taschenbücher. Thieme, 1993. ISBN 9783137874010. URL `https://books.google.de/books?id=a-ZFAAAAYAAJ`.

S. Nummela. Scaling of the mammalian middle ear. *Hearing Research*, 85:18–30, 1995.

K. K. Ohlemiller, J. S. Kanwal, and N. Suga. Facilitative responses to species-specific calls in cortical FM-FM neurons of the mustached bat. *Neuroreports*, 7(11):1749–1755, 1996.

J. F. Olsen and N. Suga. Combination-sensitive neurons in the medial geniculate body of the mustached bat: encoding of target range information. *Journal of Neurophysiology*, 65(6):1275–96, 1991. ISSN 0022-3077. 10.1152/jn.1991.65.6.1254.

W. E. O'Neill, J. R. Holt, and M. S. Gordon. Responses of neurons in the intermediate and ventral nuclei of the lateral lemniscus of the mustached bat to sinusoidal and pseudorandom amplitude modulations. In *Assoc Res Otolaryngol Abstr*, volume 15, page 140, 1992.

J. Ostwald. Encoding of Natural Insect Echoes and Sinusoidally Modulated Stimuli by Neurons in the Auditory Cortex of the Greater Horseshoe Bat, Rhinolophus Ferrumequinum BT - Animal Sonar: Processes and Performance. pages 483–487. Springer

US, Boston, MA, 1988. ISBN 978-1-4684-7493-0. 10.1007/978-1-4684-7493-0_48. URL https://doi.org/10.1007/978-1-4684-7493-0{_}48.

T. J. Park and G. D. Pollak. GABA shapes sensitivity to interaural intensity disparities in the mustache bat's inferior colliculus: Implications for encoding sound location. *Journal of Neuroscience*, 13(5):2050–2067, 1993. ISSN 02706474. 10.1523/jneurosci .13-05-02050.1993.

T. Paus. Primate anterior cingulate cortex: where motor control, drive and cognition interface. *Nature reviews neuroscience*, 2(6):417–424, 2001. ISSN 1471-0048.

R. Pelleg-Toiba and Z. Wollberg. Discrimination of communication calls in the squirrel monkey: "Call detectors" or "cell ensembles". *Journal of Basic and Clinical Physiology and Pharmacology*, 2(4):257–272, 1991. ISSN 21910286. 10.1515/JBCPP.1991.2.4.257.

J. O. Pickles. *Auditory pathways: Anatomy and physiology*, volume 129. Elsevier B.V., 1 edition, 2015. 10.1016/B978-0-444-62630-1.00001-9. URL http://dx.doi.org/10.1016/B978-0-444-62630-1.00001-9.

G. W. Pierce and D. R. Griffin. Experimental determination of supersonic notes emitted by bats. *Journal of Mammalogy*, 19(4):454–455, 1938. ISSN 1545-1542.

G. D. Pollak and J. H. Casseday. The neural basis of echolocation in bats. *Zoophysiology*, 25:V–IX, 1989. ISSN 0720-1842.

C. V. Portfors and J. J. Wenstrup. Excitatory and facilitatory frequency response areas in the inferior colliculus of the mustached bat. *Hearing Research*, 168(1-2):131–138, 2002. ISSN 03785955. 10.1016/S0378-5955(02)00376-3.

Y. Prat, M. Taub, and Y. Yovel. Vocal learning in a social mammal: Demonstrated by isolation and playback experiments in bats. *Science Advances*, 1(2):1–6, 2015. ISSN 23752548. 10.1126/sciadv.1500019.

J. P. Rauschecker, B. Tian, and M. Hauser. Processing of complex sounds in the macaque nonprimary auditory cortex. *Science*, 268(5207):111–114, 1995. ISSN 00368075. 10 .1126/science.7701330.

K. Reimer. Coding of sinusoidally amplitude modulated acoustic stimuli in the inferior colliculus of the rufous horseshoe bat, Rhinolophus rouxi. *Journal of Comparative Physiology A*, 161(2):305–313, 1987. ISSN 03407594. 10.1007/BF00615250.

R. D. Rogers, B. J. Everitt, A. Baldacchino, A. J. Blackshaw, R. Swainson, K. Wynne, N. B. Baker, J. Hunter, T. Carthy, E. Booker, M. London, J. F.W. Deakin, B. J. Sahakian, and T. W. Robbins. Dissociable deficits in the decision-making cognition of chronic amphetamine abusers, opiate abusers, patients with focal damage to prefrontal cortex, and tryptophan-depleted normal volunteersEvidence for monoaminergic mechanisms. *Neuropsychopharmacology*, 20(4):322–339, 1999. ISSN 0893133X. 10.1016/S0893-133X(98)00091-8.

L. M. Romanski and P. S. Goldman-Rakic. An auditory domain in primate prefrontal cortex. *Nature Neuroscience*, 5(1):15–16, 2002. ISSN 10976256. 10.1038/nn781.

L. M. Romanski, J. F. Bates, and P. S. Goldman-Rakic. Auditory belt and parabelt projections to the prefrontal cortex in the rhesus monkey. *Journal of Comparative Neurology*, 403(2):141–157, 1999a. ISSN 00219967. 10.1002/(SICI)1096-9861(19990111)403:2⟨141::AID-CNE1⟩3.0.CO;2-V.

L. M. Romanski, B. Tian, J. Fritz, M. Mishkin, P. S. Goldman-Rakic, and J. P. Rauschecker. Dual streams of auditory afferents target multiple domains in the primate prefrontal cortex. *Nature Neuroscience*, 2(12):1131–1136, 1999b. ISSN 10976256. 10.1038/16056.

M. F. S. Rushworth, M. A. P. Noonan, E. D. Boorman, M. E. Walton, and T. E. Behrens. Frontal Cortex and Reward-Guided Learning and Decision-Making. *Neuron*, 70(6):1054–1069, 2011. ISSN 08966273. 10.1016/j.neuron.2011.05.014. URL `http://dx.doi.org/10.1016/j.neuron.2011.05.014`.

J. M. Russ, G. Jones, I .J. Mackie, and P. A. Racey. Interspecific responses to distress calls in bats (Chiroptera: Vespertilionidae): A function for convergence in call design? *Animal Behaviour*, 67(6):1005–1014, 2004. ISSN 00033472. 10.1016/j.anbehav.2003.09.003.

J W H Schnupp, Thomas M Hall, Rory F Kokelaar, and Bashir Ahmed. Plasticity of Temporal Pattern Codes for Vocalization Stimuli in Primary Auditory Cortex. *Journal of Neuroscience*, 26(18):4785–4795, 2006. ISSN 0270-6474. 10.1523/JNEUROSCI.4330-05.2006.

C. E. Schreiner and J. V. Urbas. Representation of amplitude modulation in the auditory cortex of the cat. II. Comparison between cortical fields. *Hearing Research*, 32:49–64, 1988.

G. Schuller, S. Radtke-Schuller, and M. Betz. A stereotaxic method for small animals using experimentally determined reference profiles. *Journal of Neuroscience Methods*, 18(4):339–350, 1986. ISSN 01650270. 10.1016/0165-0270(86)90022-1.

C. S. Simões, P. V. R. Vianney, M. M. de Moura, M. A. M. Freire, L. E. Mello, K. Sameshima, J. F. Araújo, M. A. L. Nicolelis, C. V. Mello, and S. Ribeiro. Activation of frontal neocortical areas by vocal production in marmosets. *Frontiers in Integrative Neuroscience*, 4(SEPTEMBER 2010):1–12, 2010. ISSN 16625145. 10.3389/fnint.2010.00123.

M. S. Springer, E. C. Teeling, O. Madsen, M. J. Stanhope, and W. W. De Jong. Integrated fossil and molecular data reconstruct bat echolocation. *Proceedings of the National Academy of Sciences of the United States of America*, 98(11):6241–6246, 2001. ISSN 00278424. 10.1073/pnas.111551998.

N. Suga and P. H. Jen. Further studies on the peripheral auditory system of 'CF-FM' bats specialized for fine frequency analysis of Doppler-shifted echoes. *Journal of Experimental Biology*, 69:207–232, 1977. ISSN 00220949.

J. Thomas, C. F. Moss, and M. Vater. Echolocation in Bats and Dolphins. *Bibliovault OAI Repository, the University of Chicago Press*, jan 2007.

D. J. Tollin and T. C. T. Yin. Sound Localization: Neural Mechanisms. *Encyclopedia of Neuroscience*, pages 137–144, 2009. 10.1016/B978-008045046-9.00267-9.

D. E. Valentine, S. R. Sinha, and C. F. Moss. Orienting responses and vocalizations produced by microstimulation in the superior colliculus of the echolocating bat, Eptesicus fuscus. *Journal of Comparative Physiology A: Neuroethology, Sensory, Neural, and Behavioral Physiology*, 188(2):89–108, 2002. ISSN 03407594. 10.1007/s00359-001-0275-5.

M. Vater. Single unit responses in cochlear nucleus of horseshoe bats to sinusoidal frequency and amplitude modulated signals. *Journal of Comparative Physiology A*, 149(3):369–388, 1982. ISSN 03407594. 10.1007/BF00619153.

M. Vater and M. Lenoir. Ultrastructure of the horseshoe bat's organ of Corti. I. Scanning electron microscopy. *Journal of Comparative Neurology*, 318(4):367–379, 1992. ISSN 0021-9967.

G. Von Békésy and E. G. Wever. *Experiments in hearing*, volume 8. McGraw-Hill New York, 1960.

X. Wang and S. C. Kadia. Differential representation of species-specific primate vocalizations in the auditory cortices of marmoset and cat. *Journal of Neurophysiology*, 86 (5):2616–2620, 2001. ISSN 0022-3077. 10.1152/jn.2001.86.5.2616.

X. Wang, M. M. Merzenich, R. Beitel, and C. E. Schreiner. Representation of a species-specific vocalization in the primary auditory cortex of the common marmoset: temporal and spectral characteristics. *Journal of Neurophysiology*, 74(6):2685–2706, 1995. ISSN 0022-3077. 10.1126/SCIENCE.644320.

K. Weineck, F. García-Rosales, and J. C. Hechavarría. Neural oscillations in the fronto-striatal network predict vocal output in bats. *PLOS Biology*, 18(3):e3000658, mar 2020. URL `https://doi.org/10.1371/journal.pbio.3000658`.

J. P. Wilson and V. Bruns. Middle-ear mechanics in the CF-bat Rhinolophus ferrumequinum. *Hearing Research*, 10(1):1–13, 1983. ISSN 03785955. 10.1016/0378-5955(83)90015-1.

A Acknowledgements

I would especially like to thank my supervisor Uwe Firzlaff, who gave me the benefit of the doubt and hired a teacher for a neuroscience position, therefore giving me the opportunity of a career in academia. Furthermore, his expertise and humour made these last 3.5 years both educational and enjoyable and I hope to collaborate with him in the future.
Furthermore, I would like to thank Harald Luksch, who always had an open ear for the questions and troubles that come with the job. His style of delivery during his lectures and his knowledge kindled my interest in neuroscience.
Sadly, Lutz Wiegrebe passed away before completion of this thesis. His willingness to help out when problems arose and his spot-on criticism are just some of his traits and I am grateful for his input.
Also, I would like to thank the technicians Birgit Seibel, Gaby Schwabedissen and especially Yvonne Schwarz, who were a great help in these 3.5 years.
Additionally, I would like to thank all my colleagues at the Zoology in Freising for many a good time, ranging from field trips to the notorious Freibierfest.
And finally, I would like to thank my parents and my partner Chrissy for putting up with me when things were not going too smoothly.

The work in this thesis was supported by the Human Frontier Science Program (France) Grant (RGP0058) awarded to Uwe Firzlaff.

B Supporting documents concerning copyright

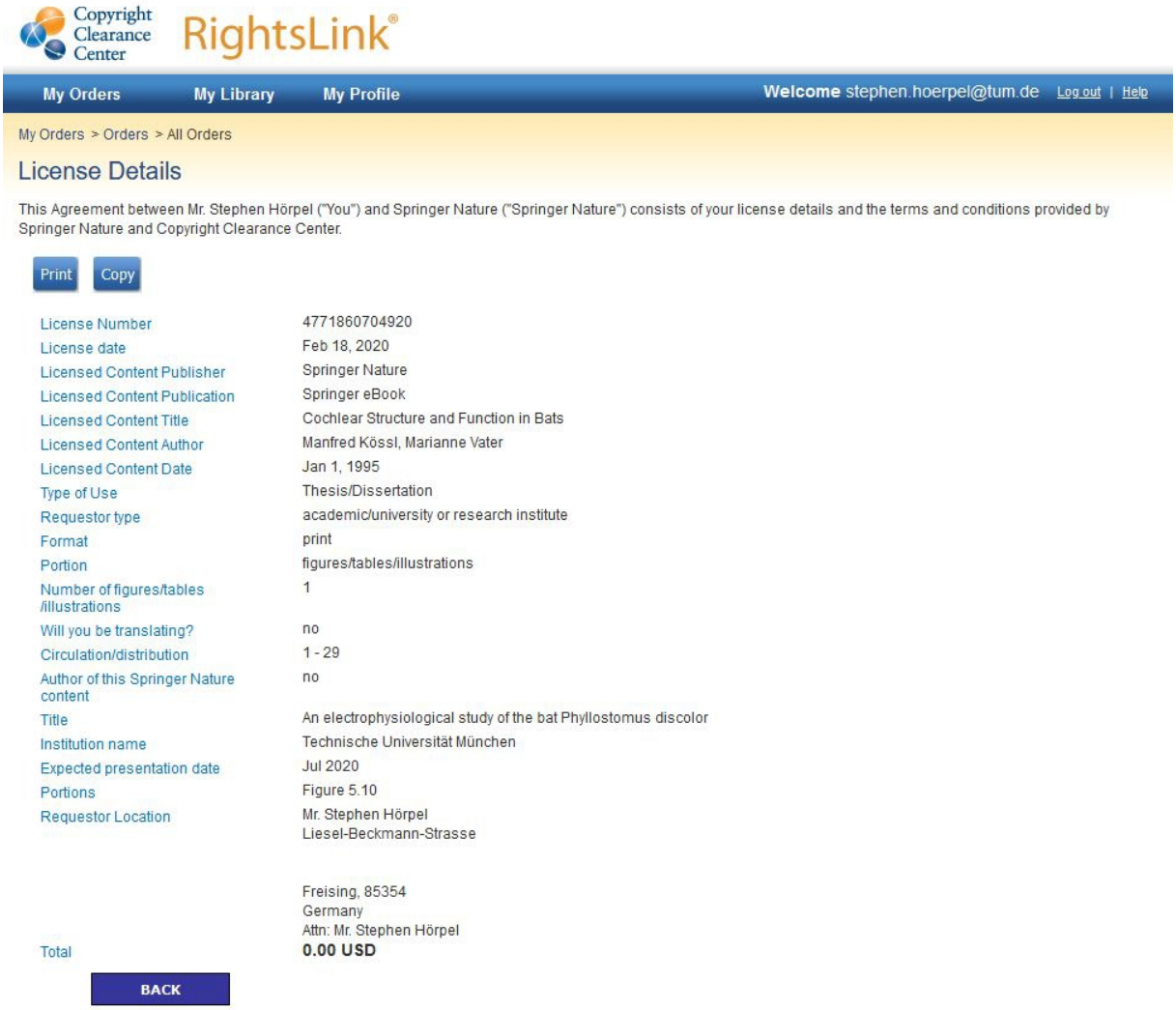
Copyright Clearance Center RightsLink®

My Orders | My Library | My Profile | Welcome stephen.hoerpel@tum.de | Log out | Help

My Orders > Orders > All Orders

License Details

This Agreement between Mr. Stephen Hörpel ("You") and Springer Nature ("Springer Nature") consists of your license details and the terms and conditions provided by Springer Nature and Copyright Clearance Center.

Print Copy

License Number	4771860704920
License date	Feb 18, 2020
Licensed Content Publisher	Springer Nature
Licensed Content Publication	Springer eBook
Licensed Content Title	Cochlear Structure and Function in Bats
Licensed Content Author	Manfred Kössl, Marianne Vater
Licensed Content Date	Jan 1, 1995
Type of Use	Thesis/Dissertation
Requestor type	academic/university or research institute
Format	print
Portion	figures/tables/illustrations
Number of figures/tables /illustrations	1
Will you be translating?	no
Circulation/distribution	1 - 29
Author of this Springer Nature content	no
Title	An electrophysiological study of the bat Phyllostomus discolor
Institution name	Technische Universität München
Expected presentation date	Jul 2020
Portions	Figure 5.10
Requestor Location	Mr. Stephen Hörpel Liesel-Beckmann-Strasse Freising, 85354 Germany Attn: Mr. Stephen Hörpel
Total	**0.00 USD**

BACK

Figure B.1: License for reproduction from the *Springer Nature*.

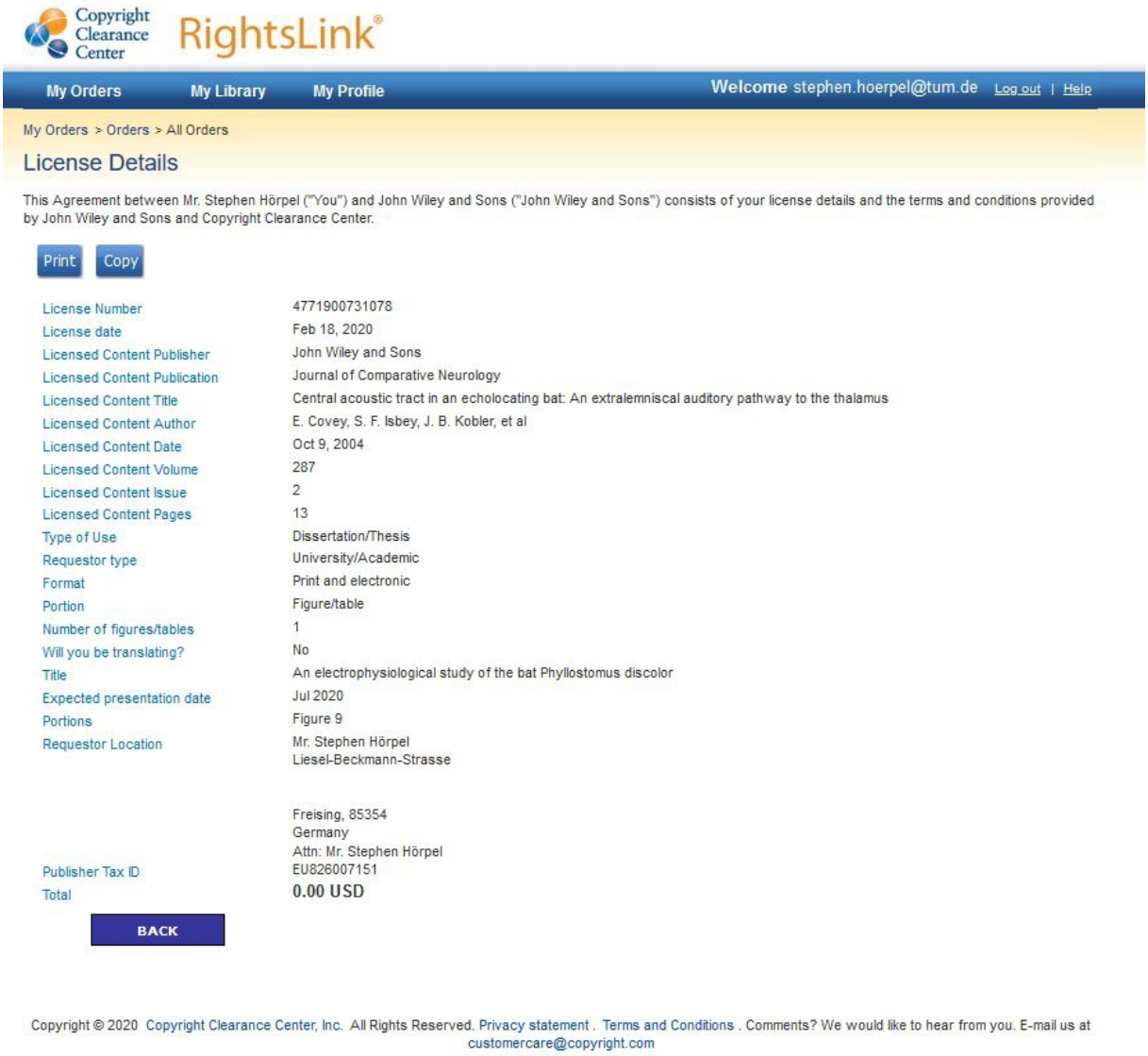

Copyright Clearance Center RightsLink®

My Orders | My Library | My Profile | Welcome stephen.hoerpel@tum.de Log out | Help

My Orders > Orders > All Orders

License Details

This Agreement between Mr. Stephen Hörpel ("You") and John Wiley and Sons ("John Wiley and Sons") consists of your license details and the terms and conditions provided by John Wiley and Sons and Copyright Clearance Center.

Print Copy

License Number	4771900731078
License date	Feb 18, 2020
Licensed Content Publisher	John Wiley and Sons
Licensed Content Publication	Journal of Comparative Neurology
Licensed Content Title	Central acoustic tract in an echolocating bat: An extralemniscal auditory pathway to the thalamus
Licensed Content Author	E. Covey, S. F. Isbey, J. B. Kobler, et al
Licensed Content Date	Oct 9, 2004
Licensed Content Volume	287
Licensed Content Issue	2
Licensed Content Pages	13
Type of Use	Dissertation/Thesis
Requestor type	University/Academic
Format	Print and electronic
Portion	Figure/table
Number of figures/tables	1
Will you be translating?	No
Title	An electrophysiological study of the bat Phyllostomus discolor
Expected presentation date	Jul 2020
Portions	Figure 9
Requestor Location	Mr. Stephen Hörpel Liesel-Beckmann-Strasse Freising, 85354 Germany Attn: Mr. Stephen Hörpel
Publisher Tax ID	EU826007151
Total	**0.00 USD**

BACK

Figure B.2: License for reproduction from *John Wiley and Sons*.

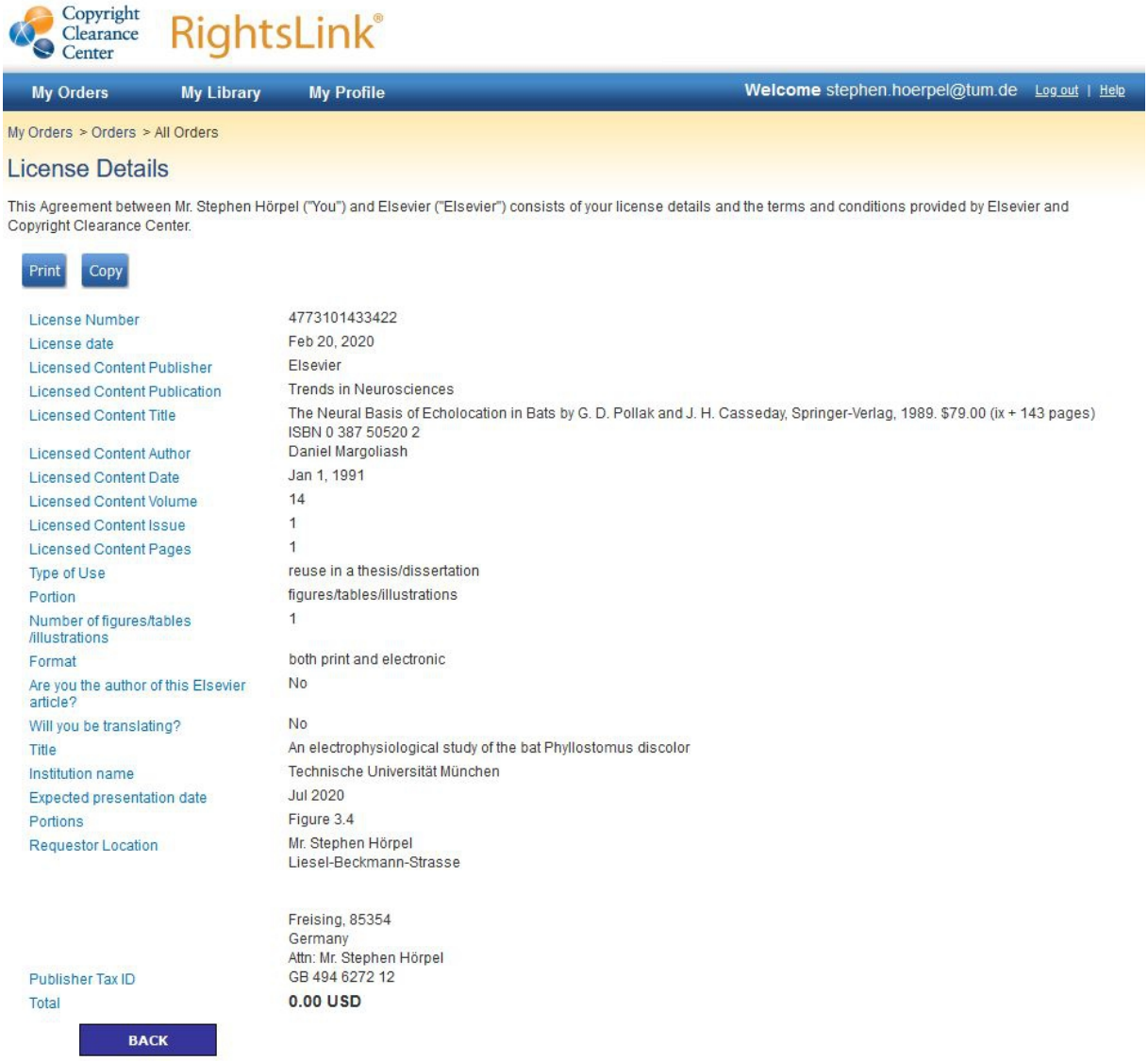

Copyright Clearance Center RightsLink®

My Orders | My Library | My Profile | Welcome stephen.hoerpel@tum.de | Log out | Help

My Orders > Orders > All Orders

License Details

This Agreement between Mr. Stephen Hörpel ("You") and Elsevier ("Elsevier") consists of your license details and the terms and conditions provided by Elsevier and Copyright Clearance Center.

Print Copy

License Number	4773101433422
License date	Feb 20, 2020
Licensed Content Publisher	Elsevier
Licensed Content Publication	Trends in Neurosciences
Licensed Content Title	The Neural Basis of Echolocation in Bats by G. D. Pollak and J. H. Casseday, Springer-Verlag, 1989. $79.00 (ix + 143 pages) ISBN 0 387 50520 2
Licensed Content Author	Daniel Margoliash
Licensed Content Date	Jan 1, 1991
Licensed Content Volume	14
Licensed Content Issue	1
Licensed Content Pages	1
Type of Use	reuse in a thesis/dissertation
Portion	figures/tables/illustrations
Number of figures/tables /illustrations	1
Format	both print and electronic
Are you the author of this Elsevier article?	No
Will you be translating?	No
Title	An electrophysiological study of the bat Phyllostomus discolor
Institution name	Technische Universität München
Expected presentation date	Jul 2020
Portions	Figure 3.4
Requestor Location	Mr. Stephen Hörpel Liesel-Beckmann-Strasse Freising, 85354 Germany Attn: Mr. Stephen Hörpel
Publisher Tax ID	GB 494 6272 12
Total	**0.00 USD**

BACK

Figure B.3: License for reproduction from *Elsevier*.

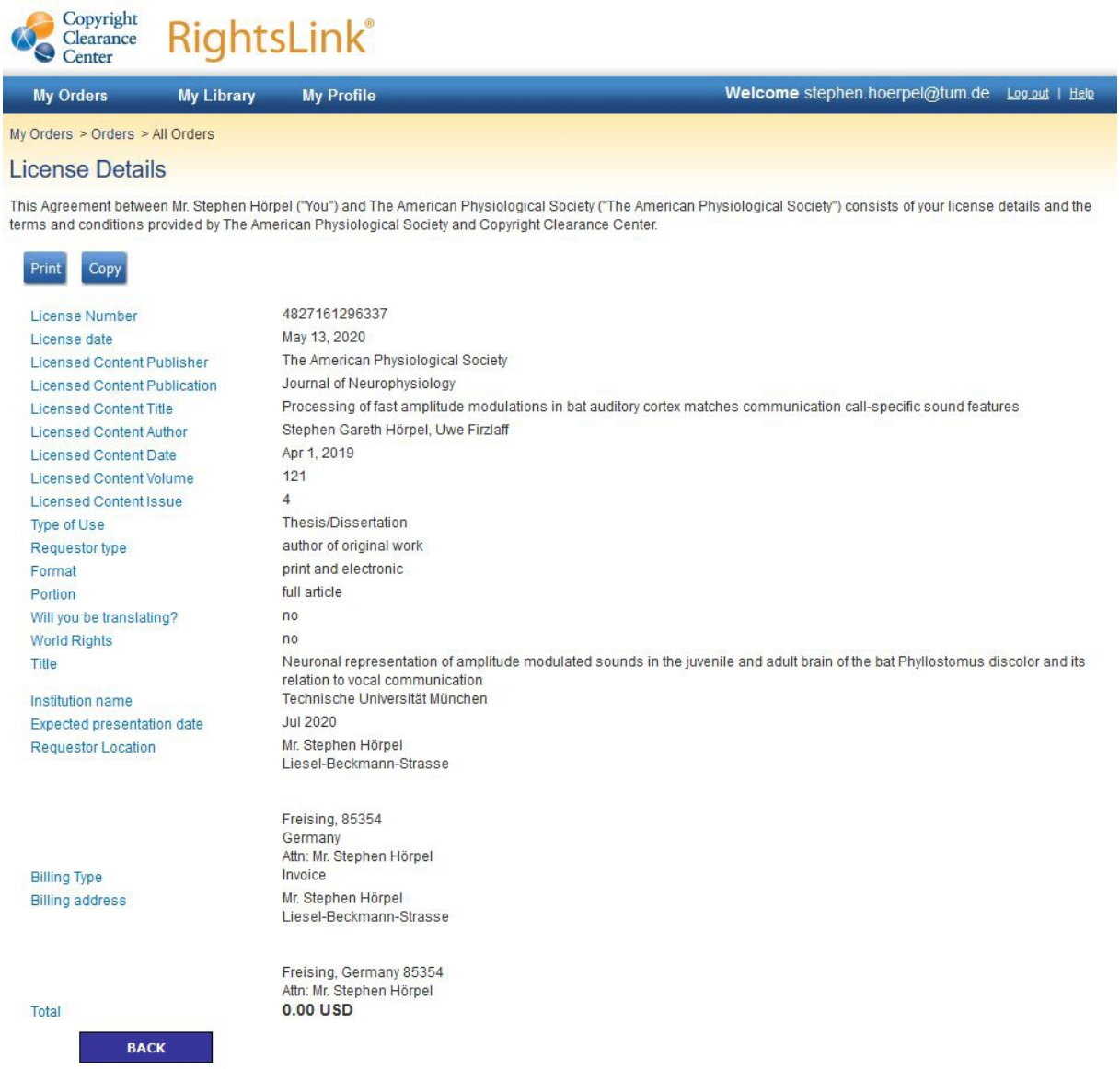

Copyright Clearance Center RightsLink®

My Orders | My Library | My Profile | Welcome stephen.hoerpel@tum.de | Log out | Help

My Orders > Orders > All Orders

License Details

This Agreement between Mr. Stephen Hörpel ("You") and The American Physiological Society ("The American Physiological Society") consists of your license details and the terms and conditions provided by The American Physiological Society and Copyright Clearance Center.

Print Copy

License Number	4827161296337
License date	May 13, 2020
Licensed Content Publisher	The American Physiological Society
Licensed Content Publication	Journal of Neurophysiology
Licensed Content Title	Processing of fast amplitude modulations in bat auditory cortex matches communication call-specific sound features
Licensed Content Author	Stephen Gareth Hörpel, Uwe Firzlaff
Licensed Content Date	Apr 1, 2019
Licensed Content Volume	121
Licensed Content Issue	4
Type of Use	Thesis/Dissertation
Requestor type	author of original work
Format	print and electronic
Portion	full article
Will you be translating?	no
World Rights	no
Title	Neuronal representation of amplitude modulated sounds in the juvenile and adult brain of the bat Phyllostomus discolor and its relation to vocal communication
Institution name	Technische Universität München
Expected presentation date	Jul 2020
Requestor Location	Mr. Stephen Hörpel Liesel-Beckmann-Strasse Freising, 85354 Germany Attn: Mr. Stephen Hörpel
Billing Type	Invoice
Billing address	Mr. Stephen Hörpel Liesel-Beckmann-Strasse Freising, Germany 85354 Attn: Mr. Stephen Hörpel
Total	**0.00 USD**

BACK

Figure B.4: License for reproduction from the *Journal of Neurophysiology*.

Figure B.5: Proof of reproduction permission from the journal *Hearing Research*.